ELSEVIER

EARTH-SCIENCE
REVIEWS

Invited review

Secular change and the onset of plate tectonics on Earth

Richard M. Palin[a,*], M. Santosh[b,c], Wentao Cao[d], Shan-Shan Li[b], David Hernández-Uribe[e], Andrew Parsons[a]

[a] Department of Earth Sciences, University of Oxford, South Parks Road, Oxford OX1 3AN, UK
[b] School of Earth Sciences and Resources, China University of Geosciences Beijing, 29 Xueyuan Road, Beijing 100083, China
[c] Department of Earth Science, University of Adelaide, Adelaide, SA 5005, Australia
[d] Department of Geology & Environmental Sciences, State University of New York at Fredonia, Fredonia, NY 14063, USA
[e] Department of Geology and Geological Engineering, Colorado School of Mines, Golden, CO 80401, USA

A B S T R A C T

The Earth as a planetary system has experienced significant change since its formation c. 4.54 Gyr ago. Some of these changes have been gradual, such as secular cooling of the mantle, and some have been abrupt, such as the rapid increase in free oxygen in the atmosphere at the Archean–Proterozoic transition. Many of these changes have directly affected tectonic processes on Earth and are manifest by temporal trends within the sedimentary, igneous, and metamorphic rock record. Indeed, the timing of global onset of mobile-lid (subduction-driven) plate tectonics on our planet remains one of the fundamental points of debate within the geosciences today, and constraining the age and cause of this transition has profound implications for understanding our own planet's long-term evolution, and that for other rocky bodies in our solar system. Interpretations based on various sources of evidence have led different authors to propose a very wide range of ages for the onset of subduction-driven tectonics, which span almost all of Earth history from the Hadean to the Neoproterozoic, with this uncertainty stemming from the varying reliability of different proxies. Here, we review evidence for paleo-subduction preserved within the geological record, with a focus on metamorphic rocks and the geodynamic information that can be derived from them. First, we describe the different types of tectonic/geodynamic regimes that may occur on Earth or any other silicate body, and then review different models for the thermal evolution of the Earth and the geodynamic conditions necessary for plate tectonics to stabilize on a rocky planet. The community's current understanding of the petrology and structure of Archean and Proterozoic oceanic and continental crust is then discussed in comparison with modern-day equivalents, including how and why they differ. We then summarize evidence for the operation of subduction through time, including petrological (metamorphic), tectonic, and geochemical/isotopic data, and the results of petrological and geodynamical modeling. The styles of metamorphism in the Archean are then examined and we discuss how the secular distribution of metamorphic rock types can inform the type of geodynamic regime that operated at any point in time. In conclusion, we argue that most independent observations from the geological record and results of lithospheric-scale geodynamic modeling support a global-scale initiation of plate tectonics no later than c. 3 Ga, just preceding the Archean–Proterozoic transition. Evidence for subduction in Early Archean terranes is likely accounted for by localized occurrences of plume-induced subduction initiation, although these did not develop into a stable, globally connected network of plate boundaries until later in Earth history. Finally, we provide a discussion of major unresolved questions related to this review's theme and provide suggested directions for future research.

1. Introduction

Without doubt, one of the most important unresolved questions in the geosciences concerns when plate tectonics began to operate on Earth at a global scale (Stern, 2005; Condie and Kröner, 2008; Shirey et al., 2008; Hawkesworth et al., 2010; Korenaga, 2013; Turner et al., 2014; Condie, 2018; Palin and Dyck, 2018). Understanding the causes and consequences of initiation of this geodynamic regime, and identifying what alternative(s) may have existed beforehand also has significant implications for studying the evolution of other rocky planets in our solar system (Head and Solomon, 1981; Phillips et al., 1981; Sleep, 1994; Solomatov and Moresi, 1996; O'Neill et al., 2007; Watters

and Nimmo, 2010; Wade et al., 2017; Stern et al., 2018) and beyond (Van Heck and Tackley, 2011; Foley et al., 2012; Noack and Breuer, 2014). The hallmark of modern-day plate tectonics on Earth is the independent horizontal motion of lithospheric plates, facilitated at divergent plate boundaries by seafloor spreading, at transform plate boundaries by strike-slip fault motion, and at convergent plate boundaries by one-sided subduction (Tao and O'Connell, 1992; King, 2001; Bercovici, 2003; Gerya et al., 2008). This tectonic 'conveyor belt' allows oceanic lithosphere to be efficiently recycled back into the mantle from whence it originated (Sleep, 1975; Kirby et al., 1991), with the gravitational pull of subducting slabs now understood to be the dominant driving force for surface plate motion (Forsyth and Uyeda, 1975; Conrad and Lithgow-Bertelloni, 2002; Schellart, 2004; Weller et al., 2019). Consequently, proving the existence of plate tectonics at any point in geological time requires proving operation of the Wilson Cycle, or else independent plate motion and rotation (Van der Voo, 1982).

In this contribution, we review the current state of understanding of the veracity of various lines of evidence proposed to support or refute the operation of plate tectonics since the Earth's formation at c. 4.54 Ga (Patterson, 1956). Papers published in the past few decades have suggested ages of onset that encompass almost all of geological time (Fig. 1), beginning in the Hadean (c. 4.2–4.0 Ga: Hopkins et al., 2008; Ernst, 2017a; Maruyama et al., 2018), through the Eoarchean (c. 3.9–3.6 Ga: Komiya et al., 1999; Nutman et al., 2002; Turner et al., 2014) and Mesoarchean (c. 3.2–3.0 Ga: Cawood et al., 2006; van Kranendonk et al., 2007; Condie and Kröner, 2008; Shirey and Richardson, 2011; Tang et al., 2016), to the Neoproterozoic (c. 1.0–0.8 Ga; Stern, 2005; Hamilton, 2011; Stern et al., 2016). Further, while some studies do not directly interpret the age of initiation, they provide valuable minimum age constraints on the operation of

subduction, as interpreted from Mesoarchean rocks of the Barberton Terrane, South Africa (Moyen et al., 2006), the Kola Peninsula, Russia (Mints et al., 2010), and Paleoproterozoic rocks from the West African Craton (Ganne et al., 2011), Tanzania (Möller et al., 1995), and the Trans-Hudson orogen, Canada (Weller and St-Onge, 2017).

Before performing detailed analysis of these geological indicators, it is important to firstly define key terms used to describe different tectonic regimes that may form on rocky planets with convecting mantles, and to provide a brief introduction to the thermal history of the Earth. A wide range of nomenclature has been introduced in recent years to describe different tectono-magmatic states, with the boundaries between each having become somewhat blurred. Subsequently, various lines of geological evidence for the operation of plate tectonics throughout Earth history are discussed, with an emphasis on metamorphic processes and products as indicators of the occurrence of subduction. Finally, we outline several issues related to this general topic that remain unanswered today and provide suggestions for future directions of study that would offer the best chances to resolve these matters.

1.1. Styles of tectonic regimes that characterize rocky planets

Rocky planets that are massive enough to allow solid-state convection in their mantles can exhibit a variety of geodynamic regimes at their surfaces, which may readily transition between different states over the thermal lifetime of the parent body (Petersen et al., 2015). All discussion of 'plates' in this work and related literature refers specifically to discrete masses of a planet's lithosphere (Barrell, 1914: Fig. 2), which defines the uppermost solid layer of the Earth, and is distinguished from the underlying asthenosphere by changes in the
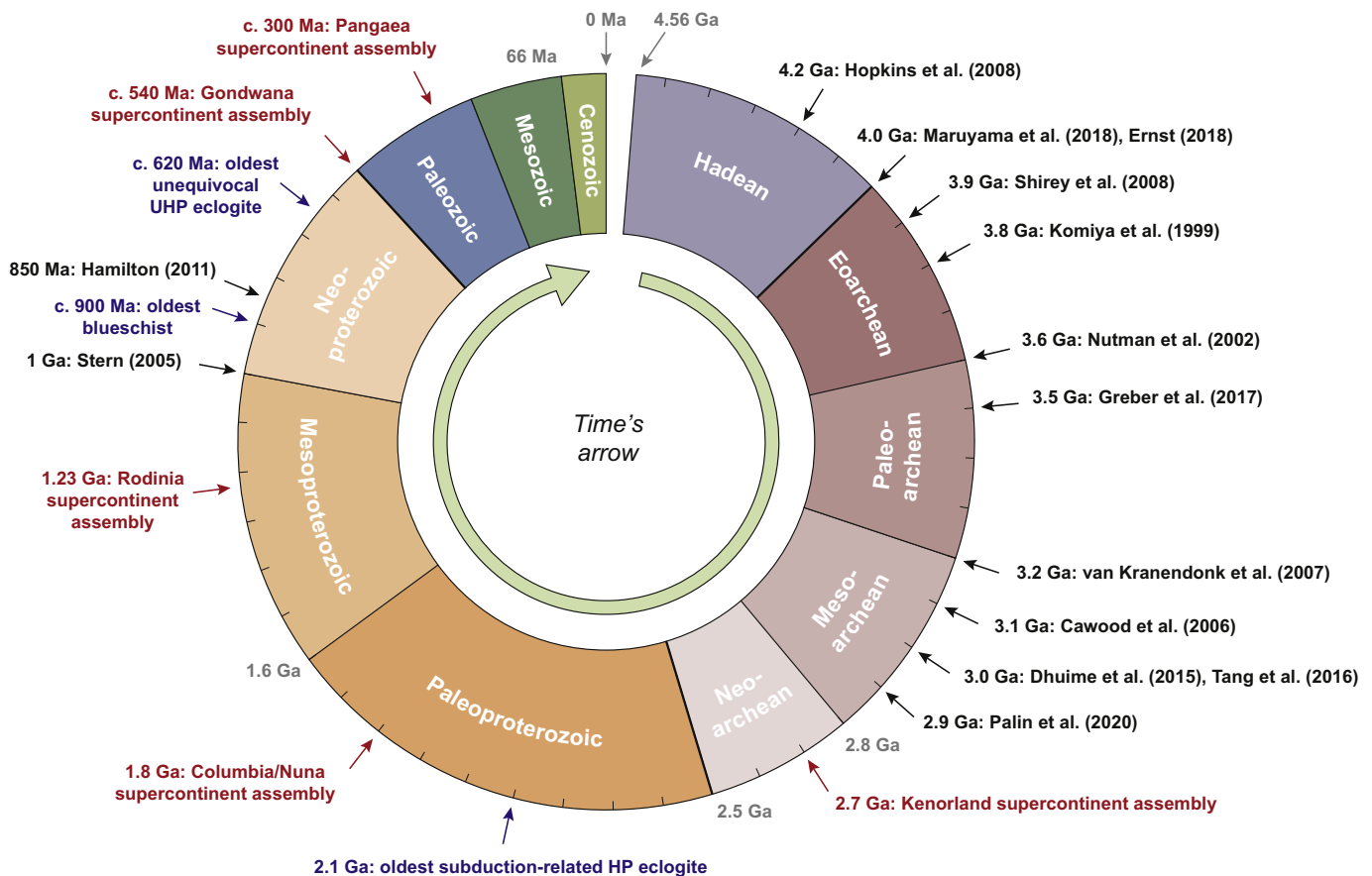

Fig. 1. Geological time chart showing a representative selection of proposed timings for the initiation of plate tectonics on Earth. Selected global-scale tectonic events and milestones are included for reference. See text for discussion of key features.
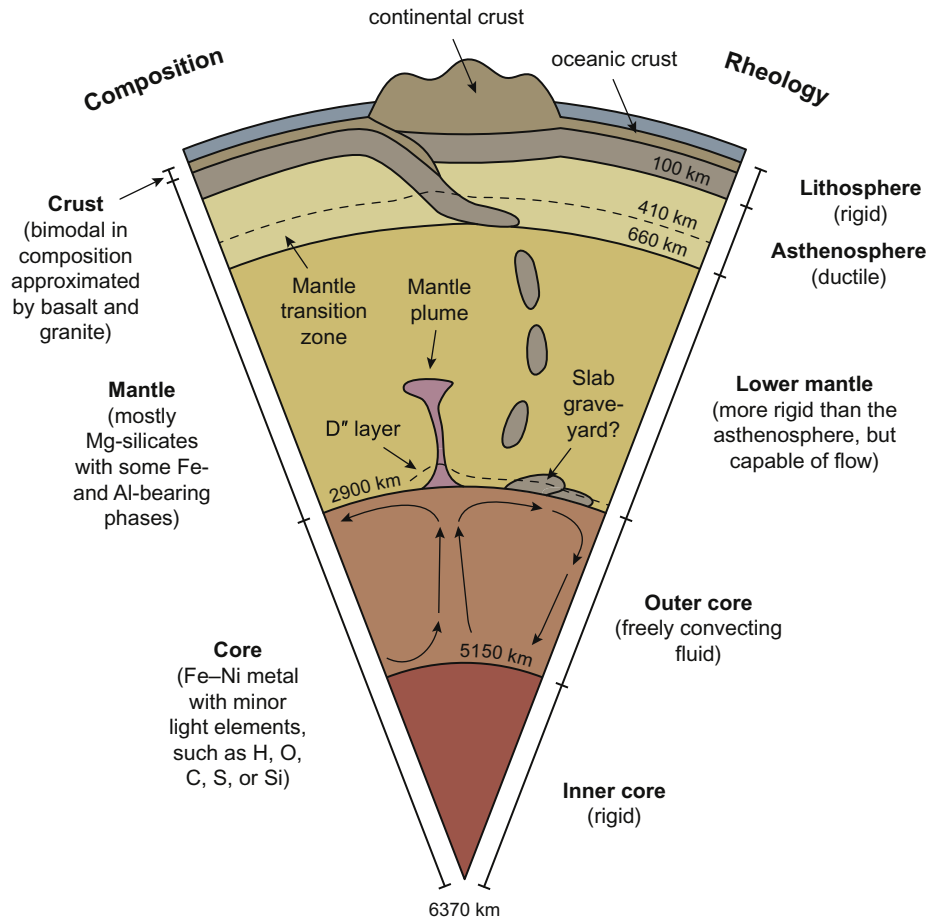
Fig. 2. Schematic cross section through the present-day Earth outlining differences in composition (left) and rheology (right) between layers. Not to scale.

dominant mode of heat flow, chemical composition, and/or rheology at the interface (Anderson, 1995; Fischer et al., 2010; Green et al., 2010). From a thermal perspective, heat flow through the lithosphere is dominated by conduction, whereas the asthenosphere and lower mantle cool primarily via convection (Pollack and Chapman, 1977). These different modes and length scales of heat transfer cause Archean and Proterozoic lithosphere to exhibit distinctly different geochemical and isotopic signatures to the underlying asthenosphere, which may compositionally homogenize over geological time (Lenoir et al., 2000; O'Reilly and Griffin, 2010). Nonetheless, discrete geochemical domains are thought to have persisted over hundred-million or billion-year timescales in the lower mantle (Hofmann, 1997), indicating that it is not as well mixed. Rheologically, the lithosphere acts in a rigid manner, whereas the underlying asthenosphere is much weaker/less viscous (Eaton et al., 2009; Burov, 2011) with a Rayleigh number that predicts vigorous convection (Korenaga and Jordan, 2003). The lithosphere may alternatively be referred to as a "lid" as it represents a strong thermal boundary layer separating hot planetary interiors from the cold hydrosphere and surrounding vacuum of space. Finally, it should be emphasized that discussion in this study refers only to rocky planets with silicate crusts and mantles (Fig. 2), although lithosphere–asthenosphere nomenclature may be equally applied to ice-rich bodies with solid outer shells situated above subsurface liquid oceans (e.g. Roberts and Nimmo, 2008).

Two fundamental end-member geodynamic regimes may exist on large silicate bodies, such as the Earth: mobile and stagnant lids. Mobile lids are characterized by active yielding of the lithosphere, which allows substantial horizontal motion and mass and energy exchange with the planet's interior (asthenosphere/lower mantle) (Moresi and Solomatov, 1998). In mobile-lid regimes, the surface velocity of the lid

is around 0.8–1.8 times that of the internal velocity (Weller and Lenardic, 2018). These criteria are all satisfied by plate tectonics, which is the archetypal form of a mobile-lid tectonic regime (Tackley, 2000). For example, subduction of oceanic lithosphere at convergent plate margins allows geochemical recycling between the Earth's interior and exterior (Othman et al., 1989; Scholl and von Huene, 2007; Rapp et al., 2008; Weller et al., 2016; Hernández-Uribe and Palin, 2019a), and the velocities of plate motion are typically within an order of magnitude of convection within the upper mantle (Ogawa, 2008). By contrast, stagnant-lid regimes exhibit severely limited horizontal surface motions, with no active yielding, although different forms of vertical mass transport allow limited mixing between surface and interior (cf. Fig. 3). In these cases, surface velocities are typically around 100–1000 times more sluggish those of internal velocities (Weller and Lenardic, 2018). With all other planetary characteristics being equal, thermo-mechanical modeling has shown that stagnant-lid regimes have thicker boundary layers, lower heat fluxes, and higher internal temperatures than equivalent mobile-lid regimes (O'Neill et al., 2007). A simplistic, but useful, distinction between mobile- and stagnant-lid tectonics is that the entire lithosphere is involved in convection in the former, whereas only the warmer, weaker (basal) part of the lid is responsive to convection in the latter (Stevenson, 2003). In this latter case, material may be lost from the lid's underside and returned to the planet's interior by dripping off or delamination (Fischer and Gerya, 2016a, 2016b; Piccolo et al., 2019), as discussed below.

Fig. 3 summarizes the conceptual tectono-magmatic evolution of large silicate bodies, such as Earth, soon after initial formation. Note that mobile-lid regimes (e.g. plate tectonics) are not illustrated here, as they likely represent a special case in geodynamic parameter space (cf. Section 1.3). Both theory and some observations imply the occurrence
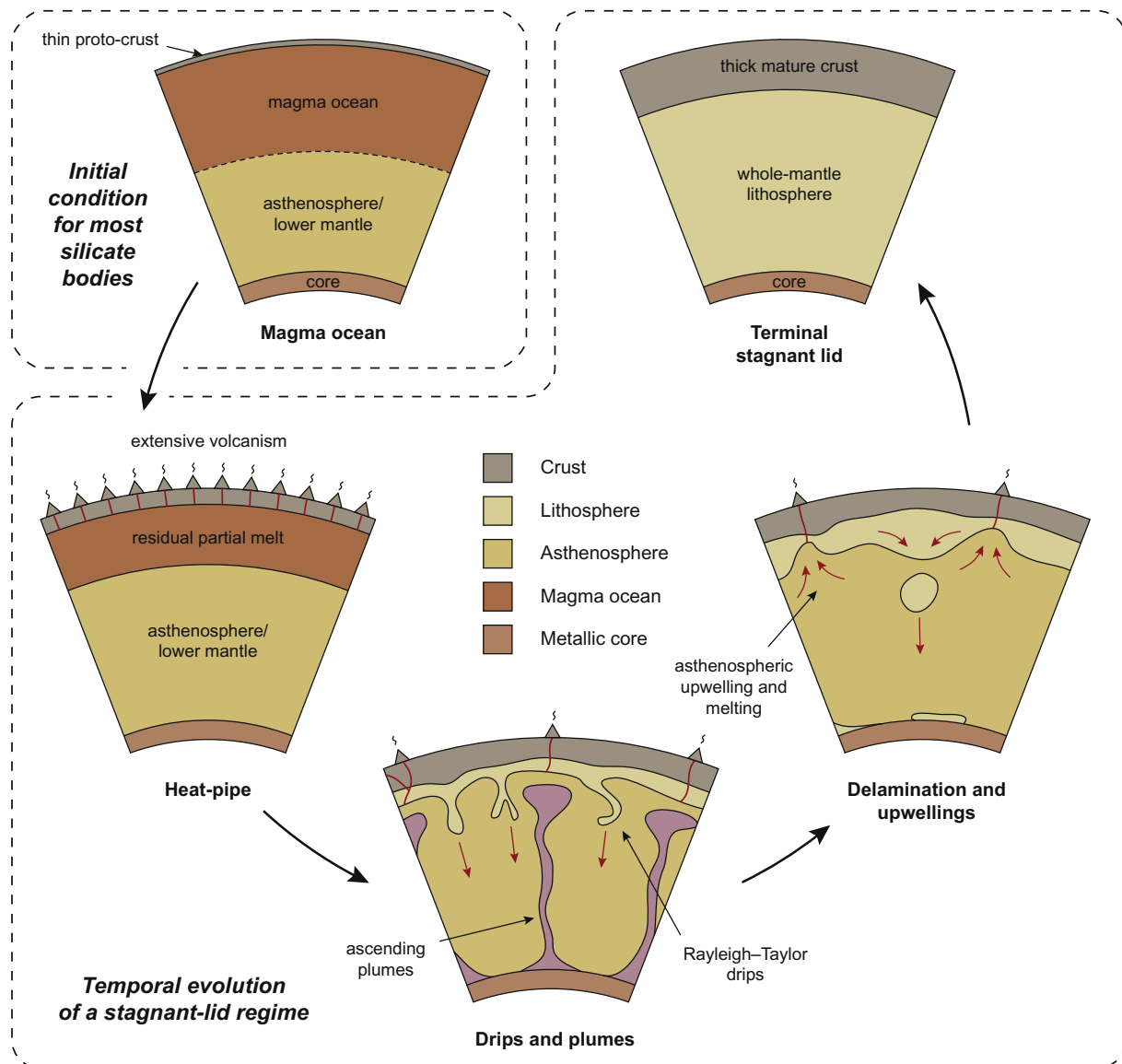
Fig. 3. Different types of stagnant-lid tectonic regimes that may exist on rocky planets following crystallization of an initial magma ocean (modified after Stern et al., 2018). Not to scale. Arrows point forwards in time representing a schematic birth-to-death evolution.

of magma ponds or oceans in the early evolution of all terrestrial planets in our solar system (Rubie et al., 2003; Elkins-Tanton, 2012; Hamano et al., 2013), which form due to heat provided by decay of radiogenic nuclides, accretion and metal–silicate differentiation, and bolide impacts (Sasaki and Nakazawa, 1986; Abe, 1997). As such, this can be considered a starting condition from which all possible tectonic regimes can evolve (Fig. 3). The initial thickness of a magma ocean depends on the planet's radius, which controls the rate of pressure increase, and so the depths at which an adiabat intersects the peridotite solidus and liquidus (Elkins-Tanton, 2012). Further, large planets with relatively low surface area-to-volume ratios cool at slower rates than small planets with relatively high surface area-to-volume ratios, and so the former are expected to retain a magma ocean for longer timescales. First-order estimations provided by integrated petrological–thermal modeling of the Hadean Earth predict a partially molten shallow magma ocean (or crystal-rich mush) to a depth of ~150–300 km below the surface (Hofmeister, 1983; Ohtani, 1985; Elkins-Tanton, 2012); however, numerical simulations of a giant impact thought to have formed the Earth–Moon system suggests that over 50 vol% of the Earth's mantle could have melted, indicating a magma ocean to at least

600 km depth (Canup, 2012; Ćuk and Stewart, 2012; Nakajima and Stevenson, 2015). Because of this uncertainty, the extent of a magma ocean on the very early Earth is debated, but even in the most extreme scenarios, complete solidification likely occurred within 1–10 Myr of inception (Elkins-Tanton, 2008; Monteux et al., 2016).

Terrestrial pseudo-analogues of the tectonic processes expected to occur on the surface of a magma ocean were described during the Mauna Ulu eruption at Kilauea volcano, Hawaii, by Duffield (1972). There, a crust-veneered lava column in the central eruptive vent was observed to exhibit a wide range of plate-like characteristics, including fragmentation and independent motion of crustal blocks, as well as their eventual sinking back into the underlying lava lake. Such features were suggested to represent a scaled-down model of primary crust formation and evolution on a magma ocean world. Upon near-terminal magma ocean crystallization, increasingly refractory melts would be expelled from crystal mush domains towards a planet's surface due to strong buoyancy contrasts with surrounding mantle residua (e.g. Turner et al., 2000). If such magmas can make their way to the planet's surface, they may erupt and crystallize as volcanic lava flows onto a thin primordial crust, which thickens over time – a stagnant-lid scenario called

heat-pipe tectonics (Fig. 3). Such a regime is suggested to have occurred on Earth during the Hadean Eon (Fig. 1: Moore and Webb, 2013) and implies that volcanism dominates over intrusive magmatism, although this is not the case for subsequent stagnant-lid modes (Rozel et al., 2017). Little is known about the veracity or likely duration of heat-pipe tectonics on the early Earth, although similar heat-pipe tectonics are thought to operate today on Jupiter's innermost satellite, Io (Kankanamge and Moore, 2019), driven by tidal heating. Future exploration of the Jovian system is likely to provide critical constraints on the parameter space in which heat-pipe tectonics may develop for extended periods of time on large planetary bodies.

Heat-pipe tectonics is an inherently short-lived form of stagnant-lid tectonics (Stern et al., 2018), as repeated eruption of lava and burial of older flows ultimately thickens the crust and so impedes magma ascent to the surface (Kankanamge and Moore, 2016). Old basaltic lava flows at the base of the crust that experience continued burial should transform to relatively dense garnet granulite at ~40 km, and even denser eclogite at ~60–80 km, depending on ambient temperature and fluid content (cf. Fukao et al., 1983; Anderson and Bass, 1986; Ellis and Maboko, 1992; Foley et al., 2003; Palin et al., 2016a, 2016b). Short-wavelength, density-driven downwellings (Rayleigh–Taylor instabilities), or "drips", provide a mechanism to return lithospheric material into the underlying mantle (Houseman et al., 1981; van Thienen et al., 2004; Fischer and Gerya, 2016a). Return-flow is expected in the form of mantle plume activity (Fig. 3), with enhanced magmatic activity occurring over these complementary regions of upwelling (e.g. Piccolo et al., 2019). By contrast with the heat-pipe model, intrusive magmatism is expected to dominate over volcanic eruption in such thick crust (Rozel et al., 2017), and tonalite–trondhjemite–granodiorite (TTG) partial melts that stalled during ascent above these plumes likely formed nuclei for Earth's first stable continental crust (Rudnick, 1995; Martin, 1993; Smithies et al., 2003; Moyen, 2011; White et al., 2017). Such a tectono-magmatic scenario is often described as a drip-and-plume regime, which represents an intermediate form of stagnant-lid tectonics (Fig. 3), or occasionally termed "plutonic squishy lid" (Cheng, 2018; Lourenço et al., 2018; O'Neill and Roberts, 2018).

Continued cooling and thickening of newly formed lithosphere encourage drips to laterally extend and plumes become more widely spaced (Sizova et al., 2015; Gerya et al., 2015). Dripping transitions to broader-scale and larger-volume delamination of dense eclogitic crust and underlying residual mantle (e.g. Zegers and van Keken, 2001; Nebel et al., 2018), which terminally descend into the asthenosphere (Fig. 3). Such a tectonic scenario, which is readily reproduced in two- and three-dimensional thermo-mechanical models of the Archean Earth (Gerya, 2014; Sizova et al., 2015; Fischer and Gerya, 2016a; Piccolo et al., 2019), is supported in the geological record by the paucity of eclogites and refractory cumulate material (see Sections 3.1 and 4.3). Larger-wavelength upwellings in the asthenospheric mantle facilitate decompression melting and continued formation of new mafic crust, which may later be buried and melted to form felsic TTGs (Kamber et al., 2005; van Hunen et al., 2008; Moyen and Martin, 2012; Kamber, 2015; Palin et al., 2016b; Feisel et al., 2018; Moyen and Laurent, 2017). Indeed, despite the apparent quiescence of this evolved form of stagnant-lid tectonics, considerable deformation and crustal growth may occur in this environment (Ernst, 2009; Debaille et al., 2013; Wade et al., 2017; Bédard, 2018).

The final state of all stagnant-lid regimes is a tectonically 'dead' planet or planetoid containing a single, globe-encircling crust (Fig. 3). Heat loss from the body's interior forces shut down of convection cells within the silicate mantle, transforming the formerly ductile asthenosphere into a thick, rigid lithosphere. Examples of this tectonic mode in our solar system today include Mercury and the Earth's Moon (Spohn, 1991; Hauck II et al., 2004).

1.2. Geodynamic conditions allowing plate tectonics

Given the rarity of plate tectonics in our solar system (cf. Stern et al., 2018), much research has been conducted into constraining the ranges of petrological and geodynamic parameter space that allow mobile-lid tectonic regimes to initiate and survive on large rocky planets, such as Earth. Numerical modeling performed by Weller et al. (2015a) and O'Neill et al. (2016), which focused on the influence of degree and rate of internal heating, showed that initially hot planetary-scale convective systems strongly promote stagnant-lid tectonic regimes. As these heat sources wane, for example due to the continued decay of radiogenic heat-producing elements, a window of opportunity for mobile-lid tectonics appears (Weller and Lenardic, 2018) by changing the effective viscosity contrast across the lithosphere–asthenosphere boundary (Korenaga, 2010, 2013), allowing yielding.

If planetary size and internal heat production allow lid fragmentation and independent plate motion, the buoyancy contrast between oceanic lithosphere and underlying asthenospheric mantle then becomes a critical factor in determining whether subduction may occur (cf. Davies, 1992). It has been shown empirically on the modern-day Earth that oceanic plate thickness and depth are proportional to age (Sclater et al., 1971; Parsons and McKenzie, 1978; Crosby et al., 2006); thus, young oceanic lithosphere is hotter and more buoyant than older, thicker, and colder equivalents (Klein et al., 2017).

If subduction could initiate on the early Earth, either locally or globally, what petrophysical and/or geodynamic conditions are required for it to be sustainable? Thermo-mechanical numerical models of convergent margin systems show that stable, one-sided subduction requires a discrete low-strength zone existing between two strong plates (Hassani et al., 1997; Sobolev and Babeyko, 2005; Tagawa et al., 2007), quantitatively defined as an effective coefficient of friction at the plate interface of < 0.1. Experimental values for dry rocks significantly exceed this cutoff, such that aqueous fluids appear to be required at the plate interface, essentially acting as lubrication (Hall et al., 2003; Gerya et al., 2008). While seawater may readily infiltrate trench openings at the Earth's surface (Peacock, 1990), water must also be continuously supplied at depth in order to maintain a weak plate interface and permit self-sustainability. Experimental petrology and thermodynamic phase equilibrium modeling has shown that aqueous fluids may be released from many components of subducted oceanic lithosphere, including surficial sediments (e.g. mudstone, carbonate ooze; Johnson and Plank, 2000; Kerrick and Connolly, 2001), hydrothermally altered oceanic crust (Liu et al., 1996; Prouteau et al., 2001; Hernández-Uribe et al., 2020), and metasomatized mantle lithosphere (Faccenda et al., 2008). These lithologies dehydrate during prograde metamorphism, releasing abundant H_2O and/or CO_2 at both fore-arc and sub-arc depths (Iwamori, 1998; Connolly, 2005; van Keken et al., 2011; Hernández-Uribe and Palin, 2019a, 2019b). As such, the presence of surface water on a terrestrial planet may be a critical factor in determining whether plate tectonics may initiate and sustain itself over million-year time-scales (Regenauer-Lieb et al., 2001; Lécuyer, 2013; Wade et al., 2017).

1.3. Thermal evolution of the Earth's mantle

As the Earth's internal heat budget fundamentally controls the window of opportunity for initiation of mobile-lid tectonics (Section 1.2), there have been many efforts to constrain our planet's thermal evolution through time (e.g. MacDonald, 1959; McKenzie and Weiss, 1975; Korenaga, 2006; Labrosse and Jaupart, 2007; Jaupart et al., 2007; Davies, 2009; Herzberg et al., 2010). However, discussion about secular changes in temperature can be complicated by the lack of a consistent reference frame. For example, the crust, the mantle, and the core all have different absolute temperatures and have likely cooled at different rates since planetary differentiation. As temperature decreases vertically through the modern-day mantle at ~0.3 °C/km, and the absolute depth of the lithosphere–asthenosphere boundary varies laterally
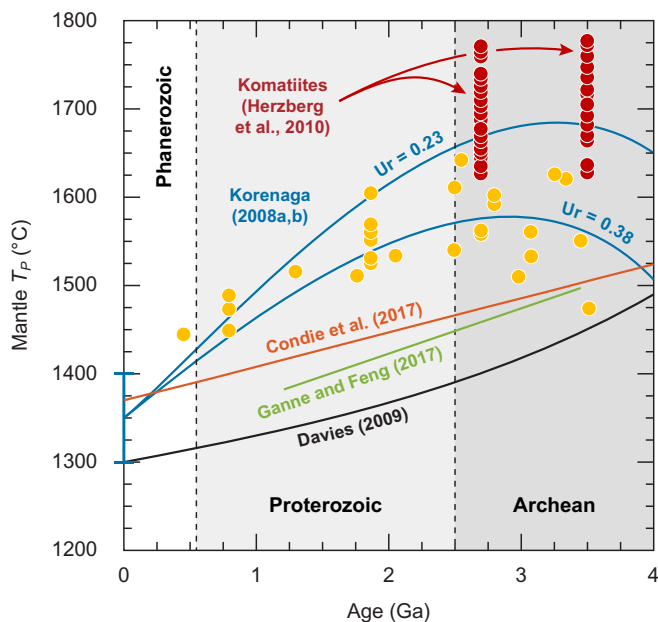
Fig. 4. Reported changes in ambient depleted mantle T_P over time. Yellow circles represent successful primary magma solutions for low- to medium-MgO basalts, calculated by Herzberg et al. (2010) and dark red circles represent equivalent data for komatiites. Present day mantle T_P is estimated to be 1350 ± 50 °C and Ur = convective Urey ratio (see main text for discussion).

according to tectonic setting, it is convenient to consider the mantle potential temperature (T_P) instead of the absolute temperature at any depth within the Earth. Mantle T_P is the adiabatic extrapolation of the mantle geotherm to the Earth's surface and reflects the balance between (1) heat lost by convective mantle cooling and conduction through the Earth's lithosphere, and (2) heat gained by radioactive decay in the mantle and conductive heating at the core–mantle boundary (e.g. Anderson, 2000; Korenaga, 2011).

The magnitude and rate of change of mantle T_P since the Earth's formation can be constrained in numerous ways. Thermal modeling and extrapolation backwards in time of the present-day ratio of heat production to heat loss – the convective Urey ratio (Ur) = 0.23 ± 0.15 – was shown by Korenaga (2008a, 2008b) to produce a concave-upwards thermal-evolution curve for mantle T_P, which peaked in the Meso-Archean (~2.8–3.2 Ga) (Fig. 4). This treatment interprets an ambient upper mantle T_P of between ~1675 °C (Ur = 0.23) and ~ 1575 °C (Ur = 0.38) at that time. When compared to today's ambient T_P value of ~1350 °C, mantle cooling rates of ~75–100 °C/Ga are implied by these models. First-order constraints on the value of Ur throughout geological time are provided by geophysical and geochemical models of the Earth (cf. Turcotte, 1980), such as the assumption of chondritic concentrations of radiogenic heat-producing elements (Leitch and Yuen, 1989; Breuer and Spohn, 1993).

During the past decade, it has been increasingly recognized that robust constraints can additionally be placed on the value of Ur and absolute mantle T_P using petrological data. While thermobarometry can be performed on metamorphic rocks in Archean high-grade terranes to constrain heat flow through the early crust (e.g. England and Bickle, 1984), the composition of primary mantle-derived magmas is more sensitive to physicochemical conditions within the source region, such as fluid content, pressure, and temperature. In a landmark study, Herzberg et al. (2010) used thermodynamic modeling to calculate the liquidus temperatures for 33 non-arc basalts of various ages (shown in Fig. 4) to constrain the ambient temperature of the mantle from which they were derived. These primary magma solutions generally lie between curves for Ur = 0.23 and Ur = 0.38, indicating Archean upper-mantle T_P values around 1500–1600 °C. Equivalent calculations for

komatiitic basalts suggest liquidus temperatures of ~1650–1800 °C, consistent with independent experimental and field evidence that such high-MgO lavas form above mantle plumes (Campbell et al., 1989; Arndt et al., 1997; Herzberg, 1999; Arndt, 2003; Herzberg et al., 2007).

In contrast to the high Archean mantle T_P values proposed by Korenaga (2008a, 2008b) and Herzberg et al. (2010), other workers argue for a less extreme scenario (Fig. 4). Both Ganne and Feng (2017) and Condie et al. (2016) applied the same petrological modeling technique for deriving primary magma solutions as conducted by Herzberg et al. (2010) to significantly larger global datasets of non-arc basaltic lavas. Both studies concluded that ambient Archean mantle T_P outside periods of supercontinent formation was ~1450–1500 °C (Fig. 4), defining a more subdued secular cooling rate of ~30–50 °C/ Gyr. While seemingly small (ΔT ~ 150 °C), the differences in interpreted Archean mantle T_P have significant implications for thermo-mechanical models of early Earth geodynamics, the viability of subduction, and continental crust formation. As mantle T_P is a controlling factor on the structure and composition of oceanic lithosphere created from it (see Section 2.1; McKenzie and Bickle, 1988; Takahashi and Brearley, 1990), several studies following the Herzberg et al. (2010) paradigm of a hot Archean mantle have demonstrated that oceanic lithosphere was too buoyant to subduct (Van Hunen and van den Berg, 2008; van Hunen and Moyen, 2012), whereas oceanic lithosphere formed from a relatively cool Archean mantle would have a larger density and viscosity contrast across the lithosphere–asthenosphere boundary. Based solely on these thermo-petrological arguments, subduction initiation may therefore be interpreted to have become viable at an earlier point in geological time than previously assumed. Recent geodynamic models have also recognized the importance of this re-evaluation of Archean mantle T_P for crust-forming mechanisms in stagnant-lid environments (Section 4.4: Piccolo et al., 2019), and time will tell whether it is necessary to revise the results and interpretations of earlier studies if the conclusions of Ganne and Feng (2017) and Condie et al. (2016) are proven correct.

2. Petrology and architecture of Archean crust

The Archean rock record is represented by 35 fragments of continental lithosphere (Bleeker, 2003) that cover ~5% of the Earth's surface (Artemieva, 2006). These regions are dominated by tonalite--trondhjemite–granodiorite (TTG) granitoids (Jahn et al., 1981; Moyen and Martin, 2012; White et al., 2017) and mafic-to-ultramafic volcanic rocks (Nisbet et al., 1977; Wilson et al., 1978; Xie et al., 1993), with rare supracrustal rocks (Moorbath et al., 1977; Boak and Dymek, 1982; Jackson et al., 1994). Many of these mafic/ultramafic volcaniclastic sequences are metamorphosed to greenschist-facies pressure–temperature (P–T) conditions, and so are often referred to as "greenstone" belts (Condie, 1981; Powell et al., 1995; Polat and Hofmann, 2003). By contrast, many TTG magmas are highly deformed with well-defined foliations (Fripp et al., 1980; Chardon et al., 1996; Marshak, 1999) and so likely experienced intense post-emplacement amphibolite- and granulite-facies metamorphism and recrystallization. For this reason, they are often referred to as "gray gneisses" (e.g. McGregor, 1979; Gao et al., 2011; White et al., 2017). These Archean bi-modal lithological associations are sometimes described as "granite–greenstone" terranes (e.g. Dziggel et al., 2002; van Kranendonk et al., 2004), although TTGs are not granitic sensu stricto in composition or mineralogy (Streckeisen, 1974; Le Bas et al., 1986), and so this term is not used herein. In addition, whether greenstone terranes represent obducted and metamorphosed fragments of ancient oceanic crust is a topic of current debate (Bickle et al., 1994; Furnes et al., 2014a), although Archean gray gneisses are unequivocally thought to be components of Earth's earliest continents (Adam et al., 2012; Hastie et al., 2016; Wiemer et al., 2018). As such, discussion below concerning the petrology and architecture of oceanic crust focuses primarily on theoretical considerations and the results of thermal–petrological
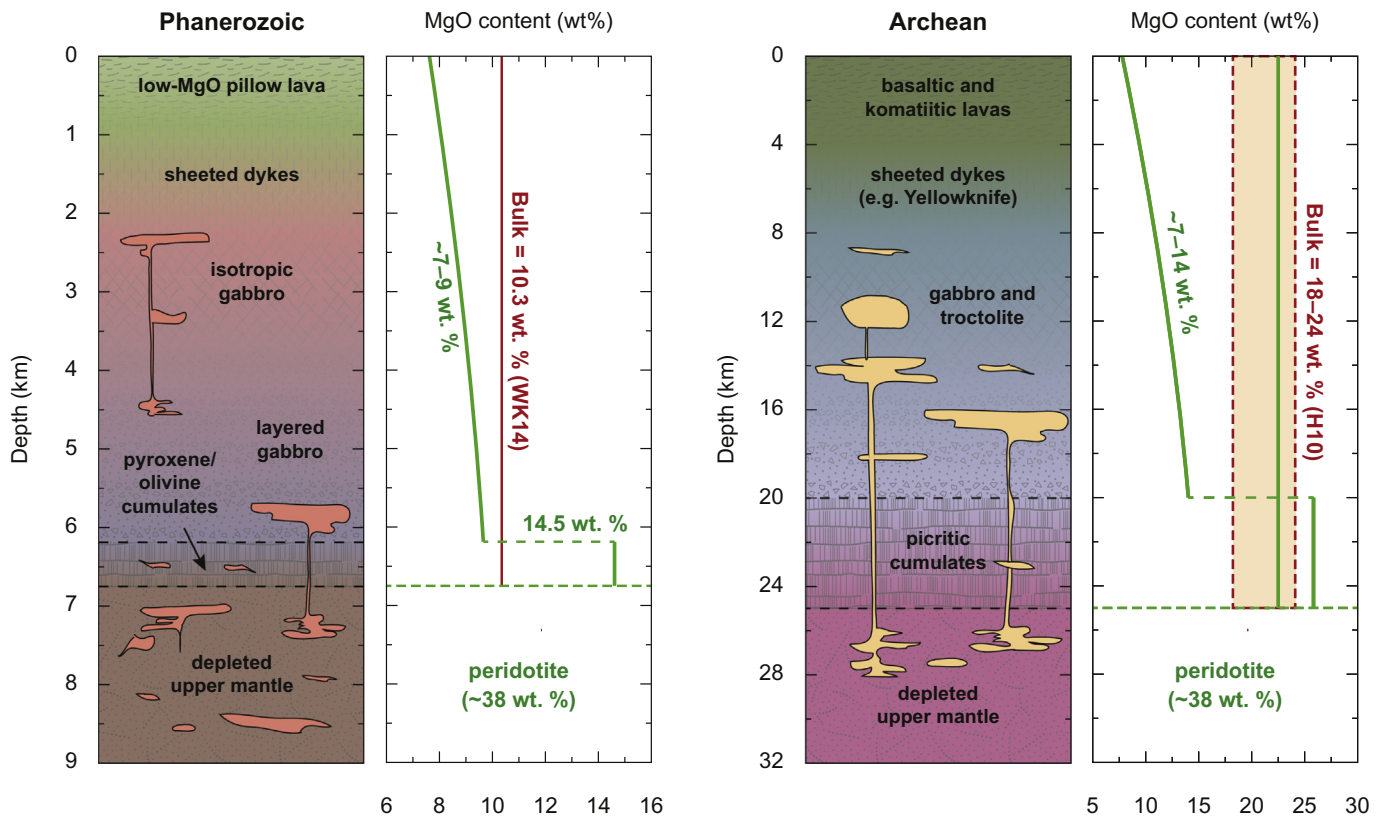
Fig. 5. Schematic cross sections through Phanerozoic and (interpreted) Archean oceanic crust and upper mantle (after Palin and Dyck, 2018). Modern-day structure, petrology, and MgO contents are from White and Klein (2014), and Archean structure and petrology are after Foley et al. (2003) and Nair and Chacko (2008). Bulk MgO content for Archean crust is after Herzberg et al. (2010) (H10) and Klein et al. (2017) (K17).

modeling, whereas discussion about the Archean continental crust focuses mostly on observational evidence.

2.1. Oceanic crust

Oceanic crust produced at mid-ocean ridge spreading centers on Earth today varies in structure and thickness depending on the rate of spreading at the central ridge (Bown and White, 1994; Dilek and Furnes, 2011, 2014). Specifically, very slow (< 2 cm/yr) and slow (< 5.5 cm/yr) spreading ridges have deep median rift valleys and thin oceanic crust at the spreading axis (Michael et al., 2003), whereas intermediate (> 5.5 cm/yr) and fast (> 10 cm/yr) spreading ridges have more subdued topography at the ridge axis and generate relatively thicker crust (Chen, 1992). In the classical Penrose ophiolite model, which is representative of intermediate- and fast-spreading ridges, the crustal section is ~6–7 km thick (Fig. 5), has an average bulk MgO content of ~10 wt%, and crystallizes from small mantle melt fractions (*F*) of 0.08–0.10 (Sleep, 1975; McKenzie and Bickle, 1988; Herzberg et al., 2010). This architecture has been deduced from direct examination of fragments obducted onto continental margins – ophiolites (e.g. Miyashiro, 1975) – and by in-situ seismic reflection and refraction studies (Spudich and Orcutt, 1980), and deep-sea drilling programs (Humphris et al., 1995). Immediately beneath a thin sedimentary veneer, the uppermost portion of the solid crust (mid-ocean ridge basalt – MORB) is comprised of pillow basalts with an MgO content of ~7 wt% (White and Klein, 2014). This horizon varies in thickness according to the spreading rate of the parent mid-ocean ridge (Nicolas et al., 1994; Carbotte and Scheirer, 2004), but spans, on average, 500–1000 m (Anderson et al., 1982; Girardeau et al., 1985). Below this extrusive horizon is a thicker sheeted dike complex (Fig. 5) that facilitates eruptions at the surface, and is underlain itself by coarser-crystalline gabbroic rocks that may be isotropic or layered (Pallister, 1981; Quick

and Denlinger, 1993). Ultramafic olivine- and pyroxene-rich cumulate horizons occur at the base of the crust (Kay and Kay, 1985; Natland and Dick, 2001).

A necessary petrological result of a hotter Archean mantle T_P is deeper and more voluminous melting of peridotite ($F = 0.25$–0.45) during adiabatic decompression, which is expected to produce a thicker (~25–40 km) crust (McKenzie and Bickle, 1988) with a higher bulk MgO content of ~18–24 wt% (Fig. 5: Abbott et al., 1994; van Thienen et al., 2004; Herzberg et al., 2010). As such, with mantle cooling over time, the structure and bulk composition of oceanic lithosphere is likely to have showed continual change. Experimental modeling of primary magmas produced from assumed mantle protolith compositions, T_P values, and higher F predict that the uppermost, MORB-like portions of such a primitive crust Archean oceanic crust would have bulk MgO contents in the range ~11–15 wt% (e.g. Ziaja et al., 2014). In support of these experimental results, Weller et al. (2019) recently performed thermodynamic calculations simulating isentropic fractional melting of Archean mantle by using petrological phase equilibrium modeling, yielding similar MgO ranges. Integrated mass-balance calculations showed that oceanic crusts generated at conservative mantle T_P values of 1425 and 1550 °C (cf. Ganne and Feng, 2017; Fig. 4) must have had minimum thicknesses of 13.8 and 24.3 km, respectively (Table 1). Both depth-integrated mantle-melt compositions were picritic, with MgO contents of 14.3 and 17.4 wt% for these isentropes (Table 1).

A schematic model of the general chemistry and structure of Archean oceanic crust and underling mantle lithosphere is presented in Fig. 5 (after Palin and Dyck, 2018), based in part on the results of these experiments and models. Secular cooling of the mantle over time thus requires that the maficity of primary mantle-derived oceanic lithosphere to have decreased since the Meso-Archean, regardless of the magnitude of change (cf. Section 5.2). Nonetheless, identification of fragments of primary oceanic crust in Archean cratons is fraught with

Table 1

Calculated oceanic crust bulk compositions (wt% oxide) and thicknesses (km) determined from isentropic fractional melting and crystallization modeling (Weller et al., 2019). T_P = mantle potential temperature, Mg# = molar Mg/(Mg + Fe^{2+}). Compositions of the melt-depleted, residual mantle for each T_P are also shown. High mantle T_P values may be taken to represent Archean crust, medium T_P values Proterozoic crust, and low T_P values Phanerozoic crust. The composition of KLB-1 fertile mantle is given for reference.

Model parameters	SiO$_2$	Al$_2$O$_3$	CaO	MgO	FeO	Na$_2$O	Fe$_2$O$_3$	Cr$_2$O$_3$	Mg#	Thickness (km)
T_P = 1300 °C crust	48.11	15.63	13.29	12.11	8.16	1.98	0.48	0.24	0.73	7.5
T_P = 1425 °C crust	47.69	13.33	12.96	14.31	9.28	1.64	0.50	0.31	0.73	13.8
T_P = 1550 °C crust	47.59	10.71	11.89	17.40	10.20	1.33	0.55	0.33	0.75	24.3
T_P = 1300 °C residual mantle	44.48	1.76	1.59	43.59	7.92	0.06	0.27	0.33	0.91	48.5
T_P = 1425 °C residual mantle	44.43	1.72	1.26	44.25	7.70	0.06	0.26	0.32	0.91	70.9
T_P = 1550 °C residual mantle	44.30	1.80	0.97	44.90	7.41	0.06	0.24	0.32	0.92	96.6
KLB-1 fertile mantle	44.94	3.52	3.08	39.60	7.95	0.30	0.30	0.32	0.90	–

difficulty (Helmstaedt et al., 1986; Bickle et al., 1994; Kusky et al., 2001; Zhai et al., 2002; Zhao et al., 2007) as a range of non-equilibrium processes (e.g. fractional crystallization and/or magma mixing during ascent) are likely to have affected the mineralogy and composition of the resultant crustal products (O'Hara, 1977; Grove et al., 1992; Morgan and Chen, 1993). Advances in modeling of mantle melting beneath ridge systems and the multi-scale magmatic processes of melt ascent and crystallization are likely to open new avenues of research in this field in the future (Kinzler and Grove, 1992; Presnall et al., 2002).

The proposal that the bulk composition of oceanic crust has evolved continuously since the Meso-Archean has been a topic of surprisingly intense debate in recent years, despite much evidence from the geological record supporting the results of experiments and thermal–petrological models. While nearly all basalts in the Precambrian rock record have undergone some degree of metamorphism (Gill, 1979), many trace-element ratios used to discriminate intraplate vs. plate margin environments of magma genesis are insensitive to thermal alteration (e.g. Floyd and Winchester, 1978; Monecke et al., 2002; Payne et al., 2010; Sheraton, 1984; Winchester and Floyd, 1976). As such, it is possible to differentiate plume-derived magmas, which are typically picritic or komatiitic in nature owing to elevated mantle T_P at plume heads, from plate-margin magmas (e.g. MORBs) and assess the secular compositional evolution of each independently.

Analyses of geochemical databases of (meta)basalt major-, minor-, and trace-element compositions have been attempted by several authors, with the key findings of each summarized in Table 2. Early workers focused on differences in trace-element ratios between relatively small numbers of Phanerozoic and Archean examples, and made comparisons of bulk-rock at a common Mg# [=100 × Mg/ (Mg + Fe^{2+})] (e.g. Gill, 1979). Subsequent studies have utilized datasets that provide extensive spatial and temporal coverage of the global geological record, alongside applying statistical tests to quantify the significance of trends identified. For example, Furnes et al. (2014a)

analyzed metabasalt compositions with depleted mantle incompatible trace element ratios from all major Precambrian greenstone belts worldwide and reported a statistically significant decrease in bulk-rock MgO content from ~15 wt% at 3.5 *Ga* to ~7 wt% today. A similar study by Condie et al. (2016) reported a that basalts older than 3 *Ga* were only slightly more mafic than Phanerozoic examples, with a mean MgO content of ~9 wt%. Importantly, however, neither study considered spatiotemporal data clustering, such that these calculated mean compositions could simply reflect sampling bias in their respective databases.

Such preservation and/or sampling issues was addressed directly by Keller and Schoene (2012) and Ganne and Feng (2017), who integrated a Monte Carlo re-sampling procedure into their geochemical analysis in order to minimize spatiotemporal bias. Keller and Schoene (2012) reported a clear secular decrease in MgO content from the Archean to the Phanerozoic within the intrusive and extrusive mafic rock record, but did not discriminate between likely environments of formation for each sample. Ganne and Feng (2017) repeated this analysis on extrusive mafic magmas only and reported successful primary magma solutions for Archean primary melt fractions that had an average MgO content of ~20 wt%, and equivalent interpreted basalt compositions with a mean MgO content of ~13 wt%. This high-MgO content exceeds that reported for modern-day MORB (White and Klein, 2014) and correlates with field evidence of strongly mafic pillow lavas (> 12 wt% MgO) with MORB-like geochemical trace element ratios that are present in many Archean greenstone belts (e.g. Isua; Komiya et al., 2004; Pilbara; Ohta et al., 1996). However, in the absence of verified fragments of Archean oceanic crust within the geological record (Bickle et al., 1994), the results of Big Data analysis, experimental petrology, and thermodynamic modeling will always remain inconclusive.

2.2. Continental crust

Interpreting the structure and composition of Archean continental crust is theoretically much simpler than for oceanic crust, as remnants of the former are readily preserved in the geological record (De Wit et al., 1992; Martin, 1994). However, unlike the oceanic crust, which experienced a simple and predictable change in thickness and bulk composition due to secular mantle cooling, the formation and continued growth of the continents is a more stochastic process that is incompletely understood even on the modern-day Earth (Arndt and Goldstein, 1987; Bohlen and Mezger, 1989; Hacker et al., 2011; Spencer et al., 2017).

Present-day structure of the continental crust is generally stratified based on seismic velocities and heat flow. Regardless of whether a three-layer (upper, middle, and lower crust; e.g. Christensen and Mooney, 1995; Rudnick and Fountain, 1995; Rudnick and Gao, 2003, 2014) or two-layer (upper and lower crust; Hacker et al., 2011, 2015) model is assumed, a good agreement exists for the granodioritic composition of the upper continental crust (Rudnick and Gao, 2014 and references therein). The composition of the lower continental crust is

Table 2

Reported secular trends in oceanic crust composition since the Early Archean based on basalts preserved within the geological record (from Palin and Dyck, 2018). Only elements reported as showing secular variation are noted here: if an element is absent from this table, it was either reported by the author(s) in question to have remained approximately constant over time or was not discussed. N.B. Mg# = molar Mg/(Mg + Fe^{2+}), [1]basalts with depleted mantle (DM) trace element geochemistry.

Lithology	Increase	Decrease	Study
Tholeiitic basalt	Al, Ti, Zr, P	Cr, Ni, Co	Gill (1979)
Tholeiitic basalt	Al	Cr, Ni, Co	Condie (1985)
Basalt	K, Na	Mg, Cr, Ni	Keller and Schoene (2012)
Basalt/greenstone	Al, Ti, Zr	Mg, Ni	Furnes et al., 2014b
Depleted mantle (DM) basalt[1]	Na, Ti, Mg#	Fe, Mn	Condie et al. (2016)
Archean basalt	Al	Mg	Ganne and Feng (2017)

still under debate, and is proposed to vary from a middle crust of amphibolite-facies metamorphic rocks and a predominantly mafic lower crust (Rudnick and Gao, 2014 and references therein) to a lower crust with only 10–20% mafic materials and a large proportion of rocks with 49–62 wt% SiO_2 (Hacker et al., 2015; Zhang et al., 2020).

The original composition and formation of early continental crust remains enigmatic due to poor preservation of primary components, which have been frequently overprinted by subsequent geological processes (e.g. metamorphism or partial melting). Only a small percentage of preserved continental crust is Archean in age (Goodwin, 1996). Although arguably present in a mafic section in the Nuvvuagittuq belt, Superior Province, Canada (O'Neil et al., 2008, 2011; O'Neil and Carlson, 2017), Hadean crust has not been found at the present-day Earth's surface, which may be due to its expected high density due to having an ultramafic or mafic composition, which may have caused it to be recycled back into the mantle (Kröner, 1985). Currently, the oldest known coherent crust occurs within the c. 3.8 *Ga* Acasta gneiss complex in the Northwest Territories of Canada (Bowring and Williams, 1999), and is composed of gabbroic and granitoid gneisses (e.g. Iizuka et al., 2007). Reimink et al. (2018) recently showed that the Acasta gneisses were derived from partial melting of hydrated Hadean mafic crust in an Iceland-like mantle plume-related setting (see also Reimink et al., 2014), not due to bolide impacts, as suggested by some studies (e.g. Johnson et al., 2018). The volumetrically dominant lithology in Archean terranes – TTG gneisses – is typically interpreted as formed through partial melting of amphibolite or eclogite due to drip tectonics (Nebel et al., 2018) or subduction of oceanic plateaus (e.g. Martin et al., 2014; Hastie et al., 2016).

Geochemical methods have been used to augment the interpretation of early continental crust composition. Dhuime et al. (2015) examined a large number (> 13,000) of samples with Nd model ages from the Hadean to the Phanerozoic, and back-calculated Rb/Sr ratios of their original crustal sources. The calculated Rb/Sr ratios significantly increase at ~3 Ga, which they interpreted as the continental crust having become more felsic in composition based on positive correlation between Rb/Sr ratio and SiO_2 contents in modern-day igneous rocks. Using Ni/Co and Cr/Zn ratios, which are positively correlated with MgO content in igneous and metamorphic rocks, Tang et al. (2016) demonstrated that the Archean upper continental crust experienced a transition from highly mafic (> 11 wt% MgO) at 3.0 *Ga* to felsic (~4 wt% MgO) at 2.5 *Ga*. This transition also marks the calculated increase of granites sensu *lato* from 10 to 40% to over 80%, and the decrease of basalt and komatiite to less than 20% in upper continental crust. These lines of evidence indicate that the upper continental crust became dominantly felsic in the Late Archean (Rollinson, 2017). Late studies also suggested that the composition of the Archean middle continental crust changed from being dominated by sodic TTG suites to having a more potassic granitoid composition from 3.0–2.5 *Ga* (e.g. Nebel et al., 2018), which has been interpreted as the evidence for the onset of plate tectonics in the Late Archean (Laurent et al., 2014).

The changing growth rate of continental crust through time is a long-standing debate (e.g. Condie and Aster, 2010; Dhuime et al., 2012; Roberts and Spencer, 2015 and references therein). Numerous models have been proposed, ranging from very early growth (Armstrong, 1981), to pulsed growth (e.g. Condie and Aster, 2010) and late growth (Goodwin, 1996). Readers are directed to detailed reviews by Kemp and Hawkesworth (2014) and Hawkesworth et al. (2017) for more information, the detail of which is beyond the scope of this review. However, one emerging approach to highlight here is the use of Big Data analysis of global zircon achieve to retrieve the continental growth (e.g. Dhuime et al., 2012; Roberts and Spencer, 2015). Fig. 6 displays the correlation of global zircon U−Pb ages (Roberts and Spencer, 2015) with timing the supercontinent formation. One key feature of this dataset is the abundance of zircon ages at 3.0–2.5 *Ga*, which has been suggested by some studies to have implications for changing geodynamic regimes. However, it has been noted that such U−Pb datasets cannot fully track continental growth, as some ages record crustal reworking and isotopic resetting; therefore, ƐHf model ages and oxygen isotope correction methods have been proposed to limit the bias from reworked zircon. Using such corrected data, Dhuime et al. (2012) yielded a volumetric growth curve (Fig. 6) for continental crust, which indicates a faster growth rate prior to c. 2.9 *Ga* and a slower rate afterward. This inflection point may indicate that a significant change of Earth's geodynamic processes occurred at this time (Dhuime et al., 2012).

The large-scale emergence of the continents from being dominantly submarine to dominantly subaerial is also thought to have dramatically influenced the evolution of life, and thus also has implications for exobiology and the search for habitable planets (see Section 7.1; Flament et al., 2008). The Great Oxygenation Event (GOE) at 2.45–2.22 Ga (Bekker et al., 2004; Guo et al., 2009; Gumsley et al., 2017) marks the rapid appearance of free oxygen in the Earth's atmosphere (Anbar et al., 2007; Sessions et al., 2009), and has been variably related to the rise of multicellular oxygen-producing cyanobacteria (Schirrmeister et al., 2013), loss of hydrogen from the atmosphere (Catling et al., 2001), a gradual change in the redox state of volcanic gases during the Late Archean, (Holland, 2002), or a geologically abrupt period of mantle overturn and/or intense plume activity near the Archean–Proterozoic transition (Kump et al., 2001; Ciborowski and Kerr, 2016). Alongside these propositions, some authors suggest that the GOE was a direct result of changing tectonic processes on Earth across the Archean–Proterozoic boundary. For example, Lenton et al. (2004) suggested that oxygenation was driven by the global appearance of shallow-shelf seas, where reduced organic carbon could be deposited and buried. Further, Campbell and Allen (2008) correlated spikes in atmospheric oxygen concentration during episodes of supercontinent formation. In this scenario, widespread continental uplift during collisional orogenesis is supposed to have increased the rate and volume of erosion, which in turn released nutrients into the ocean to feed photosynthetic cyanobacteria. Similar feedback mechanisms between tectonic activity and climate are well documented in the Phanerozoic rock record (e.g. Macdonald et al., 2019), so likely also occurred in the geological past.

3. Evidence for the operation of subduction throughout Earth history

The wide range of interpretations presented in Fig. 1 for the onset of global tectonics result from the debated reliability of different lines of evidence for plate tectonic processes operating, alongside different weightings given to these different types of data. Here, we discuss the strengths and weaknesses of some of the major forms of each. For simplicity, these plate tectonic indicators are divided into three main groups – petrological, tectonic, and geochemical/isotopic lines of evidence – although many criteria cross these boundaries and should not be considered as being restricted to one typology. Finally, a fourth group is discussed: thermo-mechanical (geodynamic) and petrological modeling. While such models are, by definition, simulations of nature, their results can be directly compared against evidence preserved within the rock record. Thus, interrogation of parameter space and interpretation of the results produced can provide indirect constraints on the likelihood of subduction having operated based on correlation with known time-dependent variables (see Section 1.3).

3.1. Petrological evidence

Petrological evidence for subduction is categorized here as being the fundamental lithologies that are reported to form only in convergent plate margin settings, although the veracity of such claims is also assessed for each.
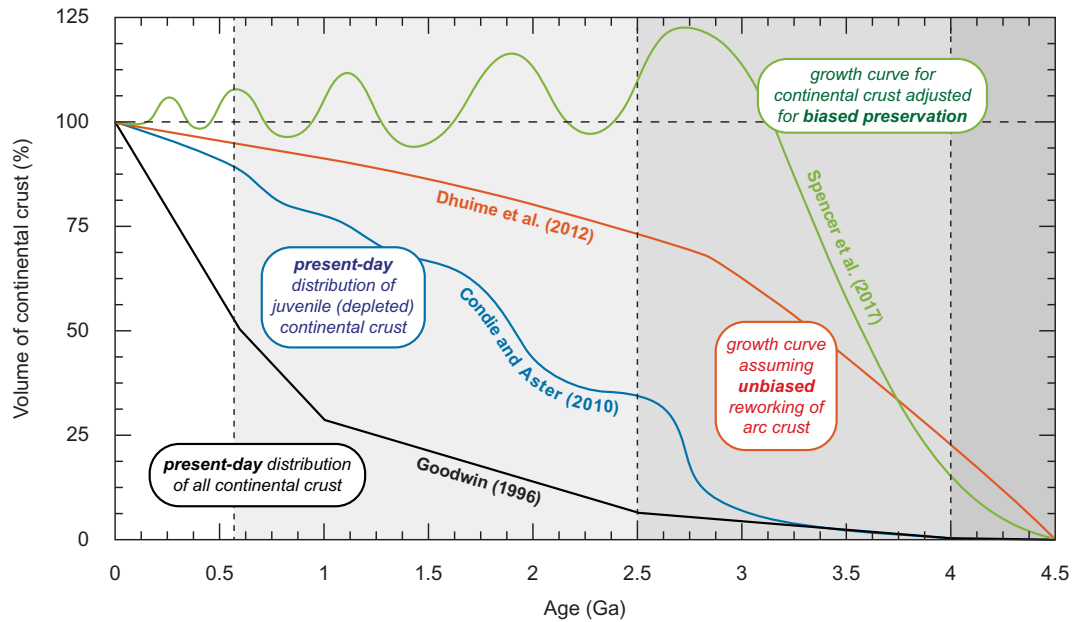
Fig. 6. Example end-member continental growth curves reported in the literature, normalized to the volume of continental crust on Earth today. See main text for discussion.

3.1.1. Blueschists

Blueschists are defined within the metamorphic facies classification system (Eskola, 1920; Fyfe, 1958) as high-*P*/low-*T* metabasic rocks that are dominated by the Na-rich clinoamphibole, glaucophane (Bailey, 1961; Ernst, 1963). Such glaucophane-rich assemblages stabilize along geothermal gradients of ~150–350 °C/GPa and to a maximum temperature of ~500–550 °C (Fig. 7; Maruyama et al., 1996; Clarke et al., 2006; Palin and White, 2016); thus, they characterize the shallow levels of subduction zones. However, while sediments or felsic igneous rocks

may be subducted and metamorphosed at blueschist-facies *P–T* conditions, the mineral assemblages that form are not necessarily diagnostic of such low geotherms (Evans, 1990), meaning that a distinct focus has been placed on the occurrence of metamafic blueschists sensu stricto in the rock record as evidence (or not) for the operation of subduction through geological time. The common association of exotic blocks of serpentinized peridotite within tectonic mélange (Ernst, 2003; Festa et al., 2010; Weller et al., 2015b; Balestro et al., 2018; Wakabayashi, 2019) supports the interpretation that they form during oceanic slab
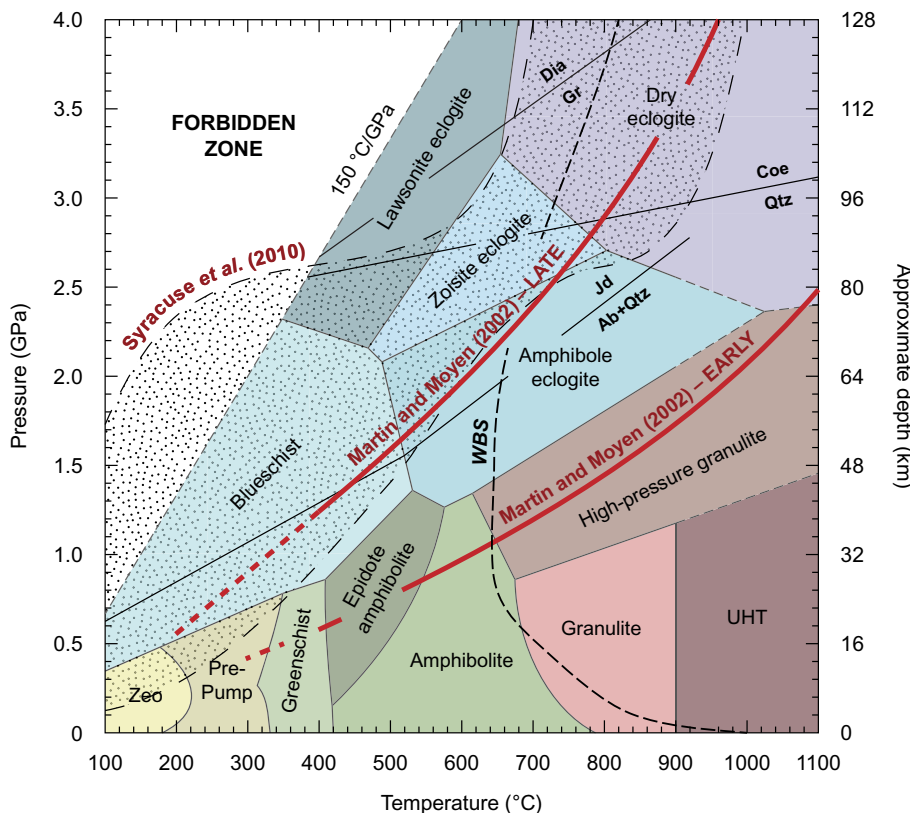

Fig. 7. Classical metamorphic facies diagram (modified after Maruyama et al., 1996 and Palin and Dyck, 2018) superimposed with oceanic slab-top pressure–temperature (*P–T*) paths representative of modern-day (Syracuse et al., 2010) and interpreted Archean examples (Martin and Moyen, 2002). Zeo – zeolite; UHT – ultrahigh temperature; WBS – wet basalt solidus; Jd – jadeite; Ab – albite; Qtz – quartz; Coe – coesite; Dia – diamond; Gr – graphite.

subduction and so their presence can be viewed as sufficient, but not necessary evidence of subduction/mobile lid tectonics having operated at the time of terrane formation. However, many blueschist-absent mélanges may still represent examples of ancient stages of subduction, such as a Neoarchean mélange (c. 2.5 Ga) from the North China Craton that hosts serpentinite exotic blocks (Peng et al., 2020). Such occurrences are described in more detail in Section 3.2.1.

The oldest blueschists on Earth are Neoproterozoic in age (c. 0.8 Ga; Maruyama et al., 1996) and their striking absence from the geological record before this time has been attributed to a wide range of factors (cf. Korenaga, 2016). Some workers have argued that their appearance marks the onset of global subduction at c. 0.8–0.9 Ga (e.g. Stern, 2005), although this interpretation is not widely accepted (cf. Ernst, 2017b). In a scenario where plate tectonics/subduction had begun to operate on Earth before the Neoproterozoic, which is agreed upon by the majority of the geological community (Fig. 1), the lack of older blueschists may alternatively by attributed to preservation bias (Möller et al., 1995; Keller and Schoene, 2018) or that a hotter Archean mantle could have increased subduction zone geotherms outside of those required to stabilize glaucophane (Bjørnerud and Austrheim, 2004). Alternatively, there may have been a compositional control on blueschist formation in the Archean and Proterozoic, whereby high-MgO basalts typical of Precambrian oceanic crust (Takahashi and Brearley, 1990; Klein et al., 2017; Weller et al., 2019) would not have been able to stabilize sodic amphibole (Palin and White, 2016; Palin and Dyck, 2018), even if metamorphosed to blueschist-facies *P–T* conditions. All three factors likely contribute independently to this anomaly in the rock record, although additional research is needed to determine the relative importance of each. These ideas are revisited in more detail in Section 4.3.

3.1.2. Jadeitites and lawsonite-bearing rocks

Jadeite is a sodic clinopyroxene of composition $NaAlSi_2O_6$ that is stable in meta-igneous rocks of mafic and intermediate composition at high-*P*/low-*T* conditions (Robertson et al., 1957; Birch and LeComte, 1960; Newton and Kennedy, 1968) characteristic of the blueschist and eclogite facies. As such, lithologies comprised of > 90% jadeite (jadeitite) have long been recognized as diagnostic indicators of subduction (cf. Harlow et al., 2015). To date, however, only 19 jadeitite localities are known worldwide; all of which occur in five Phanerozoic orogenic belts (Caribbean, circum-Pacific, Alps/Himalayas, Uralides, and Central Asia/Altaids). The oldest jadeitites formed at c. 470–440 *Ma* (Oya-Wakasa, Japan; Nishimura and Shibata, 1989).

Akin to blueschists, all jadeitite occurrences are found in close spatial association with serpentinite-matrix mélanges and/or rocks with other high-pressure/low-temperature parageneses (Harlow et al., 2014). Experimental petrology, petrography, and phase equilibrium modeling suggest that jadeitites form either as direct precipitates from hydrous fluid released from a subducted slab into the overlying mantle wedge, or as a metasomatic replacement of oceanic plagiogranite, graywacke, or metabasite along the channel margin (cf. Harlow et al., 2015 and references therein). The subsequent exposure of jadeitites requires a late-stage Wilson Cycle compressional event that exhumes the subduction channel boundary as a serpentinite mélange (Tsujimori and Harlow, 2012). Due to their rarity even in modern-day convergent plate margin settings, jadeitites should be considered sufficient – but not necessary – evidence of subduction.

Lawsonite is a hydrous sorosilicate with a composition of $CaAl_2Si_2O_7(OH)_2H_2O$ that is stable at low geothermal gradients (d*T*/d*P* < 350 °C/GPa; Tsujimori and Ernst, 2014; Palin and White, 2016), and is thought to be a significant reservoir of structurally bound H_2O content (11–12 wt%) in subducted metabasalt. Lawsonite is stable up to ~10 GPa and may so carry H_2O and other trace elements (REE, *Sr*, Th, and U) into the mantle more effectively than other hydrous phases, such as amphibole, epidote, and chlorite (Pawley, 1994; Schmidt and Poli, 1998; Spandler et al., 2003; Usui et al., 2007; Martin et al., 2014).

Lawsonite-bearing lithologies often occur in close spatial association

with serpentinite-matrix mélanges and/or rocks with other high-*P*/low-*T* parageneses, even in UHP terranes (Tsujimori et al., 2006; Tsujimori and Ernst, 2014). Rare lawsonite eclogites occur as xenoliths in rhyolitic tephras and in diatremes of serpentinized ultramafic microbreccia (Hoffman and Keller, 1979; Usui et al., 2003; Hernández-Uribe and Palin, 2019b), indicating the operation of subduction and transport of slab-top fragments back to the Earth's surface via volcanism. Lawsonite blueschist is relatively more common than lawsonite eclogite (Tsujimori and Ernst, 2014), probably due to its lower density, which promotes exhumation prior to its transition to lawsonite-eclogite subfacies assemblages (Hernández and Palin, 2019a). The oldest known lawsonite blueschist formed at c. 560–550 *Ma* (Anglesey, Wales; Kawai et al., 2007), whereas as the oldest known lawsonite eclogite formed at c. 490–450 *Ma* (North Qilian orogen, China; Song et al., 2004).

Lawsonite stability is favored in Ca-rich rocks such as metabasites (e.g. basalts and gabbros) and is relatively rare in rocks with a metasedimentary protoliths (Evans and Brown, 1986; Poli and Schmidt, 2002). As such, lawsonite-bearing rocks are considered indicators of subduction of mafic oceanic crust (Stern, 2005; Tsujimori et al., 2006). While experimental petrology and phase equilibrium modeling suggest that lawsonite-bearing rocks should be common in the rock record (Schmidt and Poli, 1998; Clarke et al., 2006), natural samples are relatively rare (Tsujimori and Ernst, 2014). Existing explanations for theuncommon occurrences of lawsonite-bearing lithologies – the so-called the lawsonite paradox – rely on the exceptional conditions (i.e. a high amount of free water at high pressure) thought necessary to form and preserve lawsonite during exhumation (Zack et al., 2004; Clarke et al., 2006; Whitney and Davis, 2006; Tsujimori et al., 2006; Wei and Clarke, 2011). However, recent study has shown that typical subduction zone geotherms do not promote lawsonite stability, which should only stabilize in particularly cold examples (Penniston-Dorland et al., 2015), thus accounting for the limited occurrence of these rocks in the geological record.

3.1.3. Ultrahigh-pressure (UHP) metamorphism

Ultrahigh-pressure (UHP) metamorphism is defined by achieving *P–T* conditions sufficient to transform quartz to coesite (~26–28 kbar at ~500–900 °C; Fig. 7) (Hacker, 2006). The oldest such coesite-bearing rocks that have been reliably dated belong to the Pan-African belt in northern Mali, and formed at 620 *Ma* (Jahn et al., 2001). Conventionally, UHP metamorphism has been viewed as a diagnostic indicator of deep subduction, owing to depths of > 100 km within the Earth being required to achieve such pressures under lithostatic conditions (Li et al., 2010). Thus, the absence of coesite-bearing UHP rocks from the geological record prior to 620 *Ma* has also been used by some workers to argue for the non-operation of subduction (e.g. Stern, 2005). There are, however, two fundamental problems with this viewpoint. First, several geodynamical studies performed in recent years have shown that pressure within the Earth's crust and upper mantle may deviate significantly from purely lithostatic values; an effect known as tectonic overpressure (e.g. Petrini and Podladchikov, 2000; Li et al., 2010; Schmalholz and Podladchikov, 2013; Gerya, 2015). Reuber et al. (2016) demonstrated that coesite-forming *P–T* conditions may be achieved at depths as shallow as ~40 km in deforming continental crust where there are strong rheological/lithological contrasts, such as mafic intrusions into felsic host rock. This implies – in theory – that UHP conditions may be achieved by crustal materials in the absence of subduction. Nonetheless, even in subducted oceanic lithosphere, tectonic overpressure may reach values up to 0.5 GPa at relatively shallow depths (< 50 km; So and Yuen, 2015; Palin et al., 2017), casting doubt on the reliability of the HP–UHP quartz–coesite transition as a necessary criterion for steep subduction. As a result, uniformitarianistic arguments for a late onset of plate tectonics based on the absence of coesite-bearing UHP rocks in the geological record before this time are weakened.

Second, the somewhat arbitrary choice of the quartz–coesite

transition as representing a diagnostic indicator of modern-day style plate tectonics is countered by high-pressure eclogite-facies rocks preserved in Phanerozoic orogens that record peak metamorphic pressures just below the HP–UHP transition, but which undoubtedly formed during steep subduction (e.g. Erzgebirge, Czech Republic, Klápová et al., 1998; Tso Morari, northwest Himalaya, St-Onge et al., 2013). Within the past ten years, deeply subducted mafic eclogites have been discovered within Meso-Archean rocks of the Kola Peninsula, Russia, which equilibrated at *P–T* conditions of ~16 kbar and ~750 °C at c. 2.87 *Ga* (Mints et al., 2010), the Fennoscandian Shield, which equilibrated at ~24 kbar and ~700 °C at c. 2.82–2.72 *Ga* (Dokukina et al., 2014), the Paleoproterozoic Congo Craton, Democratic Republic of the Congo, which equilibrated at ~23 kbar and 550 °C at c. 2.10 *Ga* (François et al., 2018), the Paleoproterozoic Nagssugtoqidian Orogen, south-east Greenland, which equilibrated at ~19 kbar and ~810 °C at c. 1.89 *Ga* (Müller et al., 2018a, 2018b), and the Mesoproterozoic Trans-Hudson orogen, Canada, which reached *P–T* conditions of ~26 kbar and ~700 °C at c. 1.8 *Ga* (Weller and St-Onge, 2017). All of these new discoveries are of critical significance for interpretation of the metamorphic rock record and strongly argue that subduction was operational on Earth – at least locally in these regions – by the Archean–Proterozoic transition. Other tectonic evidence can be invoked to support or deny claims that these subduction events were connected by a global plate boundary network, as discussed in Section 5.3.

3.1.4. Ophiolites

Ophiolites are complete or partial sections through the oceanic lithosphere that have been tectonically emplaced (obducted) onto a continental margin (Miyashiro, 1975; Dewey, 1976; Moores, 1982). Most known examples on Earth today were emplaced either from downgoing oceanic lithosphere via subduction-accretion or from the upper plate in a subduction zone through trench–continent collision (Dilek and Furnes, 2014). Excluding those formed via emplacement beneath a hyper-extended margin, such ophioites are typically diagnostic indicators of sea-floor spreading and subsequent ocean–continent plate margin convergence (i.e. subduction) (Stern et al., 2012). The identification of ophiolites in the geological record has been a highly contentious field of research in recent years. Akin to blueschists, jadeites, and UHP rocks, their presence in a metamorphic terrane would be viewed as very strong evidence for the operation of subduction, as no numerical simulations have been able to replicate their emplacement in intraplate tectonic environments (Agard et al., 2014; Edwards et al., 2015; Duretz et al., 2016). Different types of ophiolitic fragments also occur within mélange and so also record convergent plate boundary processes associated with the evolution of both active and passive margins (e.g. Festa et al., 2010). Several such cases are documented from Neoproterozoic (c. 0.6 *Ga*: Hajná et al., 2019) to Paleoproterozoic (c. 1.9 *Ga*: Liu and Zhang, 2019) and Neoarchean (c. 2.5 *Ga*: Peng et al., 2020) terranes.

Complete ophiolites (cf. Section 2.1) containing pelagic sediments, pillow basalts, sheeted dikes, gabbros, and tectonized ultramafic rocks (dunite, harzburgite, and lherzolite) are rare on Earth today, and many workers have instead searched for fragmented/partial sections as evidence for the past operation of plate tectonics. Ideally, several disparate components should be preserved in a single orogenic belt if oceanic lithosphere was episodically obducted or incorporated into accretionary prisms along active plate margins (Condie and Kröner, 2008). The oldest undisputed ophiolites on Earth are the Purtuniq ophiolite, Cape Smith belt, Trans-Hudson orogen, Canada (c. 2.0 *Ga*; Scott et al., 1992), the Jormua ophiolite, Finland (c. 1.95 *Ga*; Peltonen et al., 1996), and the Payson ophiolite, Arizona, USA (c. 1.73 *Ga*; Dann, 1997). More contentious examples include the Dongwanzi greenstone belt, North China Craton, which has been proposed by Kusky et al. (2001) to contain obducted fragments of Archean oceanic crust (c. 2.5 *Ga*), although this interpretation has been strongly contested (Zhai et al., 2002; Zhao et al., 2007). Sheeted dikes and associated pillow basalts in the Isua supracrustal sequence (c. 3.8 *Ga*), Greenland, have also been interpreted to represent fragments of a Paleoarchean ophiolite complex (Furnes et al., 2009; Friend and Nutman, 2010), although again this interpretation is not universally accepted (e.g. Hamilton, 2007). This issue is revisited in Section 5.1.

3.1.5. Andesites and arc/back-arc assemblages

The petrology and geochemistry of volcanic rocks found today in arc complexes have long been used to infer the likelihood of similar subduction-zone processes having operated in the Archean (e.g. Barley et al., 2006; Polat, 2012). In particular, calc-alkaline andesites, which are ubiquitous in Phanerozoic accretionary and collisional orogens, also occur throughout the geological record. Neoarchean (c. 2.7 *Ga*) andesites from the East Yilgarn craton, Western Australia, have a similar petrology and incompatible trace-element signature to those of modern island-arc examples, although their higher Ni and MgO contents have been interpreted by some workers to record formation above a mantle plume (Barnes and van Kranendonk, 2014). While not all Archean greenstone belts may preserve convergent-margin arc/back-arc assemblages, there are many examples documented in sequences as old as the Early Archean (see below).

Archean greenstones have been divided into two major types by some workers based on their overall petrological composition: "mafic-type" sequences that consist chiefly of pillow basalt and komatiite, and "arc-type" sequences that additionally contain calc-alkaline volcanics and related sediments (Thurston and Chivers, 1990; Condie, 1994; Condie and Benn, 2006). Arc-type andesite-bearing successions are widespread in the Superior, Slave, Yilgarn, and Eastern and Southern Africa Archean cratons (e.g. Boily and Dion, 2002). These andesitic members are often accompanied by graywacke and various volcaniclastic rocks that are commonly deposited in an arc system. Field mapping and sedimentologic studies of arc-type greenstone sequences in the Raquette Lake Formation, Slave Province, indicate the presence of high-energy clastic sedimentary facies that were deposited contemporaneously with ignimbrite (Mueller and Corcoran, 2001), resembling volcaniclastic strata that occur along modern-day continental-margin arcs, such as Japan. Boninite, shoshonite, and high-Mg andesite have also been reported from several Archean greenstones belts that formed at 3.4 *Ga* (Parman et al., 2001; Smithies et al., 2004). Such successions argue strongly for the operation of subduction and arc volcanism by at least this time in Earth history, although they alone cannot confirm the existence of a global network of plate boundaries (cf. Section 5.3).

3.2. Tectonic evidence

Tectonic evidence for the operation of subduction-driven plate motion focuses on large-scale morphological features that require dominantly horizontal tectonic forces, or else those that infer independent plate motion or rotation.

3.2.1. Accretionary and non-accretionary subduction complexes

Accretionary prisms are the hallmarks of oceanward growth of continental margins – an important continent-building process associated with horizontal plate motion and convergence. Importantly, accretionary prims also illustrate the process of downward younging of the accreted sediments. An evaluation of the accretionary prisms in Japan shows that individual units become more voluminous as they get younger, which implies that part or all of the older units were tectonically eroded and dragged down into the mantle (Isozaki et al., 2010). This process is driven by sediment subduction at convergent margins with modern examples along the Japanese and Chilean trenches, where older fore-arc crust has been eroded from the bottom (Yamamoto et al., 2009, and references therein). Isozaki et al. (2010) also illustrated that accretionary growth during the past ca. 500 million years of subduction history in Japan was not a continuous process, but alternated with

subduction erosion. Tectonic erosion along convergent margins by down-going oceanic plate includes diverse processes of arc subduction and sediment subduction as well as erosion of the hydrated mantle wedge (Yamamoto et al., 2009). Thus, accretionary prisms also mark the sites of continental convergence and destruction.

A typical feature of accretionary prisms is the occurrence of diverse types of mélange: complex geological units carrying chaotic rock assemblages that often display block-in-matrix fabric (Festa et al., 2010). Recent classification of mélanges suggests a close relationship between processes and mechanisms of their formation with diagnostic features of tectonic, sedimentary and diapiric origin (Festa et al., 2019). Among these, sedimentary mélanges are diagnostic of subduction processes (i.e. accretionary and non-accretionary) along convergent margins, and are characterized by the dominant association of basalt and limestone clasts within a mudstone matrix, often considered to have been derived from ancient seamounts (Wakita, 2019). The paucity of accretionary prisms in the rock record prior to c. 0.9 *Ga* has been used as evidence against the existence of Proterozoic and Archean subduction (Hamilton, 1998), although several mélange-like terranes have been identified in Archean terranes and have been interpreted as accretionary prisms (Komiya et al., 1999; Kitajima et al., 2001; Peng et al., 2020). For example, the Schreiber-Hemlo greenstone belt (2.75–2.70 *Ga*) in the Superior Province of Canada was described by Polat and Kerrich (1999) and Yang et al. (2019) to contain a tectonic (accretionary) mélange, as have other Meso- to Late-Archean deformed sedimentary-volcanic sequences, including the Abitibi greenstone belt, Quebec (Mueller et al., 1996), and the Tokwe terrane, Zimbabwe (Kusky, 1998). Though controversial, some researchers suggest that the Isua supracrustal sequence, which formed at c. 3.8 *Ga*, is an Eoarchean example (Shervais, 2006), thus suggesting that subduction was operating very early in Earth history (Turner et al., 2014), although this may represent an example of localized plume-induced subduction initiation instead (Section 5.3).

3.2.2. Paired metamorphic belts

Parallel linear metamorphic belts showing contrasting metamorphic mineral assemblages of low-temperature/high-pressure (LT/HP) and high-temperature/low-pressure (HT/LP) assemblages are referred to as paired metamorphic belts, and were first described from the active convergent margin of SW Japan (Miyashiro, 1961). Paired metamorphic belts are defined as penecontemporaneous belts of contrasting type of metamorphism that record different apparent thermal gradients – one warmer and the other colder – which are juxtaposed through tectonic processes. A typical example is the Ryoke and Sambagawa metamorphic belts in SW Japan that were superposed through shortening induced by forearc contraction during opening of the Japan sea (Isozaki et al., 2010).

Paired high-pressure (HP) and high-temperature (HT) metamorphic belts can also form through tectonic erosion along convergent plate margins (Santosh and Kusky, 2010). Substantial erosion of the accretionary wedge and sediment subduction such as in the case of Central American trench, Alaskan forearc, and SW Pacific provide examples for flux of hydrous material into the deep mantle (Yamamoto et al., 2009; Santosh, 2010). The subducted material undergoes HP metamorphism, whereas in the adjacent arc, mafic magmas underplated at the base of the crust cause HT metamorphism, generating paired metamorphic belts. Paired HP and ultra-high temperature (UHT) metamorphic belts have also been described from Precambrian terranes, such as those along the Palghat-Cauvery Suture Zone in southern India, considered as the Cambrian Gondwana collisional suture (Santosh et al., 2009). A wide accretionary belt with typical features of ocean plate stratigraphy (Wahrhaftig, 1984; Kusky et al., 2013) developed in this region, associated with subduction of the Mozambique ocean during the Neoproterozoic, and is characterized by granitoids at the higher crustal level, and HP–UHT paired sequences together with mafic-ultramafic rocks at the lower level. Santosh and Kusky (2010) proposed a ridge subduction

and slab-window model with asthenospheric upwelling to explain such paired HP–UHT metamorphic belts. Paired metamorphic belts thus provide evidence for subduction, tectonic erosion, crustal shortening and exhumation along convergent plate boundaries, and this duality of thermal regimes can be traced back through the geological record as far as c. 3.3 *Ga* (e.g. Li et al., 2020).

3.2.3. Collisional and accretionary orogens

The convergence of tectonic plates, forcing closure of intervening oceans, and final collisional amalgamation of continental blocks to build major orogenic belts on Earth can be classified into two endmember types: collisional and accretionary orogens (also known as Pacific-type and Himalayan-type, respectively; Maruyama et al., 1996; Cawood et al., 2009; Santosh et al., 2009). Accretionary-type orogens are composed of accretionary complexes carrying MORB, seamounts, ocean island basalt (OIB), carbonates, and deep-sea sediments that belong to the oceanic plate, and medium- to high-grade metamorphic rocks and subduction-related batholiths belonging to the continental arc. A fore-arc basin often occurs in between. Collisional-type orogens are characterized by passive continental-margin sequences, with an orogenic core of regional metamorphic rocks. A collisional suture with remnants of oceanic components marks the zone of ocean closure. Cawood et al. (2009) further subdivided accretionary orogens into retreating and advancing types. Advancing orogens, such as the Andes, have a foreland fold and thrust belt and crustal thickening, whereas retreating orogens, such as those that occur in the modern western Pacific, are characterized by a back-arc basin. Accretionary orogens are major sites of both crust formation through lateral growth as well as destruction through tectonic erosion caused by the downgoing oceanic lithosphere (Scholl and von Huene, 2010). One of the best examples of accretionary orogenesis is the Central Asian Orogenic Belt (CAOB), considered as the world's largest Phanerozoic accretionary orogen, where multiple subduction-accretion-collision events have been recorded (Xiao et al., 2015).

Accretionary orogens along modern convergent margins often preserve an original ocean plate stratigraphy (OPS) that can be used to reconstruct the history of the oceanic plate from its birth at a MOR to its demise at the trench. An OPS comprises a composite stratigraphic succession of the ocean floor which is incorporated in the accretionary complex (Matsuda and Isozaki, 1991; Santosh, 2010), and thus includes MORB, chert, OIB and trench sediment (Isozaki et al., 2010). Remnants of OPS can also be traced in Precambrian suture zones along which ocean closure and continent assembly occurred (Santosh et al., 2009). Safonova and Santosh (2014) described examples of typical OPS sequences from Central and East Asia (including Russia, Kazakhstan, Kyrgyzstan, Tajikistan, Mongolia, and China) and the Western Pacific (China, Japan, Russia) where fragments of oceanic island basalts (OIBs) and ophiolite units occur within the accreted sequences. Petrological and geochemical data on these rocks indicate extensive plume-related magmatism in the Paleo-Asian and Paleo-Pacific Oceans. The OIB-bearing OPS units in CAOB and Western Pacific were correlated to two superplumes: the late Neoproterozoic Asian and the Cretaceous Pacific plumes. The accreted seamounts also play an important role in the outward growth of continental margins by enhancing the accumulation of fore-arc sediments (Safonova and Santosh, 2014).

It has long been believed that subduction-accretion complexes such as those along the Western Pacific margin are major sites of juvenile crustal growth. However, based on an extensive dataset of Sr−Nd isotope of Cretaceous, Miocene and Quaternary granitoids from SW Japan, Jahn (2010) showed that the magmas from which these rocks formed incorporated a substantial volume of recycled ancient continental crust. Independently, Kröner et al. (2014) showed that the crustal evolution of the CAOB, regarded as the hallmark of juvenile crustal growth, preserves evidence for abundant reworking of older crust of varying proportions throughout its accretionary history. Thus, modern accretionary orogens may not be entirely composed of juvenile components, but may

incorporate variable amounts of recycled older crustal components (e.g. Spencer et al., 2017). As such, both ancient and modern collisional and accretionary orogens are markers of convergent tectonics, with OPS accreted on to continents representing firm evidence for the horizontal movement of oceanic lithosphere from ridge to trench.

3.2.4. Supercontinent assembly

Supercontinents are large landmasses that form a closely packed assembly through the convergence of multiple continental fragments carrying ancient cratons, together with accreted terranes (Rogers and Santosh, 2004). Although some supercontinents such as Ur (3.0 *Ga*) and Kenorland (2.7–2.5 *Ga*) have been proposed to have existed on the Archean Earth, the first coherent supercontinent is thought to have assembled at c. 2.0–1.8 *Ga*, termed Columbia/Nuna (Hoffman, 1997; Rogers and Santosh, 2002; Meert and Santosh, 2017). Following this, several other younger supercontinents have been documented, including Rodinia (1.2–1.1 *Ga*), Gondwana (0.54 *Ga*) and Pangaea (0.30–0.25 *Ga*) (Fig. 1: Rogers and Santosh, 2004; Nance et al., 2014). The episodic assembly, evolution and dispersion of supercontinents exert a major impact on growth and destruction of continental crust and its resources, mantle dynamics, surface processes and evolution of life (Santosh, 2010; Stern et al., 2018). Diverse models have been proposed for the assembly and breakup of supercontinents (see Nance et al., 2014, for a comprehensive review), among which double-sided subduction (Maruyama et al., 2007) or multiple subduction (Santosh et al., 2009) are postulated to be key factors that promote the rapid assembly of continental fragments into supercontinents. In the case of multiple subduction, a Y-shaped convergent triple junction would accelerate plate refrigeration and thus promote stronger downwelling compared to other regions of the mantle, termed super-downwelling (Santosh et al., 2009). This process would pull together dispersed continental fragments into a close-packed assembly. Indeed, Maruyama et al. (2007) considered the Western Pacific region as the frontier of a future supercontinent termed "Amasia" to be assembled within the next 250 Myr.

The voluminous subducted materials during ocean closure associated with supercontinent assembly temporarily accumulate in the mantle transition zone at 410–660 km depth (Fig. 2), from where they sink to the core–mantle boundary and accumulate as 'slab graveyards' (Fig. 2: Maruyama et al., 2007). Melting of the slab graveyards through heating from the core provides a potential trigger for the formation of superplumes, which ascend from the core–mantle boundary, eventually diverging into hot spots (Condie, 2001) and rifting the supercontinent. Plumes rising from the core–mantle boundary facilitate heat and mass transport between different layers of the Earth (Maruyama et al., 2007). The insulation of mantle heat radiation by large supercontinents on the surface also triggers the break-up of supercontinent assembly. The role of mantle plumes associated with the break-up of supercontinents is marked by large igneous provinces (LIPs) and giant dike swarms. Major LIPs and regional magmatic events have been well documented to have driven the disruption of the Proterozoic supercontinents Columbia and Rodinia (Ernst et al., 2008).

One important implication of the supercontinent cycle is the impact on the rate and mechanisms of crustal growth and destruction (Nance et al., 2014). Condie (2004) proposed a correlation between the increased rate of production of juvenile crust and the formation of supercontinents. The spikes in zircon age spectra of orogenic granitoids were correlated with continental growth and supercontinent formation (Condie and Aster, 2010). Based on magmatic zircon grains in detrital populations of river sands, Rino et al. (2008) suggested continuous growth of continental crust since the Archean with an abrupt increase during the Late Archean and Early Proterozoic, and significant contribution during the Neoproterozoic. Hawkesworth et al. (2010) noted that although the peaks in crystallization ages might mark the times of supercontinent assembly, these may also correspond to an increased preservation potential for magmas rather than enhanced crust

generation. However, Roberts (2012) proposed a contrasting model based on $\varepsilon_{Hf}(t)$-time space of global zircon database which envisages increased continental loss during supercontinent amalgamation. Recent evaluations indicate that the preserved crustal record on our planet is the balance between the volume of crust generated by magmatic processes and the volume destroyed through return to the mantle by tectonic erosion and lower crustal delamination (Spencer et al., 2017). Other workers suggest that the preserved volume of Archean TTG on Earth today is far far less than that predicted by geodynamic models, and that much of the TTG record has been recycled back into the mantle via subduction (Kawai et al., 2013). However, due to various limitations of the data base and analytical techniques, the estimates of preserved continental crust and growth curves represent only a minimum of total crustal growth. Thus, the episodic assembly and disruption of supercontinents likely began during the Mesoarchean (c. 3 *Ga*) and provides evidence for large-scale horizontal plate motion, facilitated by subduction-driven tectonic processes, although uncertainty remains regarding whether these amalgamations can prove the existence of a global network of plate boundaries.

3.2.5. Paleomagnetism

Investigations of Precambrian plate tectonics from a paleomagnetic perspective are based on comparisons of apparent polar wander paths (APWPs) from Archean cratons (e.g. Buchan, 2013). Early paleomagnetic studies were hindered by the difficulties of finding suitable stratigraphic sections (i.e. horizontal, undeformed, and not remagnetized), disagreements between paleomagnetic constraints and bedrock geology, and large uncertainties associated with geochronological constraints (e.g. Dewey and Spall, 1975; Irving and Lapointe, 1975; Mitchell et al., 2014). More recently, advances in isotope geochronology and paleomagnetic analyses, including improved statistical approaches and best practices for identifying primary magnetism (e.g. Van der Voo, 1990; Buchan, 2013), have led to a robust demonstration of relative motions between cratons since c. 1.7 *Ga* during formation and break-up of the Columbia and Rodinia supercontinents (e.g. Li et al., 2008; Buchan, 2013; Pisarevsky et al., 2014; Meert and Santosh, 2017; Merdith et al., 2017). Further back in time still, APWPs from the Slave and Superior cratons record significant divergence between these blocks during 2.2–2.0 *Ga*, followed by their accretion during formation of the Nuna continent (the core of the Columbia supercontinent) by c. 1.8 *Ga* (Evans and Halls, 2010; Mitchell et al., 2014; Buchan et al., 2016). Similarly, paleomagnetic data from Laurentian and Baltican Archean cratons, which formed the other constituent parts of Nuna, record relative lateral motions between c. 2.1 *Ga* and c. 1.7 *Ga* (Lubnina et al., 2017; Meert and Santosh, 2017). Most recently, it has been argued that paleomagnetic data record ~5000 km lateral displacement between the Superior and Kaapvaal cratons between c. 2.7 and c. 2.4 *Ga* (Cawood et al., 2018). Based on the above works, it can be argued that paleomagnetic studies robustly demonstrate the activity of plate tectonics on Earth since c. 1.7 *Ga* (Buchan, 2013; Pisarevsky et al., 2014) and provide a strong argument for its occurrence at c. 2.2 to 2.0 *Ga* (Mitchell et al., 2014, Buchan et al., 2016), and possibly as far back as c. 2.7 *Ga* (Cawood et al., 2018).

3.3. Geochemical and isotopic evidence

3.3.1. Geochemical constraints on geodynamic environments

Geochemical and isotopic data are used extensively to determine the tectonic environments and mechanisms of formation of Phanerozoic rocks, particularly mafic lavas (Winchester and Floyd, 1976; Pearce, 1996, 2008). Different geochemical reservoirs within the mantle allow discrimination between basalts generated in divergent plate-boundary settings (MORs) from those that form above subduction zones in island arcs (Hofmann, 1997; Sepidbar et al., 2019). As such, geochemical fingerprinting has potential to act as a powerful tool for tracking the existence of different geodynamic settings through time by analysis of

the geochemical characteristics of mafic lavas through time (Keller and Schoene, 2018). Nonetheless, there remains great debate concerning whether isotopic and trace element signatures that characterize modern-day or Phanerozoic environments are applicable to the early Earth (Pearce, 2008; Payne et al., 2010; Verma and Verma, 2013; Condie, 2015), and some authors caution use of this technique in its entirety, given notable overlap in fields that define different distinct tectonic settings on Earth today (Wood et al., 1979; Maniar and Piccoli, 1989; Snow, 2006; Vermeesch, 2006; Li et al., 2015).

Using Nb–Th–Zr systematics in young oceanic basalts with well-constrained environments of formation, three mantle source domains can be identified (cf. Condie, 2003): enriched mantle (EM), depleted mantle (DM), and hydrated mantle (HM). While primitive (unmodified) mantle (PM) has its own unique Nb/Th and Zr/Nb ratios, these signatures do not show up in basalt melt fractions unless by chance, given crystal–melt partitioning during the mantle melting process (Blundy and Wood, 2003). DM has high values for each ratio (Nb/Th > 8 and Zr/Nb > 20); EM has high Nb/Th ratios but typically low Zr/Nb ratios (< 20); and HM has very low Nb/Th (< 8) and variable Zr/Nb ratios (Condie, 2015). DM signatures are characteristic of asthenospheric mantle below mid-ocean ridges, but also may appear in mantle wedges above subduction zones (Saunders et al., 1988). EM signatures occur in basalts erupted on oceanic plateaus and islands, as it is thought to occur in mantle plumes that initiate in the middle and lower mantle (Hofmann, 1997; Hofmann and White, 1982; Stracke, 2012). Finally, HM is characteristic of arc/back-arc geodynamic settings where partial melting and basalt petrogenesis takes place within a hydrated mantle wedge (e.g. Kimura and Yoshida, 2006).

A recent application of this technique to a global dataset of mafic lavas and greenstone belt components by Condie (2015) suggests that modern-day tectonic settings cannot be easily identified in rocks older than 2.2 *Ga*, based on EM and DM signatures only becoming widespread at that time. However, other studies have performed similar analyses using different incompatible trace element ratios and suggest that the majority of Archean greenstone belt basalts formed in subduction-related regimes (Furnes et al., 2014a). Here, Th/Yb–Nb/Yb and V/Ti ratios suggest that Paleo-, Meso-, and Neoarchean greenstone belts preserve trace element compositions equivalent to modern-day boninites, island arc tholeiites, and MORB (Furnes et al., 2014b). One point of contention in using such geochemical and/or tectonic discrimination diagrams for tracing geodynamic regimes through time is the uncertainty regarding the expected major-, minor-, and trace-element signatures of basalts generated in various types of stagnant lid regime (e.g. Fig. 3). HM signatures, for example, which may be viewed as diagnostic of subduction at oceanic or continental arcs today, may potentially also represent intraplate mantle that has experienced hydration due to dripping or delamination of hydrous lower crust (Bédard et al., 2003; Fischer and Gerya, 2016a, 2016b; Piccolo et al., 2019). Future work specifically focused on the geochemistry of basaltic rocks exposed on Mars and Venus, which almost certainly formed in some form of stagnant lid regime, may provide critical new insight into this problem (cf. Section 7.1; Greenough and Ya'acoby, 2013).

3.3.2. Diamonds and their inclusions

Diamond is a high-pressure polymorph of carbon that stabilizes at minimum pressures of ~3.5–4.5 GPa at ~600–1200 °C, equivalent to at least 150–180 km depth within the Earth's upper mantle (Khaliullin et al., 2011; Day, 2012: Figs. 2 and 7). A rarer variety of "superdeep" diamonds are thought to have originated from > 410 km depth, within the mantle transition zone (e.g. Timmerman et al., 2019). As such, during growth, diamonds can trap minerals, fluids, or melts that are stable at various depths within the Earth's interior. Based on their morphology and internal growth structures, natural diamonds likely crystallize from solutions within the mantle, rather than forming in the solid state (Harte, 2010). The precipitation of diamond from such carbon-bearing fluids or melts is thought to be driven by

reduction–oxidation events (Deines, 1980; Haggerty, 1986; Jacob et al., 2016).

Several important studies have used the composition of diamonds and/or their inclusions to identify transport of crustal materials into the mantle, potentially via subduction. In a landmark paper, Shirey and Richardson (2011) compiled isotopic and bulk chemical data of over 4000 silicate and sulfide inclusions in diamonds with well-constrained ages of formation from five Archean cratons worldwide. Silicate inclusions formed two major groups: p-type (peridotitic), including both harzburgitic and lherzolitic compositions, and e-type (eclogitic) parageneses, characterized by Cr- and Al-rich garnet and Na-, Fe-, and Mg-rich pyroxene. This analysis showed that diamonds older than 3.2 *Ga* contained only p-type inclusion suites, whereas e-type inclusions became dominant after c. 3.0 *Ga*. This mineralogical transition was interpreted by Shirey and Richardson (2011) to record the capture of eclogite and diamond-forming fluids in subcontinental mantle via subduction and continental collision, marking the onset of the Wilson Cycle (i.e. plate tectonics) at around 3.0 *Ga*.

Other studies have used stable isotope compositions of diamonds to infer contamination of the mantle with crustal and other Earth-surface materials. Recently, Archean placer diamonds (c. 3.5–3.1 *Ga*) from the Kaapvaal craton, South Africa, were analyzed by Smart et al. (2016) for both their nitrogen content and nitrogen and carbon isotopic signatures. High concentrations of nitrogen in these diamonds compared to the average upper mantle were interpreted as evidence for localized contamination of the Archean mantle by nitrogen-rich sediments, and carbon isotopic signatures suggested diamond formation by reduction of an oxidized fluid or melt. Both isotopic characteristics were used to argue for the introduction of oxidized sediments and aqueous fluids to the mantle by crustal recycling at subduction zones, thus indicating the operation of plate tectonics no later than c. 3.1 *Ga*. Oxygen and strontium isotopic ratios in Archean diamonds from cratonic mantle eclogite xenoliths in South Africa and Venezuela were reported by MacGregor and Manton (1986) and Schulze et al. (2003) to record seafloor alteration and the transport of metasomatized oceanic crust into the mantle during the Mesoarchean. Smit et al. (2019) compared the mass-independently fractionated sulfur, which refers to $\Delta^{33}S$ ($^{33}S/^{32}S$) and $\Delta^{36}S$ ($^{36}S/^{32}S$) relative to $\Delta^{34}S$ ($^{34}S/^{32}S$), in sulfide inclusions in diamond from Archean to Proterozoic terranes. They showed that the mass-independently fractionated sulfur was not present in sulfides in Paleoarchean diamonds, but was in sulfides in younger diamonds. Because the mass-independent fractionation can be caused by photolysis of sulfur in the atmosphere with UV light, the authors suggested that the mass-independently fractionated sulfur in diamonds younger than c. 3 *Ga* was carried into the mantle by subduction. In addition, negative Eu anomalies in majoritic garnet inclusions in diamond from the Jagersfontein kimberlite, South Africa, and the unusually light carbon isotopic signature of the host grains was interpreted by Tappert et al. (2005) to record recycling of oceanic crust into the mantle, which carried organic carbon-rich sediments with it. Nonetheless, it is important to remember that such lines of evidence do not unequivocally prove the operation of subduction, as various forms of stagnant lid tectonics allow crust–mantle mass exchange (Fig. 3) to different degrees.

3.4. Modeling

Many studies have employed various types of modeling to infer the likelihood of subduction at different times during the Archean, with the most compelling arguments coming from the results of 2-D and 3-D thermo-mechanical modeling at the crustal, lithospheric, and planetary scale (cf. Section 1.2). Petrological and geochemical modeling can also inform about whether lithologies in Archean terranes likely formed in subduction zone or intraplate environments by way of matching predicted major-, minor-, and trace-element signatures with those preserved in the geological record (e.g. Palin et al., 2016b).

3.4.1. Geodynamic modeling

Thermo-mechanical modeling represents a powerful tool with which to examine the likely effects that different physico-chemical parameters impart on crustal or mantle dynamics, although the reliability of the results of such simulations are necessarily dependent on the properties chosen a priori. Geodynamic modeling is particularly useful for constraining the likely effects of secular cooling of the mantle (cf. Section 1.3), which impacts on its viscosity and the rigidity of the lithospheric lid (Rolf et al., 2012). Mantle viscosity also directly controls the wavelength of mantle convection – with increases as mantle T_P decreases – and so feeds back on the mechanism of heat transfer (Bunge et al., 1996). Secular cooling over time is thus expected to promote the transition from short-wavelength drip-and-plume tectonics (Fig. 3) to broader-scale delamination and associated convection cell-style upwellings (Fig. 3), with plate tectonics being associated with wide aspect ratio mantle convection (Grigné et al., 2005).

Geodynamic modeling of stagnant-lid regimes has been instrumental in deciphering the form of tectonics that may have preceded the modern-day mobile-lid regime. Several workers have investigated the thermal stability of thick, mafic primary crust, and suggested that shown that eclogitization of buried lithologies could have promoted dripping and delamination of this dense material into the mantle (Fischer and Gerya, 2016a; Capitanio et al., 2019). Thermo-mechanical investigations of the viability and style of subduction through geological time have provided great insight into the conditions necessary to initiate and sustain plate tectonics on Earth (Section 1.2: Gerya et al., 2008; Van Hunen and Moyen, 2012; Gerya, 2014). Parameterizations employing different oceanic lithospheric thicknesses, crustal compositions, mantle hydration states, and mantle T_P values for Phanerozoic, Proterozoic, and Archean convergent margins suggest that hot, thick, and more mafic Archean oceanic slabs lack the competency to subduct at steep angles without breaking away from the lithosphere at the surface (Moyen and van Hunen, 2012). In some 3-D simulations, this is manifested via a form of "dripping subduction" predicted at mantle T_P values just 50–100 K greater than the present-day (Fischer and Gerya, 2016b), which is characterized by frequent dripping from the slab tip and a loss of coherence of the slab. Slab decomposition in these cases is likely the result of a hotter (weaker) mantle providing less support for the subducting mass and the thicker oceanic crust creating a larger tensile stress between the buoyant crust near the surface and dense eclogite at depth (Moyen and van Hunen, 2012). Simulations of Phanerozoic subduction systems confirm the importance of slab pull in driving plate motion at the surface (Becker and Faccenna, 2009), suggesting that eclogitization and slab fragmentation in the Archean may have been sufficient to allow transient subduction initiation, but long-term stability was not achieved until the subducted lithosphere became stronger during secular cooling.

3.4.2. Petrological modeling

An independent approach to examine the likelihood of plate tectonics/subduction at any point in geological time involves forward and inverse petrological modeling, which can characterize the metamorphic mineral assemblages and partial melts that stabilize at different P–T conditions within the Earth's crust and mantle (Vance and Mahar, 1998; Štípská and Powell, 2005; Palin et al., 2012; Jennings and Holland, 2015; Treloar et al., 2019; Parsons et al., 2020). These predictions may then be compared to lithologies preserved in Archean cratons, as different metamorphic environments are characterized by different geothermal gradients (see Section 4) and contain rocks with different major-, minor-, and trace-element signatures (e.g. Wilson, 2007; Moyen, 2011). Recent advances in the capability of petrological modeling to simulate subsolidus and suprasolidus phase equilibria (Diener et al., 2007; Diener and Powell, 2012; Green et al., 2007, 2016; Holland et al., 2018) in metamorphosed mafic igneous precursors (e.g. MORB, calc-alkaline basalt, picrite) has allowed interplay between high-grade metamorphism and melt generation to be constrained with significantly

greater precision and reliability (Palin et al., 2016a; Marsh and Kelly, 2017; Stuck and Diener, 2018; Cao et al., 2019; Kunz and White, 2019). However, care must be taken to choose appropriate lithologies as potential protoliths, as petrological modeling of Archean basalts of unsuitable geochemistry has in the past lead to spurious results (cf. Corrigendum to Johnson et al., 2017).

Early petrological modeling-based investigations of Archean continental crust petrogenesis (Nagel et al., 2012) examined the compositions of partial melts generated in convergent margin tectonic settings using MORB-like protoliths, although could not effectively examine trace element systematics or consider the effects of open-system melt loss. Following parameterization of a thermodynamic model for TTG-like silicate melt (Green et al., 2016), numerous workers have examined the melt fertility of different Archean mafic lithologies with a view to constraining the geodynamic environment and mechanisms of formation of Earth's first stable continents (e.g. Palin et al., 2016b; White et al., 2017; Zhang et al., 2017; Ge et al., 2018; Wiemer et al., 2018; Kröner et al., 2018). The results of these investigations are discussed in more detail in Section 4.4.

4. Metamorphism in the Archean

Metamorphic mineral assemblages are highly sensitive to changing P–T conditions within the Earth, so can record the degree of heating and cooling of a rock during its burial and exhumation (Anovitz and Essene, 1990; Powell and Holland, 2008; Green, 2018). When combined with isotope geochronology, absolute ages (t) can be assigned to different stages in a thermobarometric evolution (e.g. Hacker and Wang, 1995; Foster and Parrish, 2003; Palin et al., 2014a; Taylor et al., 2016; Lamont et al., 2019), thus producing a P–T–t path that describes the changing nature of geotherms in a particular tectonic setting (England and Richardson, 1977; Harris et al., 2004; Li et al., 2018a). As different geodynamic settings are characterized by different geothermal conditions, careful examination of the mineralogy, microstructures, and geochemistry of metamorphic rocks provides critical insight into the thermal evolution of the Earth's crust throughout time and space (e.g. Burke and Kidd, 1978; England and Thompson, 1984; Bohlen, 1987; Harris et al., 2004; Holder et al., 2018; Huang et al., 2019; Waters, 2019). As a result, the metamorphic rock record is often considered as the first port of call for examining the changing nature of lithospheric tectonics since the Archean–Hadean boundary.

Compilations of apparent peak metamorphic P–T conditions throughout geological time have been used by some authors to define a tripartite classification scheme that can inform about secular changes in geodynamics. In these schemes, high dT/dP types include normal and ultrahigh temperature (UHT) granulites, intermediate dT/dP types typically include high-pressure granulites (HPG) and medium- and high-temperature eclogites, and low dT/dP types include blueschists and low-temperature eclogites. The low-dT/dP limit of metamorphism on Earth is ~150 °C/GPa, with geothermal gradients below this value defining the 'Forbidden Zone' (Fig. 7; Liou et al., 2000). Fig. 8a shows the temporal distribution of such metamorphic data reported by Brown and Johnson et al. (2018), although we adopt a corrected set of dT/dP thermal gradients that more accurately reflect mineralogical transitions between key metamorphic facies (cf. Maruyama et al., 1996), and so better reveal the secular evolution of tectonic regimes. In this expanded dataset, to which we have added additional data published since its compilation, subduction-related blueschists and eclogites are considered together as having low dT/dP apparent peak gradients of 150–440 °C/GPa, HPG have intermediate dT/dP apparent peak gradients of 440–760 °C/GPa, and normal and UHT granulites have high dT/dP apparent peak gradients of 760–1500 °C/GPa (Fig. 8a). This revised 440 °C/GPa gradient for the high-pressure granulite-to-eclogite transition more closely aligns with the plagioclase-out/omphacitic clinopyroxene-in transition in mafic rocks, as constrained via phase equilibrium modeling (De Paoli et al., 2012; Palin et al., 2014b; Weller
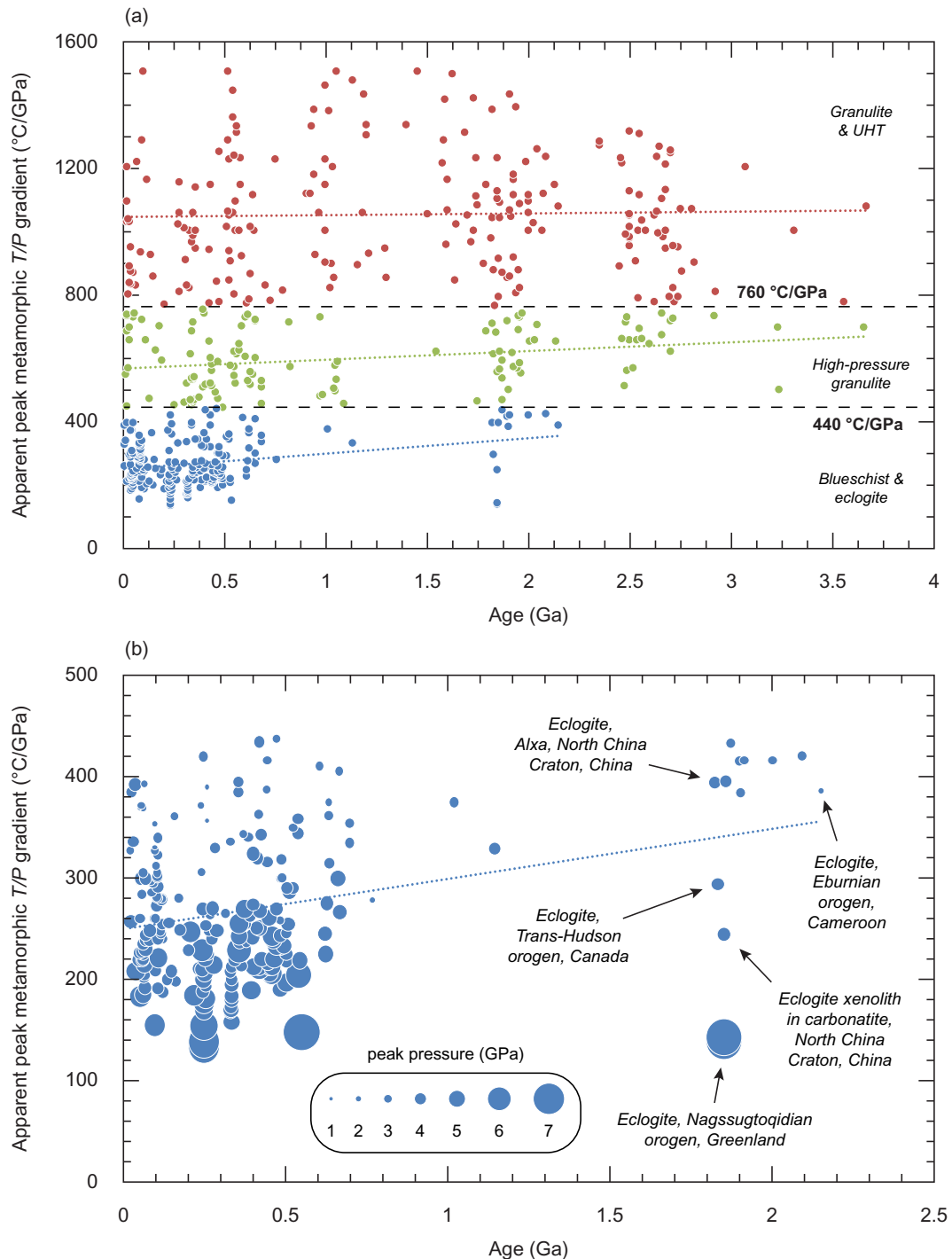
Fig. 8. (a) Reported apparent peak metamorphic temperature/pressure (d*T*/d*P*) gradients through time (data extended from Brown and Johnson, 2018). (b) Data only for low d*T*/d*P* blueschists and eclogites, with circle widths scaled for peak pressure of metamorphism. Dashed lines represent linearized trends through time. Reproduced with permission from the Mineralogical Society of America.

et al., 2015b; Hernández-Uribe et al., 2019) and experimental petrology (Green and Ringwood, 1967; Ito and Kennedy, 1971; Austrheim, 1990). The revised 760 °C/GPa gradient for the high-pressure granulite-to-normal granulite/UHT transition better fits the garnet–orthopyroxene mineralogical transition in mafic rocks, as documented in Pattison (2003), although this reaction is multi-variant in nature, such that both garnet and orthopyroxene may stably exist in mafic graulites worldwide (Brandt et al., 2003; Sajeev et al., 2004). Finally, we discard the small number of data with d*T*/d*P* > 1500 °C/GPa, as these likely formed via contact metamorphism instead of regional-scale tectonic events, and so

detail localized thermal anomalies rather than crustal-scale tectonic phenomena.

4.1. High dT/dP metamorphism

Granulite-facies metamorphism is ubiquitous throughout the rock record (Fig. 8a) and occurs prominently in Archean terranes (e.g. Jahn and Zhang, 1984; Harley, 1989). The elevated heat flow required for granulite-facies *P–T* conditions is thought to be associated with regional-scale magmatism or local concentrations of radiogenic heat-

producing elements (Warren, 1983; Ellis, 1987; Clemens, 1990; Clark et al., 2011). In the former scenario, which is likely the most general case, tectonic environments of granulite formation – at least on Earth today – include island and continental arcs at convergent plate margins, continental rifts, hot spots and at the margins of large, deep-seated batholiths (Bohlen, 1991; Collins, 2002; Santosh et al., 2003, 2012). Granulites are thus interpreted to form the bulk of the lower continental crust (Fig. 5), as supported by geophysical investigations, direct inspection of exhumed terranes, and xenoliths (Rudnick and Fountain, 1995; Gao et al., 2004; Zhang et al., 2020). However, the absolute *P–T* conditions of the prograde amphibolite–granulite transition, defined by the appearance of metamorphic orthopyroxene (Phillips, 1981), are sensitive to fluid content and its composition. A reduction in the activity of H_2O in coexisting metamorphic fluid due to dissolution of CO_2 or salts can expand orthopyroxene-bearing assemblages to relatively low temperatures (Frost and Frost, 1987; Bucher and Grapes, 2011), although such effects are often metasomatic and localized in nature and cannot be responsible for terrane-scale granulite formation (Newton, 1992). The abundance of granulites in Archean cratons is thus likely a result of elevated continental geotherms caused by a higher mantle T_P (Fig. 4) and regional-scale metamorphism due to magma emplacement and crustal thickening.

More extreme thermal regimes in the middle- to lower-crust are recorded in the rock record by UHT granulites. Crustal UHT metamorphism is defined by temperatures exceeding 900 °C at pressures below the sillimanite–kyanite transition (cf. Fig. 7; Harley, 1998; Kelsey, 2008). Diagnostic mineral assemblages of such *P–T* conditions include high-*Al* orthopyroxene + sillimanite + quartz, sapphirine + quartz, and spinel + quartz, alongside metamorphic pigeonite and ternary feldspar (Kelsey and Hand, 2015). By contrast with normal granulites, UHT metamorphism is rare in the Archean, being mostly associated with Proterozoic supercontinent accretion events (e.g. Santosh et al., 2006; Kelsey, 2008; Li et al., 2019), which themselves record evidence of horizontal plate motion.

4.2. Medium dT/dP metamorphism

The HPG metamorphic facies is transitional between true crustal granulites and hot eclogites (Fig. 7), and is bracketed here by geotherms of 440–760 °C/GPa (Fig. 8). Mineralogically, HPGs are characterized by garnet + diopsidic clinopyroxene + plagioclase + quartz in mafic rocks and kyanite + K-feldspar in intermediate and felsic rocks (O'Brien and Rötzler, 2003). Two essential types of HPG occur in the geological record: a high- to ultrahigh-temperature group and a group representing overprinted eclogites (Rudnick and Presper, 1990; Zhao et al., 2001; O'Brien and Rötzler, 2003). The former, which are considered HPG sensu stricto, form due to short-lived tectonic events that generate overthickened continental crust (Carswell and O'Brien, 1993; Liu and Zhong, 1997; Guo et al., 2002), commonly due to accretional or collisional orogeny (e.g. Zhang et al., 2020). The latter group typically has a subduction origin and so although they may contain metamorphic parageneses with *P–T* conditions representative of HPG metamorphism, their precursors provide constraints on the operation of plate tectonic activity through time. Examples of such granulitized MORB-type eclogites have recently been documented from the Paleoproterozoic Kasai Block, Democratic Republic of Congo by François et al. (2018) and record evidence of subduction having operated at 2.2–2.1 *Ga*. Near-complete granulitization of eclogite has been documented from the Himalaya (e.g. O'Brien, 2018), and is kinetically promoted by rehydration during exhumation through the crust (Sartini-Rideout et al., 2009; Palin et al., 2014b; Yardley and Bodnar, 2014). It thus remains a possibility that some Archean HPG localities may represent overprinted hot eclogites, providing further support for the operation of subduction at this time in Earth history, although much or all petrological evidence of their early tectonic evolution has been lost due to tectonic reworking. Instead of continued exploration for preserved eclogites and blueschists

in Archean terranes, which may represent a fool's errand (see below), focused study of these lesser-studied HPG lithologies represents a potentially more fruitful avenue for future breakthroughs.

4.3. Low dT/dP metamorphism

Blueschists and eclogites represent definitive petrological evidence of the operation of plate tectonics at any point in geological time (Section 3.1), as low d*T*/d*P* geothermal gradients are uniquely characteristic of subduction zones (Vidale and Benz, 1992; Peacock, 1996). While the *P–T* conditions experienced by a descending oceanic slab surface vary according to factors including plate convergence rate, dip angle, and slab age (Peacock and Wang, 1999; Syracuse et al., 2010; Penniston-Dorland et al., 2015), all except the very hottest examples pass sequentially through the zeolite, prehnite–pumpellyite, greenschist, blueschist, and eclogite facies (Fig. 7; Hernández-Uribe and Palin, 2019b). Ultrahigh-pressure (UHP) metamorphism is defined in silica-bearing rocks by the stabilization of coesite (Chopin, 1984; Smith, 1984) – a high-pressure polymorph of quartz – which occurs at ~90–100 km depth below the Earth's surface, assuming lithostatic pressure (Liou et al., 2004). However, much study in recent years into the effects of non-lithostatic "overpressure" in crust show that so-called UHP conditions can be reached in overthickened continental roots (Schmalholz and Podladchikov, 2014; Reuber et al., 2016) or at notably shallower depths in subducted oceanic slabs (Audet et al., 2009; Palin et al., 2017). For this reason, discrimination between 'normal' high-pressure eclogite and UHP eclogite as an indicator of deep subduction is becoming widely recognized as misleading for interpreting tectonic regimes on the early Earth.

The temporal distribution of low d*T*/d*P* rocks in the geological record has proven to be one of the most contentious points of debate that exists for interpretation of Archean geodynamics (cf. Stern, 2005; Palin and White, 2016). The oldest blueschists on Earth are Neoproterozoic in age (c. 0.8 *Ga*; Maruyama et al., 1996), and examples occur in almost all Phanerozoic orogenic belts worldwide (Tsujimori and Ernst, 2014). Given multiple independent lines of evidence for plate tectonics having operated since at least the Late Archean (Fig. 1), the absence of pre-0.8 *Ga* blueschists in the rock record has been variably attributed to a lack of preservation (Gibbons and Mann, 1983), a lack of exhumation (Maruyama et al., 1996), elevated subduction zone geotherms prohibiting their formation (Nisbet and Fowler, 1983), and secular change in oceanic crust composition prohibiting formation of diagnostic mineral assemblages (cf. Section 3.1.1: Palin and White, 2016). Each of these factors has merit and it is likely that all contribute in some shape or form, although a very late onset of subduction (Stern, 2005; Hamilton, 2011) is least compatible with most other independent lines of evidence.

4.4. Metamorphism and the generation of tonalite–trondhjemite–granodiorite (TTG) magmas

Magmas and their metamorphosed equivalents (gray gneisses) of TTG composition in Archean terranes represent components of the Earth's earliest-formed continental crust and formed by partial melting of hydrated metabasalt (e.g. Rapp et al., 1991; Wolf and Wyllie, 1994; Rapp and Watson, 1995). Such TTGs have considerable value for identifying the operation (or not) of subduction in the Archean (cf. Fig. 1), as patterns and secular trends in their bulk compositions provide critical petrological information about the mafic parent rock from which they separated and *P–T* conditions of metamorphism, and so the tectonic environment of their formation.

In a pioneering study, Martin and Moyen (2002) divided a global compilation of sodic Archean TTGs into three main groups based on their major- and trace-element geochemistry: (1) those with high Al_2O_3, Na_2O, Sr, and La/Yb, and low Y and Nb/Ta; (2) those with low Al_2O_3, Na_2O, Sr, and La/Yb, and high Y and Nb/Ta; and (3) those with

intermediate compositions between these end members. Such geochemical signatures constrain the minerals present in the metabasite residuum from which the TTG melts separated, with high Sr contents indicating plagioclase-poor assemblages, high La/Yb ratios indicating garnet-rich assemblages, and low Nb/Ta ratios indicating the presence of rutile and amphibole (Fig. 10: Martin and Moyen, 2002; Foley et al., 2002, 2003; Rapp et al., 2003). Experimental investigation and phase equilibrium modeling of the absolute *P–T* stability fields of these minerals (e.g. Rushmer, 1991; Rapp et al., 1991; Rapp and Watson, 1995; Foley et al., 2003; Zhang et al., 2013; Palin et al., 2016a, 2016b) has led some workers to refer to TTG types 1–3, above, as "high-pressure", "low-pressure", and "medium-pressure", respectively (Moyen and Stevens, 2006; Moyen, 2011; Moyen and Martin, 2012; Laurie and Stevens, 2012; Rozel et al., 2017; Rajesh et al., 2018). Such classifications have inherent geodynamic implications, as "high-pressure" TTGs requires separation from an eclogite-like source rock (Rapp et al., 1991, 2003), "medium-pressure" TTGs would require a garnet-bearing high-pressure granulite or garnet amphibolite, and "low-pressure" TTGs would form via partial melting of a normal (garnet-absent) amphibolite. However, while samples from individual plutons typically belong to the same "group", many Archean cratons contain mixtures of multiple groups with similar ages (Moyen, 2011), complicating tectonic interpretations.

Due to petrological similarities with modern-day adakites (Drummond and Defant, 1990; Martin, 1999), many workers have suggested that "high-pressure" TTGs formed due to slab melting in a subduction zone setting (Martin and Moyen, 2002; Rapp et al., 2003; Laurie et al., 2013), either with a steep dip angle and thick mantle wedge between both plates (Fig. 9a), or involving shallower subduction/underplating with little or no intermediate asthenospheric mantle present (Fig. 9b). Given the large proportion of felsic crust to mafic greenstone in many Archean terranes (> 80%: Kröner, 1985), melting of subducted oceanic slabs appears an efficient mechanism for

voluminous TTG generation, as a substantial amount of hydrated mafic source material may be transported to granulite- or eclogite-facies *P–T* conditions depths at convergent plate margins (Foley et al., 2002, 2003). However, subsolidus dehydration of the slab during prograde metamorphism is likely to have reduced the overall fertility of subducted Archean crust, as fluid-undersaturation suppresses the onset of partial melting to higher temperatures (Hacker et al., 2003; van Keken et al., 2011; Hernández-Uribe et al., 2020).

Alternative mechanisms proposed for TTG petrogenesis focus on vertical-growth in intraplate tectonic settings, such as anatexis of the lower levels of tectonically thickened oceanic crust or plateaux (Fig. 9c), or the foundered portions thereof (Zegers and van Keken, 2001; Bédard, 2006; Bédard, 2013; Zhang et al., 2013; Wiemer et al., 2018). Trace-element systematics of Archean sediments imply that oceanic plateaux were much more common than on the modern-day Earth (Kamber, 2010), and had equilibrium thicknesses of ~40–45 km (Vlaar et al., 1994; Korenaga, 2006). Given the density of high-MgO basalt and komatiite, this depth range would have produced metamorphic pressures of ~12–14 kbar at the plateau base, which forms garnet-bearing HPG in most mafic precursor materials (Fig. 10: Palin et al., 2016a, 2016b). Voluminous TTG generation in Archean plateau environments is perhaps unexpected based on comparison with differentiated modern-day examples (e.g. Arndt, 2003), which are nominally anhydrous at depth. However, repeated sub-aqueous eruption, hydration, and burial of lava during top-down construction of Archean examples was proposed by Kamber (2015) to transport hydrated basalt to depths enough for partial melting to occur (Fig. 9c). Hybrid models incorporating elements of lateral accretion and vertical thickening have been proposed by Bédard (2013), with horizontal cratonic motion potentially driven by large-scale convective currents in the mantle pushing on deep-seated roots.

Despite these well-refined geodynamic models, experimental petrology and thermodynamic phase equilibrium modeling has revealed
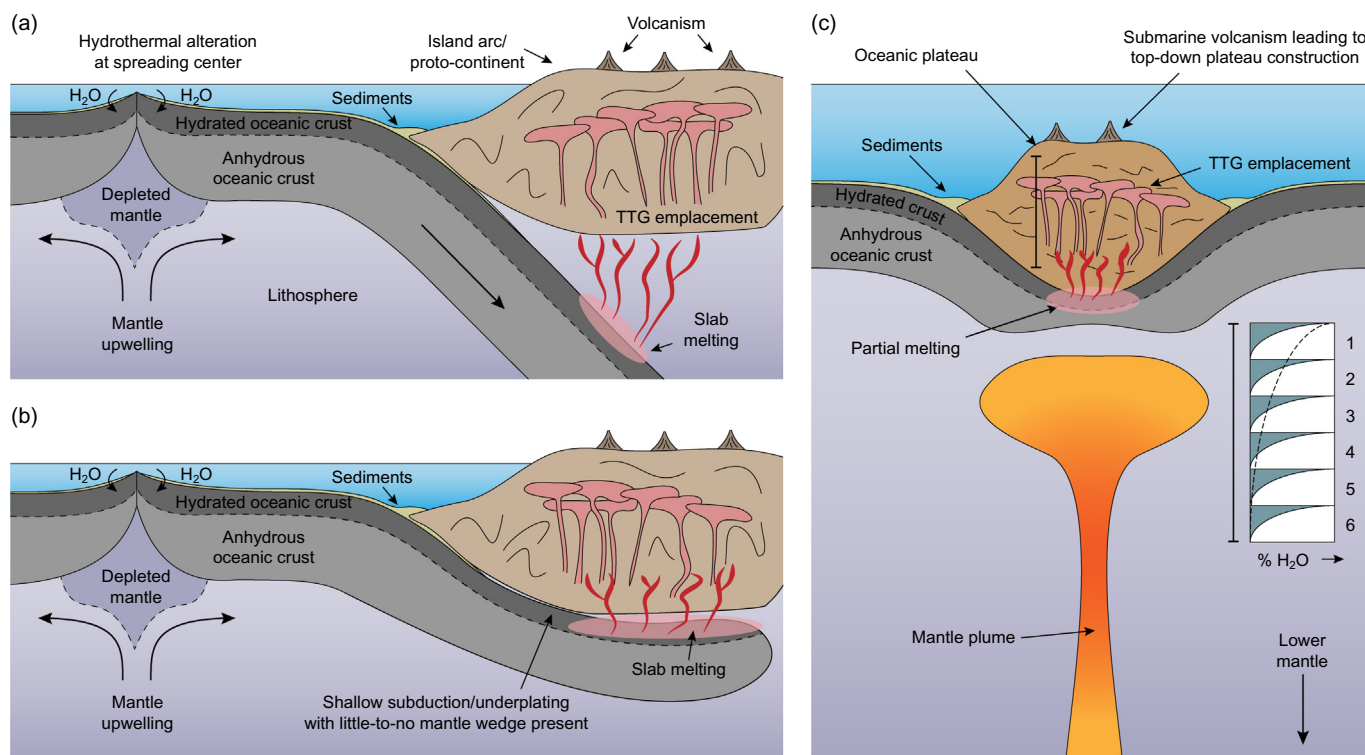

Fig. 9. Possible architectures and geological characteristics of (a) shallow and (b) steep Archean subduction zones (after Palin et al., 2016b). Note that subducted-slab melts must pass through a much thicker mantle wedge to reach the overlying arc in the case of steep subduction compared to shallow subduction. (c) Potential mechanism for TTG generation in an intraplate environment above a mantle plume. Vertical box plot shows the schematic step-like hydration state of multiply buried mafic lava flows. Figures are approximately to scale but emphasize general geodynamic concepts rather than exact crustal thicknesses or plate margin geometries.
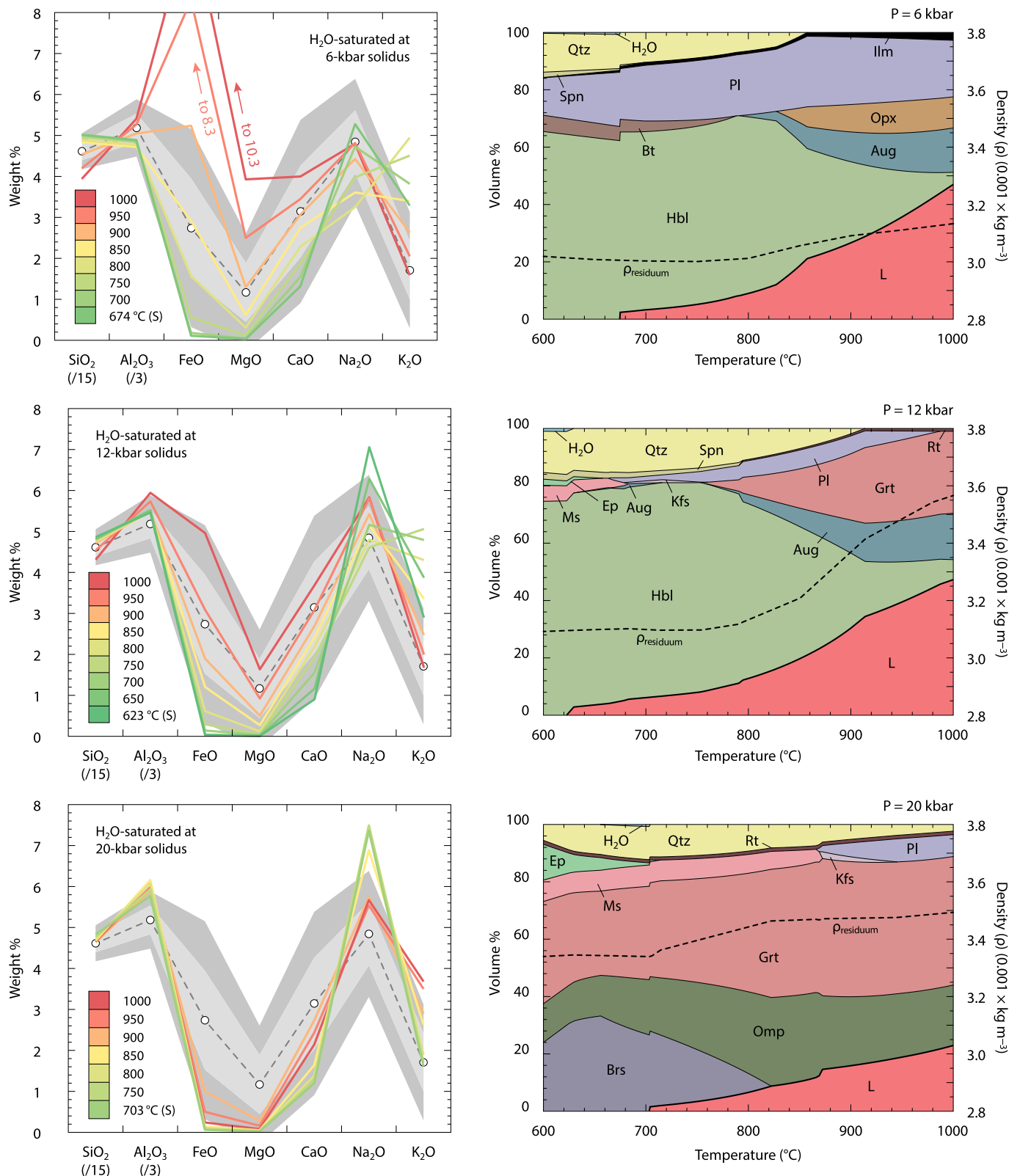
Fig. 10. Calculated mineral assemblages and partial melts compositions generated during metamorphism of an enriched Archean tholeiite (EAT) at low- (6 kbar), medium- (12 kbar) and high-pressure (20 kbar) conditions (after Palin et al., 2016b).

complexity in this tripartite major- and trace-element division of TTGs due to potential variation in the bulk composition of possible source rocks. Most experiments focused on determining the stability of garnet, plagioclase, amphibole, and rutile in metabasalt considered modern-day MORB or MORB-like amphibolites, which have a low MgO content (e.g. Rushmer, 1991; Rapp et al., 1991; Sen and Dunn, 1994; Wolf and Wyllie, 1994). While of direct relevance to Phanerozoic subduction systems, the likelihood that Archean oceanic crust was considerably
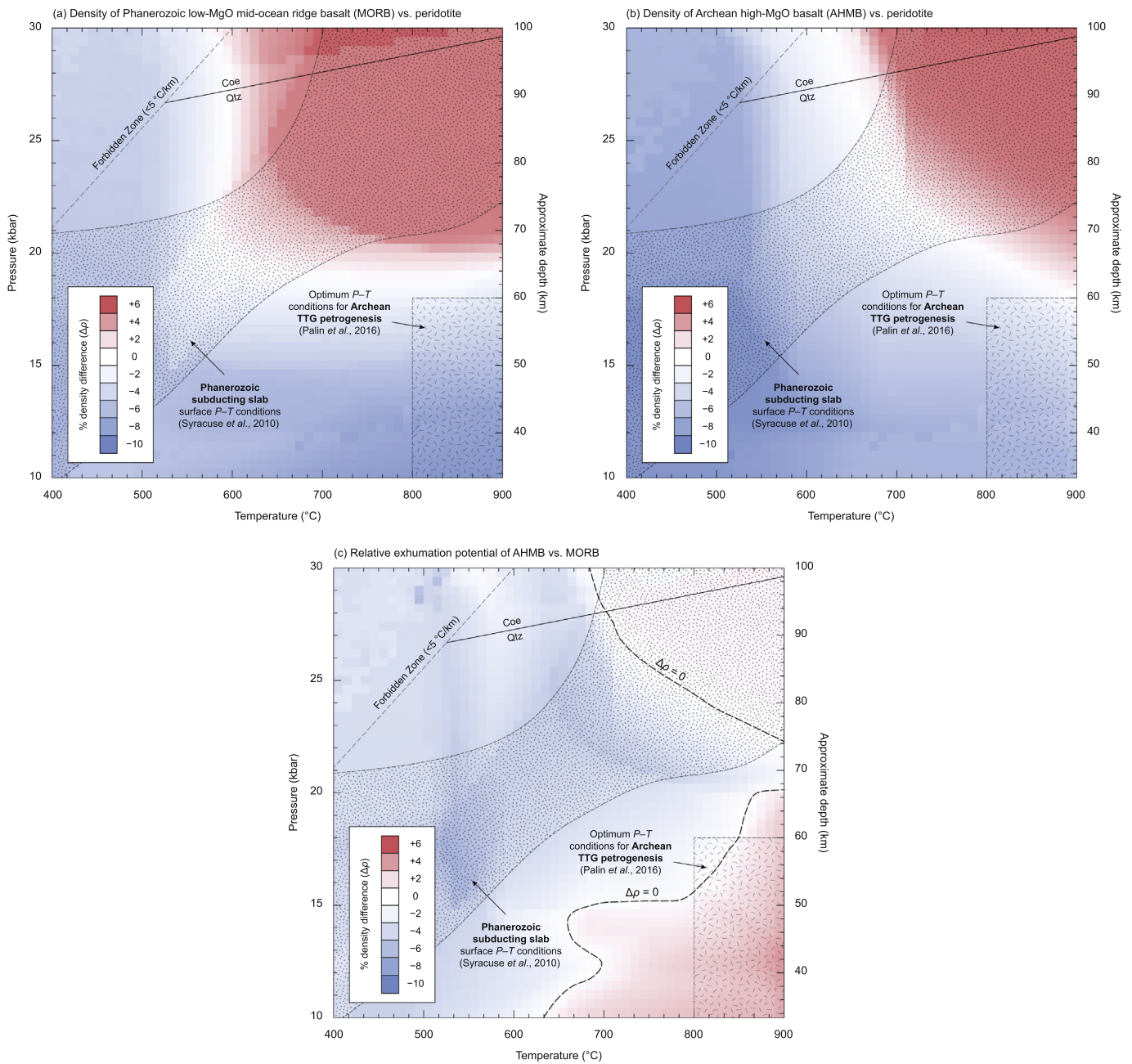
Fig. 11. Density-contrast maps for (a) Phanerozoic low-MgO and (b) Archean high-MgO basalt (AHMB) experiencing subduction (or burial/delamination) into the mantle. Color scale denotes the percentage density difference between the basalt and peridotite. Red colors indicate that the former is denser than the latter, and so is not expected to be exhumed due to buoyancy. The inverse is true for blue colors. Panel (c) shows the relative exhumation potential of both end-member basalts, such that red colors indicate that AHMB is denser than Phanerozoic low-MgO basalt at any given pressure–temperature (*P–T*) condition. Subducting slab-top geotherms for Phanerozoic subduction zones are after Syracuse et al. (2010) and the optimum *P–T* conditions for Archean TTG genesis determined by Palin et al. (2016b) are shown for reference.

more mafic than that observed today affects interpretations that can be drawn from the results of such work. For example, picritic and komatiitic basalts with higher MgO contents suppress plagioclase formation and coevally expand the limit of garnet stability to much lower pressures than for MORB, as would an unusually high FeO content. As a result, "high-pressure" signatures can be generated at moderate pressures within the crust in bulk-rock compositions that differ significantly from MORB (cf. Wade et al., 2017; Nebel et al., 2018).

Palin et al. (2016b) demonstrated that TTG magma genesis is severely restricted at pressures exceeding 20 kbar, representative of intersection of the wet basalt solidus during steep subduction. The maximum fertility of such minimally hydrated, MORB-like Archean basalts

occurred at ~12 kbar, which was interpreted by these authors to record the pressure at which shallowly subducted oceanic lithosphere may begin to melt. However, Palin et al. (2016b) defined optimum *P–T* conditions for slab melting and the production of Archean-like TTG magmas with compositional characteristics matching natural examples of > 800 °C at a pressure of less than 18 kbar (Fig. 11), such modeling cannot directly constrain whether subduction could have operated at any point in time in Earth history. Subsequent studies (e.g. Zhang et al., 2017; Ge et al., 2018; Wiemer et al., 2018; Wei et al., 2019) have corroborated these findings. Interestingly, due to metamorphic transformations during subduction allowing meta-basalt to exceed the density of surrounding mantle (Fig. 11), it is possible that the contribution

by high-pressure metamorphism is underestimated based on the paucity of exhumed HP eclogites in Proterozoic rocks (and absence in Archean terranes).

5. Unresolved issues

Despite decades of focused study, there are several unresolved issues related to the broad theme of secular change in metamorphism and tectonics through Earth history. Below, we initiate discussion on three of the topics that we consider most important for the community reaching a more holistic understanding of the early Earth and its transition into a mobile-lid plate-tectonic regime, whenever that is interpreted to have initiated.

5.1. Are greenstone belts obducted oceanic crust?

Given renewed uncertainty surrounding the thermal history of the Earth's mantle (Section 5.2), discovery of certified Archean ophiolites (or fragments thereof) would be groundbreaking within the scientific community. Claims of this nature have been made several times in the past (cf. Section 3.1.4), but the community appears reticent in accepting them. So, are none, some, or all greenstone belts obducted oceanic crust?

The geochemistry of Archean greenstones has been used as a proxy to trace magma mantle-source regions and tectonic settings of formation (Section 3.3.1), although the limitations and reliability of this technique are disputed for modern-day proxies being translated to the early Earth (Pearce and Cann, 1973; Wood, 1980; Vermeesch, 2006; Condie, 2015; Furnes and Safonova, 2019). Here we briefly discuss evidence from incompatible elements for the tectonic setting of formation and/or mantle source of basaltic rocks in the well-preserved and well-documented Neoarchean (c. 2.6–2.5 *Ga*) greenstone belts in the Dharwar Craton, India, and the North China Craton, China.

The crustal blocks in the Dharwar Craton are welded together by several greenstone belts, including the Chitradurga Suture Zone that separates the Western Dharwar Craton (WDC) and Central Dharwar Craton (CDC), and the Kolar-Kadiri greenstone belt welding the Central Dharwar Craton with the Eastern Dharwar Craton (EDC) (Manikyamba et al., 2008; Jayananda et al., 2018, 2020; Li et al., 2018b) (Fig. 12). In the Nb/Th vs. Zr/Nb tectonic discrimination diagram from Condie (2015), MORB–OIB-type (meta)basalts from the c. 2.7 *Ga* Sandur greenstones of the CDC show relatively high Zr/Nb values and variable Nb/Th values and fall into the HM field, suggesting a hydrous source mantle within continental margin setting (Manikyamba et al., 2008) (Fig. 13). The Mesoarchean greenstones from Goa in the WDC yield low Nb/Th and high Zr/Nb, also suggesting a hydrous source region, typical of a hydrated wedge above a subducting slab in a convergent margin setting (unpublished data). Similarly, the c. 2.6 *Ga* Hutti greenstone in the EDC, which underwent greenschist- to amphibolite-facies metamorphism, also shows a variably enriched geochemical affinity to MORB-type basalts, suggesting the magmas were generated through slab melting (Manikyamba et al., 2009), along with high-Mg basalts from the Kushtagi-Hungund (Fig. 12: Naqvi et al., 2006). The c. 2.5 *Ga* basalt from Nallamalai suture zone and Moyar suture zone are MORB type formed by melting of subducted oceanic plate (Samuel et al., 2014; Li et al., 2018a). The Palghat-Cauvery Shear Zone (PCSZ) separates the Dharwar Craton to the north and Southern Granulite terrane in the south, and contains c. 2.5 *Ga* mafic granulite that has a MORB geochemical signature and hydrous mantle provenance (Noack et al., 2013). In a Th_N versus Nb_N diagram (Fig. 13), basaltic rocks from greenstone belts in the Dharwar Craton and those between the south microblocks dominantly show P-MORB, E-MORB and N-MORB characteristics, suggesting formation within an enriched suprasubduction zone (Saccani, 2015). These features support independent arguments (e.g. Li et al., 2018a) showing that the greenstone belts that stitch the Dharwar Craton together (a) contain fragments of OPS – albeit

metamorphosed to greenschist-facies conditions – and (b) were obducted at convergent plate margins (e.g. Dewey, 1976; Agard et al., 2014). This suggests that plate tectonic processes and a major network of subduction zones had been established by at least the Archean–Proterozoic transition.

Akin to the Dharwar Craton, the Neoarchean North China Craton is a collage of microblocks welded by several greenstone belts (see Fig. 12b for detail: Zhai and Santosh, 2011; Tang and Santosh, 2018). The c. 2.5 *Ga* Wutai greenstones include light rare earth element (LREE)-depleted back-arc basin basalts and LREE-enriched IABs, suggesting generation in an intra-oceanic subduction and mantle upwelling setting. The alkaline and E-MORB types suggest additional material interaction with the downgoing slab and their ages correlate with the final collision of eastern and western block of the North China Craton (Gao and Santosh, 2019; Wang et al., 2004). Similar c. 2.5 *Ga* LREE-enriched MORB-type basalts and c. 2.3–2.0 *Ga* IAB or MORB-type basalts from the Zanhuang complex are interpreted to record ocean closure associated with the amalgamation of Archean microblocks and back-arc setting closure and final collision of the Eastern and Western blocks of the NCC, respectively (Li et al., 2016; Deng et al., 2013). In a Zr/Nb versus Nb/Th diagram, the basalts and metavolcanics from Zanhuang mainly fall in the HM field.

Metavolcanic rocks from eastern Heibei (c. 2.6–2.5 *Ga*) and siliceous high-MgO basalt from Taishan (c. 2.5 *Ga*) show variable LREE enrichment and an N-MORB character, together with a primitive arc basalt character suggesting partial melting of a mantle wedge associated with hydration from oceanic plate subduction (Guo et al., 2013; Peng et al., 2013). The metavolcanics from the eastern Hebei yield moderate Zr/Nb values, variable Nb/Th values, and spread from the HM to the DM and EM classification field. Further, greenstone belt components with ophiolite-like structures in the Yishui Complex at the southern margin of Jiaoliao Block contain (meta)basalt with E-MORB and N-MORB geochemical affinities, which infer an IAT mode of origin in a suprasubduction zone setting (Santosh et al., 2015a). In the Zr/Nb versus Nb/Th diagram, the plots of the basaltic rocks from Yishui Complex mostly fall into the HM and PM field, again suggesting a hydrous mantle source.

Geochemical data for (meta)basalts from these two major Archean cratons that have a similar age both support the interpretation that subduction was operating on Earth immediately prior to the Archean–Proterozoic transition. Examination of Zr/Nb vs. Nb/Th characteristics for metabasalts for both the North China Craton and Dharwar Craton shows mostly HM and DM source regions, suggesting that magmas were derived from hydrated oceanic crust, albeit with minor incorporation of variably depleted components. These conclusions are echoed by Th_N vs. Nb_N data, where most analyzed samples lie within the N-MORB, E-MORB, P-MORB and IAT fields. Such data are fully consistent with these basalts having been generated as part of oceanic lithosphere created at a divergent plate margin, as opposed to in an intraplate setting above the head of a mantle plume (e.g. Boily and Dion, 2002).

Just before the turn of the century, Bickle et al. (1994) suggested that no unequivocal Archean ophiolites have been identified. While this may have been true at this time, more exploration of Archean terranes and new laboratory techniques have shows that this is likely not the case (e.g. Section 3.1.4). One immediate issue that complicates the search for a pristine section through Archean oceanic crust (with or without upper mantle) is the structural difference between typical oceanic crust today and that predicted via thermal–petrological models for the Archean and/or Proterozoic. Due to more efficient melt formation in a hotter Archean mantle, the Archean oceanic crust would likely have been ~25–40 km in thickness (McKenzie and Bickle, 1988) with a high bulk MgO content of ~18–24 wt% (Fig. 5: Abbott et al., 1994; van Thienen et al., 2004). This architecture is in stark contrast with modern-day oceanic crust, which is ~6–7 km thick (Fig. 5), has an average bulk MgO content of 10–13 wt% (Sleep, 1975). Most
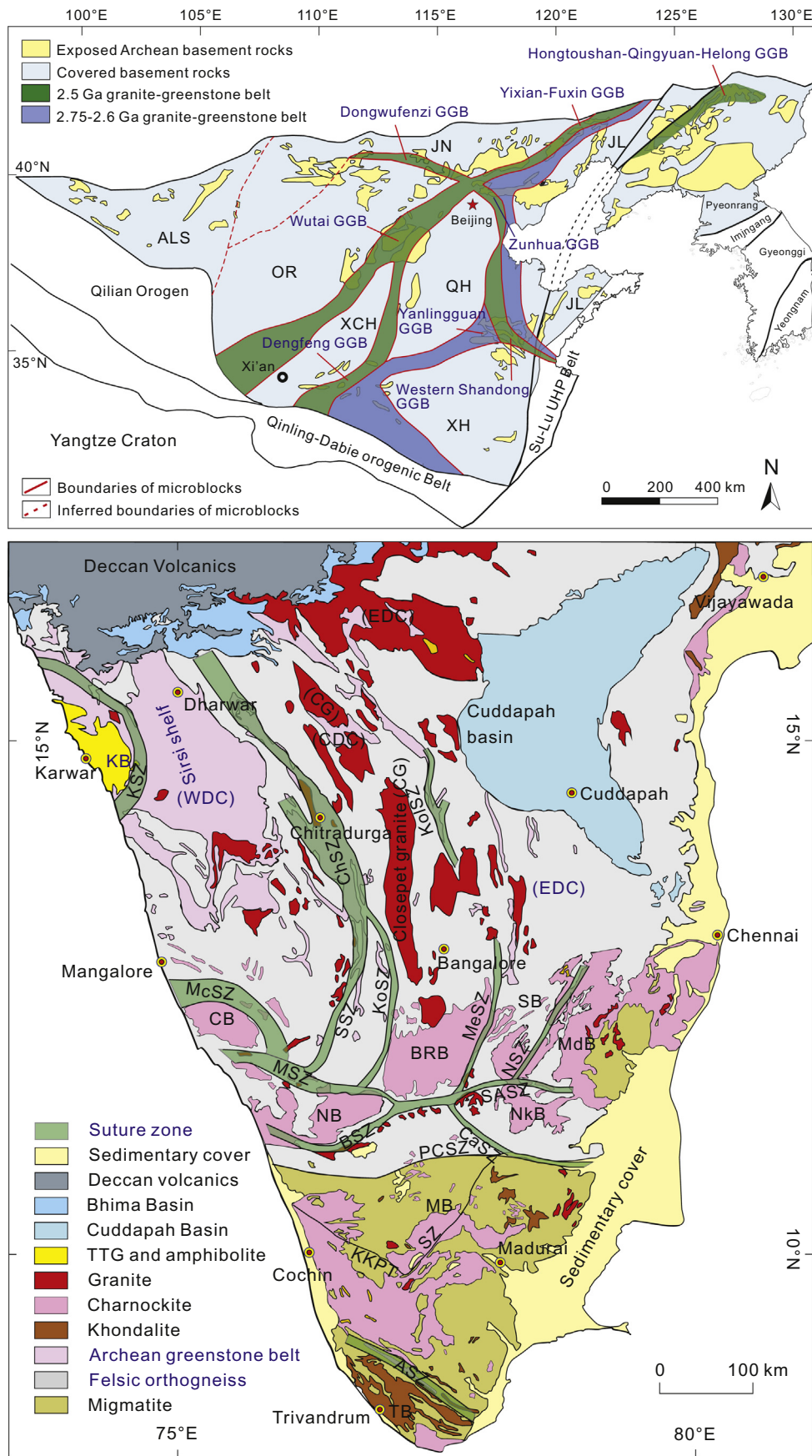
Fig. 12. Geological maps of (a) the North China Craton, China, and (b) the Dharwar Craton, India, highlighting the position of greenstone belts and Archean–Proterozoic microblocks. See main text for discussion.
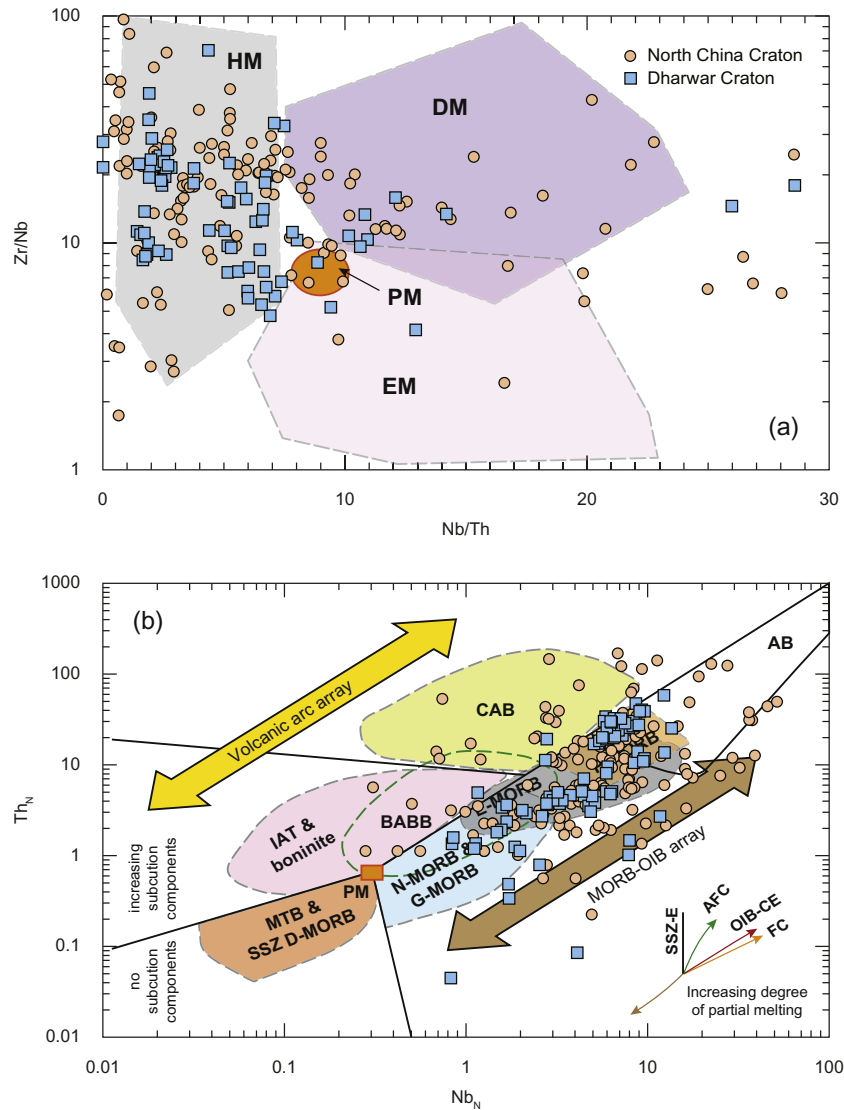
Fig. 13. Tectonic discrimination diagrams for basaltic greenstone belt components from the North China Craton and Dharwar Craton shown on (a) Zr/Nb vs. Nb/Th and (b) Th_N vs. Nb_N bivariate plots. HM = hydrated mantle; EM = enriched mantle; DM = depleted mantle; PM = primitive mantle; CAB = continental arc basalt; IAT = island arc tholeiite; BABB = back-arc basin basalt; MORB = mid-ocean ridge basalt; OIB = ocean island basalt; SSZ = supra-subduction zone; AFC = assimilation–fractional crystallization; FC = fractional crystallization; AB = alkaline basalt.

Neoproterozoic (and younger) ophiolites are less than 5 km in thickness (Condie, 2005), and are bound by thrust faults, which imply that they have been emplaced by obduction. One might then pose the question – is there a constraint on the maximum mass/volume/thickness of oceanic crust and/or lithosphere that may be mechanically emplaced onto a continental margin? To our knowledge, this has not been investigated, although if the worldwide "mean" thickness of an ophiolite (~5 km) exposed in a Phanerozoic orogenic belt is representative, then an Archean ophiolite would not resemble a complete section through the crust, but merely the uppermost portion. As shown in Fig. 5, this would likely comprise a thick sequence of pillow basalt with the uppermost portions of sheeted dikes. Notably, these are the petrological–structural components almost always observed in greenstone belts, whereas the highly mafic and/or ultramafic cumulate sequences expected to characterize the basal levels of a thicker Archean oceanic crustal section remain scarce (or absent). Further investigation of this hypothesis is clearly needed to test whether field geologists are searching for rock types that are not expected to have ever been exhumed in the first place.

5.2. Magnitude and rate of cooling of the Earth's mantle

Descriptions of the thermal evolution of the Earth and absolute temperature of the ambient Archean mantle vary significantly in the literature, with discrepancies emanating from different datasets, assumptions, and uncertainties (see Korenaga, 2006, for a review). The present-day mantle T_P is well constrained and propagation of this variable backwards in time has been used to predict the potential temperature of the Archean and Proterozoic mantle (Fig. 4). Knowledge of such a parameter is critical for effectively parameterizing two- and three-dimensional geodynamic simulations (cf. Gerya et al., 2015; Piccolo et al., 2019), for forward-modeling the volume and composition of partial melt fractions derived during adiabatic decompression of early-Earth mantle (Vlaar et al., 1994), and so modeling of crustal extraction and geochemical depletion of the upper mantle reservoir (Chase and Patchett, 1988; Maurice et al., 2003; McCoy-West et al., 2019).

Early thermal models of mantle T_P over time initially showed a clear discrepancy: Korenaga (2008a, 2008b) deduced that the Mesoarchean mantle T_P reached a maximum of ~1600–1650 °C by projecting a value

of Ur of 0.23 ± 0.15 backwards in time (Fig. 4). In these thermal models, the Paleoarchean was cooler than the Mesoarchean due to the delayed effect of radiogenic nuclides incorporated into the mantle during planetary accretion beginning their heat production. By contrast, a study published by Davies (2009) shortly afterwards suggested that there was no arch-like T_P curve, and that the Earth's mantle had experienced continual cooling since c. 4.56 *Ga*. This model inferred a mantle T_P at 3.5 *Ga* of ~1425 °C; much cooler than that put forward by Korenaga (2008a, 2008b). Apparent validation of the "high-temperature" models was provided by Herzberg et al. (2010), who calculated liquidus temperatures for 33 non-arc basalts of various ages (yellow dots on Fig. 4), with these data lying within Ur = 0.23–0.38 for the models of Korenaga (2008a, 2008b). However, as outlined in Section 1.3, subsequent analysis of much larger geochemical sets of basalt compositions by Condie et al. (2016) and Ganne and Feng (2017), facilitated by the rise of Big Data, favor the interpretation of Davies (2009). Both studies concluded that ambient Archean mantle T_P outside periods of supercontinent formation was ~1450–1500 °C (Fig. 4), defining a more subdued secular cooling rate of ~30–50 °C/Gyr compared to the conclusions of Herzberg et al. (2010).

If the results of Condie et al. (2016) and Ganne and Feng (2017) are correct, a worrying large number of studies conducted in the past decade based on "hot" Archean mantle T_P values will need re-examination. The sensitivity of thermo-mechanical models to mantle T_P values has been studied explicitly by several workers (e.g. Gerya, 2014; Fischer and Gerya, 2016a, 2016b), and the timing of transition from stagnant-lid to mobile-lid tectonics has often been defined based on a critical T_P value being passed. The point in time at which cooling of the ambient mantle crossed this threshold is dependent on interpreted models of the thermal history of the Earth. Recent modeling studies have identified this issue and have investigated how continental crust may form in intraplate geodynamic environments in a "relatively cool Archean mantle" (Piccolo et al., 2019), although much further study is required from two standpoints: firstly, to finalize the magnitude and rate of cooling of the Earth through time, whether from first principles with updated physico-chemical constraints, or from a more in-depth study of the petrological record. Secondly, tectonic, petrological, and/or geodynamic modeling should adopt fewer a priori assumptions of mantle T_P in the Precambrian, whether this has influence over the resultant architecture of oceanic crust (e.g. Palin and White, 2016; Palin and Spencer, 2018) or petrophysical properties of Archean continental crust and its ability to partially melt and internally differentiate (e.g. Nebel et al., 2018). Ideally, more advanced integrated models (e.g. Section 7.2) may be adopted in the future that take greater consideration of the effects of uncertainty related to this secular cooling until the issue approaches a more definite conclusion.

5.3. Global vs. localized onset of subduction

With the increasing number of examples of eclogite-facies metamorphic rocks and terranes of Precambrian age (cf. Fig. 8a–b) having been reported in the literature over the past decade (Section 3.1.3), it has become a topic of recent debate whether these exposures truly represent evidence for a globally connected network of subduction zones, as one would require for plate tectonics to operate, or else localized occurrences of subduction initiation that failed to subsequently stabilize (e.g. Viete and Holder, 2019). Alternatively, plate tectonic behavior may have been transient during the Proterozoic, with the Earth frequently switching between stagnant- and mobile-lid states before reaching an equilibrium (Lenardic, 2018; O'Neill et al., 2018). Without doubt, the temporal clustering of HP/UHP eclogite-facies metamorphism at c. 1.8–2.1 *Ga* in many different localities around the world is significant, as is the curious lack of such samples in the 600-Myr period afterwards (c. 1.2–1.8 *Ga*: Fig. 8b). The large-scale emergence of blueschists and eclogites in the geological record at c. 0.9 *Ga* represents a firm constraint on the latest possible onset of cold, steep subduction

(cf. Stern, 2005).

While eclogite (sensu *lato*) is not diagnostic of subduction, given the potential for overthickening of continental crust and transformation of its mafic lower levels (e.g. continental eclogite from the Pamir; Hacker et al., 2005), geochemical characteristics and field associations of many examples within this cluster of data support a subduction-related origin. For example, recently reported Paleoproterozoic (c. 1.8 *Ga*) eclogite from the Trans-Hudson orogen, Canada, by Weller and St-Onge (2017), shows comparable field relations (i.e. boudinaged and metamorphosed dikes enclosed within felsic continental basement) and peak *P–T* conditions to equivalent eclogite from the Himalayan orogeny (e.g. Wilke et al., 2010; St-Onge et al., 2013). The scale and rates of orogenesis in both the upper and lower plate in both orogenies are also comparable (St-Onge et al., 2006), which was used by Weller and St-Onge (2017) as evidence for comparable modern-day-style plate tectonic processes having operated at that point in Earth history. Although much independent evidence supports subduction of some form having operated prior to 1.8 *Ga*, early forms of subduction likely had a shallow angle of dip (Van Hunen and Moyen, 2012), thus precluding formation of UHP rocks; however, one study has purported eclogite-facies metamorphism of garnet pyroxenite from the Nagssugtoqidian orogen, Greenland, at extreme *P–T* conditions of ~7 GPa and ~975 °C (Glassley et al., 2014). This data point stands as a clear outlier to the other eclogite examples of this age, and even in modern-day environments, the geodynamic mechanism by which high-density mafic rocks could be exhumed from such mantle depths is uncertain (cf. Agard et al., 2009), although steep subduction remains one possibility.

While many forms of petrological evidence (e.g. UHP metamorphism, blueschists, jadeitites etc.) are diagnostic of subduction through Earth history, there is much evidence from the tectonic record that adds compelling independent arguments to the broader-scale conclusion that a global network of plate boundaries had been present on Earth since at least the Archean–Proterozoic transition (cf. Fig. 1). Supercontinent formation (Section 3.2.4) requires the lateral accretion of formerly separate lithospheric terranes, which is facilitated today by seafloor spreading and concomitant destruction of intermediate oceanic lithosphere in subduction zones (Shervais, 2001; Harris, 2020). While paleomagnetic data (or the lack of it: Section 3.2.5) do not allow confident plate reconstruction and/or paleolatitudinal location prior to the Middle or Early Proterozoic (Evans and Pisarevsky, 2008), the existence of supercontinents is confirmed to at least c. 2.0–1.8 *Ga* (Fig. 1): namely Columbia/Nuna (Meert, 2012). Indications of older continental assemblies dated at c. 2.7–2.5 *Ga* (Kenorland) and, potentially, at 3.0 *Ga* (Ur) have been made from various proxies (e.g. Aspler and Chiarenzelli, 1998; Mahapatro et al., 2012), including the global zircon archive, which can be used to track large-scale extraction of continental-like crust from the underlying mantle, as is associated with plume activity and/or convergent margin arc-related processes (Dewey and Horsfield, 1970; Rudnick, 1995; Clift et al., 2009).

Interrogation of these hypotheses has rightly been made by comparison with subduction-like features observed on other planets in our solar system – particularly Venus (Section 7.1.1) – which otherwise are observed to exhibit a stagnant-lid tectonic regime (Reese et al., 1999). Such features on Venus include abyssal hills on MOR-like structures (Head and Crumpler, 1987; McKenzie et al., 1992) and trench-like features with similar curvature and asymmetry as ocean–ocean plate margins on Earth (Sandwell and Schubert, 1992; Schubert and Sandwell, 1995), and suggest that localized subduction may occur on a planet that is otherwise made up of static lithospheric fragments. Although such bi-modal regimes have not been predicted in simulations of the early Earth, they are at least conceivable, or else may be partially represented by episodes of incipient subduction initiation that never stabilize (e.g. Toth and Gurnis, 1998; Gurnis et al., 2004; Ueda et al., 2008).

Field investigation and thermo-mechanical modeling of subduction initiation has been undertaken by a variety of researchers in recent
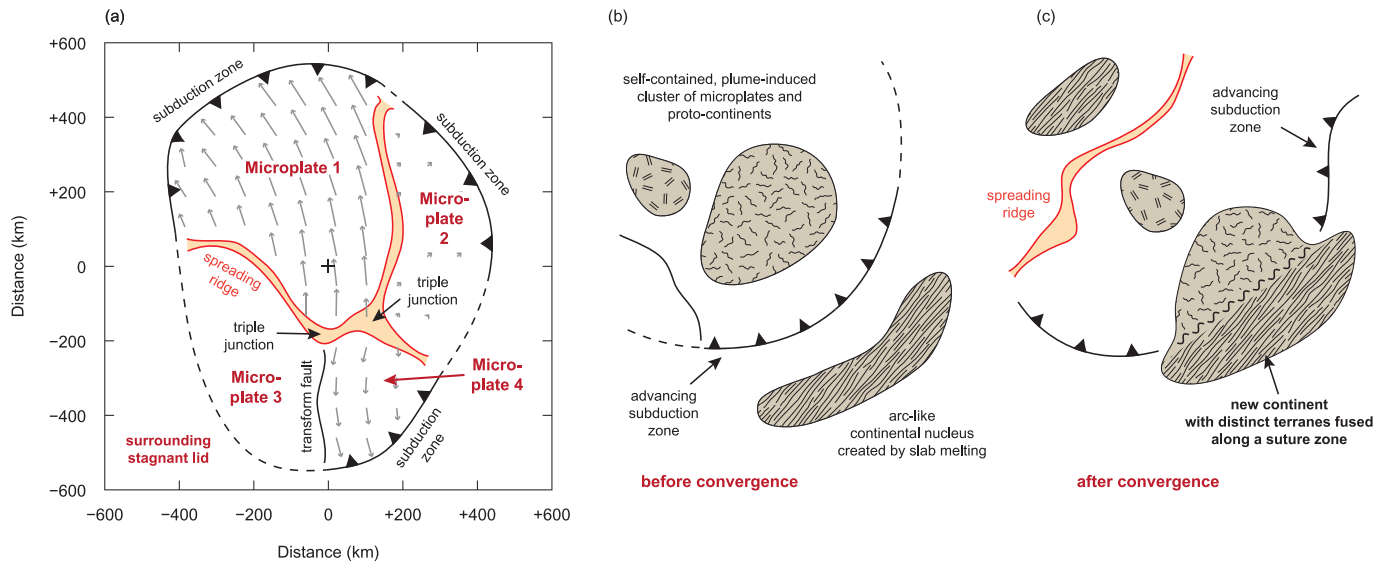
Fig. 14. Potential geodynamic scenarios allowing isolated subduction on an Earth dominated by stagnant lid tectonics. (a) Summary plan view of development of a mosaic of microplates above a mantle plume produced via 3-D numerical modeling by Gerya et al. (2015). Microplates are separated by spreading ridges or transform faults. Gray arrows represent the magnitude of the calculated second strain rate invariant at a depth of 20 km, and thus indicate the general vector of plate motion. All lithosphere outside of the marked plate boundaries exists in a stagnant lid regime. Reproduced with permission from Springer. Schematic model in plan view before (b) and after (c) collision of microcontinents and formation of suture zones by convergence of two or more plume-induced cells (modified after Brown et al., 2020). Reproduced with permission from Annual Reviews.

years, although the former technique can only inform geologists of recent (Phanerozoic) processes. A detailed and realistic numerical simulation of subduction initiation on the Archean Earth was completed by Gerya et al. (2015), where discrete and self-contained clusters of 100-km scale microplates bounded by spreading ridges, transform faults, and one-sided subduction zones were predicted to form above a mantle plume (Fig. 14a). The remaining area outside of this simulated microcosm would exhibit characteristics of a stagnant lid regime. While no proto-continents were predicted in this scenario, subduction of oceanic lithosphere would be expected to form arc-like nuclei on the overriding plate, or else melting at the base of the microplates situated directly above the plume head would likely begin to internally differentiate to generate TTG-like magmas. Although subduction in this case is localized, mantle plumes were thought to be much more abundant on the Archean Earth compared to today (Kamber, 2010). Thus, if two or more microplate clusters formed in close proximity, and if plume migration or subduction zone advancement could cause one cell to merge with another, it can be envisaged that two or more microcontinents can be brought together, akin to Phanerozoic collisional orogenesis (Fig. 14b–c). Such a collision would be characterized by at least two discrete continental terranes that have been fused along a suture zone, with associated petrological (Section 3.1) and tectonic (Section 3.2) features observed in modern day collision zones. Thus, it would have been possible to produce small-scale plate tectonic-like features on the surface of the early Earth that mostly exhibited a stagnant lid regime. Given the recent surge of reports of Paleoproterozoic examples of subduction-related eclogite in the geological record (cf. Fig. 8), continued exploration of Archean terranes coupled with detailed thermobarometry and geochronology offer the best path forwards to illuminate whether such simulations are representative of natural processes.

6. The timing of onset of plate tectonics on Earth

The timing of onset of plate tectonics on Earth is a topic that will likely never be agreed upon by the scientific community. While many lines of evidence may be used to infer the possibility of subduction and/ or independent plate motion at any given period in Earth history, few

proxies are considered definitive. Indeed, while it is argued here that some of the most robust evidence for subduction comes from the metamorphic rock record, especially in the form of blueschists (Section 3.1.1) and exhumed UHP eclogites (Section 3.1.3), neither of these lithologies have been dated to be older than c. 0.9 *Ga* (Fig. 1). Nonetheless, this does not preclude them from having formed earlier in Earth history, but never having been exhumed to the surface, or else exhumed but completely eroded or overprinted by later tectonic activity, thus aligning with other forms of evidence supporting (steep) subduction as early as the Paleoproterozoic (e.g. Shirey and Richardson, 2011 and many others). It is thus of critical importance to realize that '*the absence of evidence is not evidence of absence*' (cf. Sagan, 2011), which has been used to enforce somewhat Uniformitarianistic viewpoints of the evolution of plate tectonics in recent works. While Uniformitarianism has use in that many fundamental geologic processes observed today have presumably operated similarly throughout all of Earth history (cf. Hutton, 1795), the geodynamics of the Hadean or Early Archean Earth may simply be too far-removed to envisage (Shea, 1982).

A holistic synthesis of the arguments discussed in this review paper is provided in Fig. 15, which illustrates major secular changes in continental (Fig. 15a) and oceanic (Fig. 15b) crust, through an overview of global geodynamic regimes (Fig. 15c). The initial tectono-magmatic state of the very early Earth is likely to have been a global magma ocean (Hosono et al., 2019) of unconstrained depth (Section 1.1), capped by a thin scum-like floatation of uncertain composition. Different studies disagree on this petrological constitution, purporting that fractional crystallization and differentiation of this precursor, short-lived magma ocean produced a primary komatiitic (Reimink et al., 2016), anorthositic (Santosh et al., 2017), or silica- and potassium-rich protocrust (Boehnke et al., 2018), the latter being comparable to modern-day continents. Nonetheless, no bonafide fragments are preserved on Earth today and indications of its geochemistry and structure are restricted to rare inclusions within Hadean zircons, for example from the Jack Hills region of Western Australia (e.g. Maas et al., 1992; Hoskin, 2005; Menneken et al., 2007; Harrison, 2009). The geological mechanisms responsible for destroying this Hadean primary crust are further unresolved, but are likely both exogenic and endogenic in nature. In the
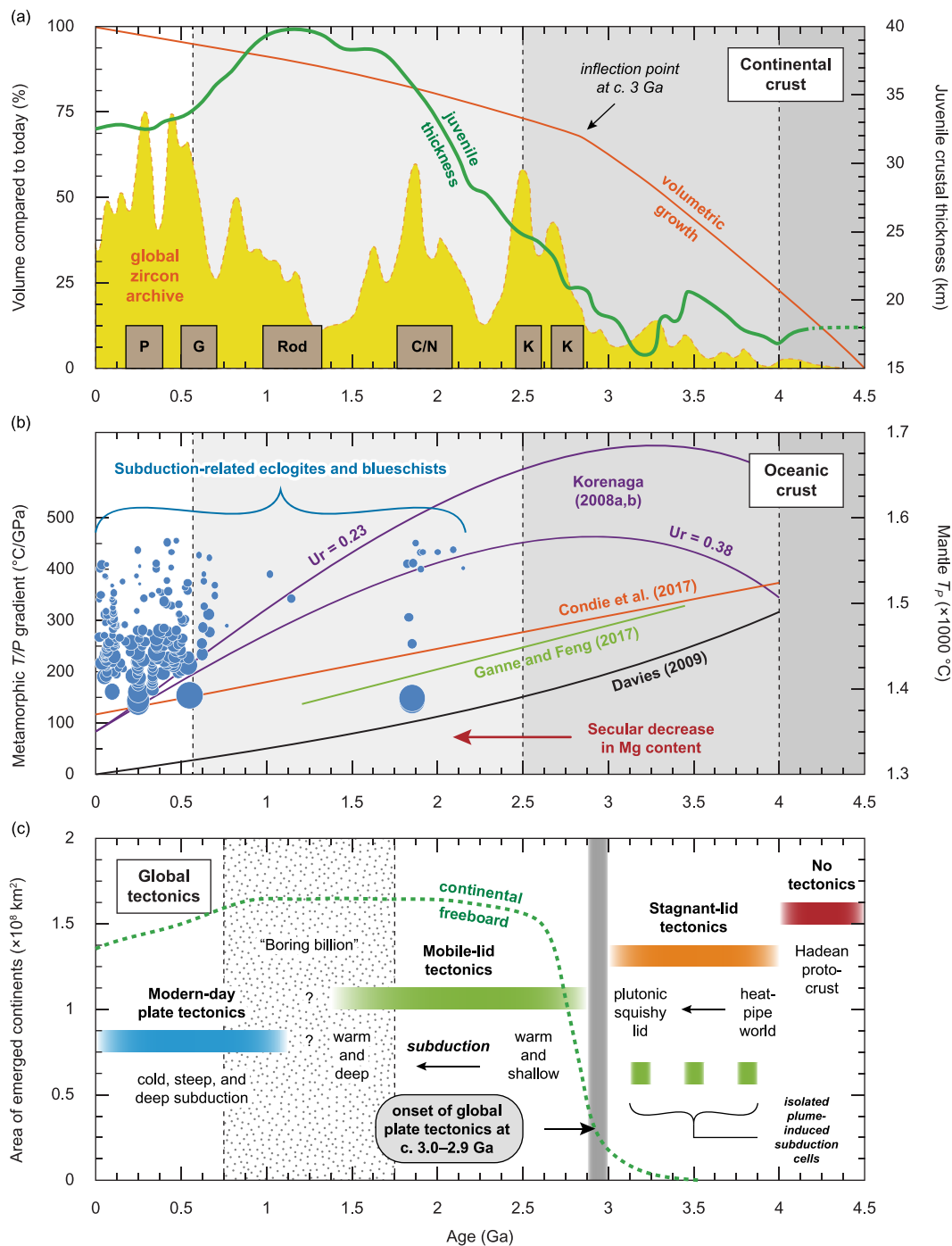
Fig. 15. Summary diagram showing key changes in the secular evolution of (a) the continental crust, (b) the oceanic crust, and (c) global geodynamics discussed in this study. Curve showing calculated continental crust juvenile thickness is after Dhuime et al. (2015), that for continental growth is after Dhuime et al. (2012), and that for continental freeboard is from Bada and Korenaga (2018). The global zircon archive curve is from Roberts and Spencer (2015).

former case, interpretations of crater densities on the surfaces of the Moon, Mercury, and Mars suggest that there was a discrete episode of increased flux of bolide impacts within the inner solar system at c. 4.2–3.9 *Ga* (Bottke and Norman, 2017), termed the late heavy bombardment. This process likely also induced widespread mixing, destruction, and/or resurfacing of the Earth's Hadean crust (Marchi et al., 2014; O'Neill et al., 2020). Endogenic solutions involve global lithospheric inversions or volcanic resurfacing events (e.g. Griffin et al., 2014), such as is thought to have occurred on Venus at c. 500 *Ma* (Strom et al., 1994: see Section 7.1.1.). Geodynamic simulations of possible early-Earth thermo-tectonic regimes suggest that such large-

scale resurfacing is plausible (e.g. Moore and Webb, 2013) and has given rise to the moniker 'heat-pipe Earth' as a term for describing a global stagnant-lid tectono-magmatic regime dominated by extrusive volcanism (Section 1.1: Fig. 3).

While Earth's first continental crust may have formed during the Hadean, it is practical to omit this from discussion, as none is preserved in the geological record. Some of the Earth's oldest preserved continental-like crustal material is exposed within the Isua Supracrustal Belt, Greenland, and has multiple radiogenic ages of c. 3.8 *Ga* (Moorbath et al., 1977; Boak and Dymek, 1982; Myers, 2001; Crowley, 2003). Field evidence and geochemical characteristics of TTG

components within the Isua belt have been used by some researchers as evidence for subduction having operated at that time (e.g. Komiya et al., 1999; Polat et al., 2002; Jenner et al., 2009; Kaczmarek et al., 2016), although few attempts at lithospheric-scale numerical modeling have been able to replicate subduction in any form at such a time in Earth history. Could such a discrepancy be a result of uncertainty in mantle T_P, which plays a critical role in determining the mode of geodynamic regime (cf. Section 5.2)? In partial contrast with geodynamic modeling, petrological modeling suggests that the major- and trace-element characteristics of Early Archean TTG magmas are consistent with derivation from shallowly subducted oceanic crust (Palin et al., 2016b) or at the base of thickened oceanic plateau (Zhang et al., 2017) formed above mantle plumes. These results are to-date inconclusive, as similar *P–T* conditions are expected in each scenario, meaning that similar metabasaltic rock types (e.g. high-pressure granulite or eclogte) may form in either tectonic model. This early continental crust is thought to be notably mafic in composition compared to Phanerozoic continental crust (Section 2.2), and relatively thin (~18 km; Dhuime et al., 2015; Fig. 15a).

Progressive cooling of the Earth during the Archean is expected to result in a continual change in the thickness and bulk-chemistry of oceanic lithosphere generated at divergent plate margins (Section 2.1), becoming increasingly less magnesian over time (Herzberg et al., 2010; Palin and White, 2016). The buoyancy of this oceanic lithosphere is expected to decrease commensurately, thus promoting transition from a pre-plate tectonic regime to one dominated by subduction, which geodynamic models suggest would be warm and shallow in this first instance (Fig. 15c). The absolute timing of this change as it occurs at a global scale is, of course, the matter of this discussion and a primary focus of this review. Much petrological evidence argues for this transition at some point during the Middle to Late Archean (c. 3.2–2.5 *Ga*: Fig. 1), and we favor interpretations that utilize bonafide petrological and/or tectonic indicators of the Wilson Cycle, including supercontinent formation (Section 3.2.4) or a sudden shift in the petrology of inclusion suites in diamonds (Section 3.3.2). Together, these indicators argue for subduction having been established at a global scale by at least c. 3 *Ga* (Fig. 15c), with indicators of subduction preserved in older terranes potentially representing localized events. Secular cooling and the onset of subduction-driven accretion at convergent margins also facilitated reworking of older materials and likely promoted more efficient internal differentiation of the continents, transforming a semi-homogenous Early Archean continental crust to a more layered Late Archean one (cf. Dhuime et al., 2015; Hawkesworth et al., 2016). Accelerated reworking is supported by a distinct change in upper crustal composition over this c. 3.0–2.5 *Ga* period (Section 2.2: Tang et al., 2016).

Emergence of the continents around the Archean–Phanerozoic transition (c. 2.5 *Ga*: Section 2.2) and progressive steepening of subduction zones throughout the Proterozoic were both direct results of continued secular cooling of the mantle (e.g. Ganne and Feng, 2017). Decreasing mantle T_P would have resulted in bulk thinning of juvenile oceanic lithosphere (Fig. 15b: Herzberg et al., 2010; Weller et al., 2019) and a decrease in its MgO content, which numerical models have shown increase the effective viscosity at the oceanic lithosphere–asthenosphere boundary (e.g. Korenaga, 2013 and references therein). Eclogitization of subducted portions of this relatively low-MgO oceanic crust (Palin and Dyck, 2018) would have provided a sufficient negative buoyancy to promote progressive steepening of the mean angle of subduction throughout Phanerozoic, with a seemingly critical threshold occurring at c. 0.9 *Ga*, when diagnostic indicators of subduction become extremely abundant in the geological record, including blueschist and UHP eclogite (Stern, 2005; Fig. 1). At this point in time in the Neoproterozoic, there is almost no doubt that subduction was a worldwide phenomenon and operated in an identical fashion to convergent margins observed on Earth today. A major curiosity in the post-Archean geological record is the preservation of HP eclogite (and one

unusual occurrence of UHP garnet-pyroxenite) at c. 1.8–2.1 *Ga* (Figs. 8 and 15b), but a notable gap between 1.8 and 1.2 *Ga* (Figs. 8 and 15b). This 600-Myr period overlaps with the proposed period of worldwide tectonic quiescence – the "Boring Billion" (c. 1.8–0.8 *Ga*) – which is bookmarked by two major glaciation and oxygenation events (Brasier and Lindsay, 1998). The Boring Billion itself is thought to record a period of stable tectonics on Earth where floral and faunal diversity stalled, although several major tectonic events are known to have occurred, including assembly of the Rodinia supercontinent (c. 1.23 *Ga*: Fig. 1) and major mantle plume-derived magmatism in central Australia (c. 1.2 *Ga*: Gorczyk et al., 2015). Whether this period represents a transitional state in global geodynamic regime – from a previously established mobile-lid regime to a new post-Archean stagnant-lid regime, with transition back again – or whether the notable paucity of evidence for subduction documents pervasive overprinting and reworking is unclear. More detailed study into rocks of this period is needed.

7. Future directions

Here, we outline key areas of research that hold much promise for developing our understanding of the initiation of plate tectonics on Earth. Many of these concepts necessarily cross disciplinary boundaries, and no single researcher is equipped to handle any one alone! Collaborative efforts between research groups with different (but complementary) expertise is required for significant advances to be made.

7.1. Extraterrestrial tectonics

Earth is the only planet in our solar system thought to have developed plate tectonics, although examination of our neighboring terrestrial bodies can shed much light on the likely tectonic regime that existed beforehand, as discussed in Section 1.2. With continual advances being made in out technical ability to deliver analytical equipment to the surfaces of other planets in the inner solar system (Cutts et al., 2007; Bajracharya et al., 2008; Păun, 2015; Trebi-Ollennu et al., 2018), or else to allow spacecraft and probes to perform orbital or fly-by investigations of more distant bodies (Wu et al., 2012; Phillips and Pappalardo, 2014; Stern et al., 2015; Lunine, 2017), we are assuredly now entering a new age of space exploration and discovery that will have unprecedented feedbacks on our understanding of the early Earth (Lowman Jr, 1989).

7.1.1. Venus

Venus is remarkably similar to Earth in terms of its size and density, exists at a similar distance from the sun, and exhibits a relatively young surface geology (e.g. Smrekar et al., 2018), which suggests comparable interior geodynamics. Indeed, many features exposed on the surface of Venus are morphologically similar to those characteristic of terrestrial plate margins, including transform faults (Ford and Pettengill, 1992), abyssal hills on MOR-like structures (Head and Crumpler, 1987; McKenzie et al., 1992), and trench-like features with similar curvature and asymmetry as ocean–ocean plate margins on Earth (Sandwell and Schubert, 1992; Schubert and Sandwell, 1995). In contrast, many other features on the Venusian surface more closely resemble those expected to form in intraplate environments, such as above the head of a mantle plume, including > 1000-km-diameter shield volcanoes (Ernst and Desnoyers, 2004; Hansen and Olive, 2010), lava flow fields of scales comparable to terrestrial flood basalts (Lancaster et al., 1995), and smaller-scale volcanic 'pancake' domes of silica-rich lava (Fink et al., 1993; Stofan et al., 2000). Indeed, at least four regions of the Venusian surface are thought to expose recent basaltic lava flows, with gravity and topography data in these locations consistent with active mantle plumes being present at depth (Kiefer and Hager, 1991; Simons et al., 1997). Given that crater counting suggests a global resurfacing event on Venus at c. 300 *Ma* (Strom et al., 1994), all of these apparent plate

boundary and intraplate tectonic features must be younger, and so likely formed coevally with one another. This hypothesis then implies localized subduction initiation, as opposed to a global network of plate boundaries, which itself may have been a transitional state for the early Earth (Moyen and van Hunen, 2012).

During recent analogue modeling of plume-induced subduction on Venus, which attempted to reproduce the structural features observed around Artemis Corona, Davaille et al. (2017) reported that hot mantle plumes impinging on the underside of the Venusian lithosphere caused tensile fractures to develop, which subsequently acted as conduits for basaltic eruptions onto the surface, akin to large igneous provinces on Earth. Spreading, loading, and flexure of newly formed oceanic-like lithosphere eventually led to subduction-like behavior along arcuate trenches. Similar results have been produced for the early Earth using geodynamic modeling (Gerya et al., 2015) and suggest that mantle plumes may be likely drivers for subduction initiation (Ueda et al., 2008; Burov and Cloetingh, 2010).

The cause of catastrophic global resurfacing on Venus at c. 300 *Ma* is debated and represents a significant "loss" of potential knowledge of the early evolution of the inner solar system. Various hypotheses have been put forward, which may readily be separated into cyclical and single-event processes. Parmentier and Hess (1992) suggested that competition between compositional stratification and thermal buoyancy may cause episodic overturn of the upper mantle, with Turcotte (1993) suggesting that this restructuring would occur over periods of ~500 Myr and would be characterized by long periods of quiescence followed by short periods of active plate tectonics. By contrast, thermomechanical modeling conducted by Solomatov and Moresi (1996) and Reese et al. (2007) suggests that the unusually thick lithosphere preserved today (200–400 km) may have formed due to a transition *from* a mobile lid regime *to* a stagnant lid regime immediately prior to c. 300 *Ma*, thus marking the onset of the terminal stagnant lid phase of silicate planetary evolution (Fig. 3). In these models, sublithospheric small-wavelength convection stops and conductive thickening of the lid suppresses the ability for mantle melts to reach the surface. Ultimately, Earth will suffer the same fate.

7.1.2. Mars

The scientific value of Mars for understanding the geodynamics of crust-forming processes in a stagnant-lid tectonic regime cannot be understated. Mars is Earth's closest planetary neighbor and so has been the target of over 50 fly-by, orbital, and surface exploration missions in the past few decades (Snyder and Moroz, 1992; Levine et al., 2010; Munévar, 2019). Mars is notably smaller than Earth, and thus cooled at a much greater rate than our home planet (Schubert and Spohn, 1990; Wade et al., 2017). Today, despite evidence for recent (< 40–100 *Ma*) volcanism on its surface (Lucchitta, 1987; Hartmann et al., 1999; Hauber et al., 2011), Mars exhibits relatively subdued seismic activity (Hansen, 2000; Giardini et al., 2020), although there is abundant evidence for active tectonics, metamorphism, and magmatism having shaped its surface soon after formation (Ingersoll, 1970; McSween Jr, 2015).

Mars' surface shows a pronounced hemispheric dichotomy (Smith et al., 1998), with low-elevation northern plains comprised of thin (~32 km) mafic crust and high-eleveation southern highlands, which are much thicker (~58 km). The boundary between both domains contains landforms that appear to have been shaped by the flow of ice and/or water, indicating that the northern plains may at one time have hosted an ocean of liquid water (Baker et al., 1991; Head et al., 1999; Di Achille and Hynek, 2010; Citron et al., 2018). The origin of this hemispheric dichotomy is much debated, and hypotheses consider endogenic (e.g. mantle plume-driven) and exogenic (e.g. bolide impacts) factors (Watters et al., 2007). In the case of an endogenic driving force, planetary-scale geodynamic modeling of early Mars suggests that a degree-1 mantle convection profile, where one hemisphere (i.e. the south) hosts an upwelling in the Martian mantle and the other

hemisphere (i.e. the north) hosts a downwelling, could be responsible for its formation (Zhong and Zuber, 2001). In this scenario, upwelling in the northern hemisphere could have acted to erode away the base of the crust, potentially redistributing it in the opposite hemisphere, or else upwelling in the southern hemisphere may lead to a greater degree of melting and extensive fracturing, producing outpourongs of lava (akin to terrestrial large igneous provinces) and a thicker crust above the plume (Roberts and Zhong, 2004). Exogenic hypotheses include a single, giant impact (Wilhelms and Squyres, 1984; Frey and Schultz, 1988) that caused catastrophic delamination of weakened lower crust in the north, implying that the ~58-km thickness recorded in the south represents a primary crustal architecture. Discussion of the validity of any particular hypothesis is far beyond the scope of this work, although ancient volcanism on the Tharsis Plateau has been attributed to mantle plume activity, such as is expected to have characterized the early Archean on Earth (cf. Fig. 3), and so many useful parallels can be drawn between Mars's evolution and that of the pre-plate tectonic Earth (Mège, 2001).

The southern highlands of Mars are of particular interest for theorizing the past operation of plate tectonics on the planet. The occurrence of large, linear crustal remnant magnetic anomalies with alternating polarities in this region (Acuña et al., 1999; Connerney et al., 1999) suggests that Mars sustained an intrinsic and dynamic magnetic field early on in its history. These magnetic anomalies are weak (or absent) adjacent to large impact basins and regions of volcanic activity, indicating erasure by thermal events. Notably, the northern plains lack such anomalies almost entirely. These Martian anomalies superficially resemble magnetic stripes that form via seafloor spreading on Earth today (Vine and Matthews, 1963); however, these extraterrestrial examples are around ten-times wider than those found on Earth and lack a well-defined spreading center (Connerney et al., 2001). Such features may be interpreted to record plate tectonic-like behavior characterized by either faster spreading and/or slower magnetic-field reversal rates, although other mechanisms have been proposed, including dike intrusion (Nimmo, 2000) and the lateral accretion of multiple micro-continents (Fairén et al., 2002) akin to the Northern Cordillera on Earth today. In either of the latter cases, significant horizontal plate motion is still required.

One additional theory of note put forward to support the operation of plate tectonics early in Martian history relates to the Valles Marineris trough system, which reportedly hosts a large-scale (> 2000-km-long and 50-km-wide) strike-slip fault zone, resembling transform faults that define transverse plate boundaries on Earth (Yin, 2012). An apparent sinistral offset of ~150 km of an ancient impact basin along this transtensional fault zone was identified by Yin (2012) from satellite imagery, and the absence of deformation in both adjoining crustal blocks was suggeststed to show that they were rigid at the time of faulting. In a similar vein to the debate surrounding magnetic stripes in the southern highlands, the scale of the Valles Marineris trough system is much larger than any equivalent examples seen on Earth, although a total displacement of ~150 km is almost identical in magnitude compared to terrestrial transform faults, such as the San Andreas fault, USA (Sieh and Jahns, 1984; Revenaugh and Reasoner, 1997), or Karakoram fault, Ladakh Himalaya (Robinson, 2009; Wang et al., 2012). Nonetheless, competing theories for formation (or accentuation) of this trough system have been proposed, including graben (rift) formation due to deformation related to magmatic overpressure in the Tharis region (Andrews-Hanna, 2011), catastrophic flooding, or collapse due to withdrawl of subsurface magma (McCauley et al., 1972). Further robotic and/or manned exploration missions, with or without sample return, present the best hope of deciphering Mars' early tectonic history, and so shed light on that of the Earth.

7.1.3. Exoplanets

While our ability to locate and characterize the orbital, physical, and/or basic geochemical properties of planets outside of our solar

system (exoplanets) has improved significantly in recent years (Borucki et al., 2010; Schneider et al., 2011; Miller et al., 2014; Pepe et al., 2014), it is impossible at this time to directly infer the operation of plate tectonics on such a body with any level of confidence. Indeed, such a discovery would make the exoplanet a prime candidate for harboring intelligent life (cf. Stern, 2016; Tosi et al., 2017), assuming extraneous factors are favorable, such as location within the circumstellar habitable zone (Abe et al., 2011).

In recent years, there has been a surge of interest in applying thermo-mechanical modeling (Foley et al., 2012; Noack and Breuer, 2014) and petrological phase equilibrium modeling to exoplanet interiors (Unterborn et al., 2014; Dorn et al., 2015) to infer the possibility of mantle convection. Indeed, it has even been proposed that the development of plate tectonics is inevitable on super-Earths (Valencia et al., 2007), which have masses ~2–10 times that of our home planet (Charbonneau et al., 2009). Exoplanets with masses significantly greater than Earth are likely to have gas- or ice-rich outer shells, such as the Jovians in our solar system. In the former case of the gas giants, the lack of well-defined solid surfaces precludes any kind of pseudo-plate-like behavior (Lunine, 2001), although convection in nitrogen-ice sheets on Sputnik Planum, Pluto, has been suggested to represent a type of "sluggish-lid" behavior (McKinnon et al., 2016). Indeed, several types of stagnant- and mobile-lid tectonic features have been reported from small bodies in our solar system, including Io (Bland and McKinnon, 2016; Moore et al., 2017) and Europa (Howell and Pappalardo, 2019), and potentially also Enceladus (Kargel and Pozio, 1996; Gioia et al., 2007), Triton (Prockter et al., 2005), and Titan (Collins et al., 2009). While exoplanets of similar masses to these Jovian satellites are too small to be identified by currently available detection techniques (Fischer et al., 2015), they very likely exist and may one day hold great scientific value for deciphering the early history of the Earth.

7.2. Integrated modeling of the early Earth

Great strides have been made in recent years in the capabilities of both geodynamic (Section 3.4.1) and petrological (Section 3.4.2) modeling as tools with which to characterize the tectonic evolution of the Earth (cf. Gerya, 2019). Each technique can provide critically important, but independent, constraints on the possible thermal characteristics of the Archean and Proterozoic mantle, and associated continental and/or oceanic crust (Diener et al., 2005; Nagel et al., 2012; Palin and White, 2016; Nicoli and Dyck, 2018; Wiemer et al., 2018; Gardiner et al., 2019). Early attempts to combine both techniques met with limited success, as an overwhelming amount of computational power is required to effectively simultaneously correlate tens-of-kilometer-scale structural deformation with the relatively fine detail of meter- or centimeter-scale mineralogical change driving metamorphic reaction and melt generation. Further, it has also only become computationally possible in recent years to expand two-dimensional simulations into a more realistic three-dimensional framework, thus allowing examination of cross sections and surficial spatial relationships well documented in exhumed Archean terranes (e.g. dome-and-keel architecture; Fischer and Gerya, 2016a). Continual improvement to thermodynamic databases (e.g. Holland and Powell, 2011) and activity–composition relations used to characterize metamorphism and anatexis in mafic and ultramafic lithologies (e.g. Holland et al., 2018) representative of subducted oceanic crust (e.g. eclogite) or adiabatically decompressed mantle now allow forward modeling to be fully integrated with lithospheric scale thermo-mechanical simulations (Rozel et al., 2017; Piccolo et al., 2019).

A relatively underused petrological modeling technique that has much relevance to continent formation on the early Earth is that of reactive transport between melt fractions as they ascend through the crust and potentially hybridize in composite magma chambers. Preliminary investigations of magma-mixing in Archean terranes have been conducted in recent years, but only in-depth investigations of the

petrological and geodynamic (e.g. rheological) effects of (pseudo)real-time melt transfer through the crust or mantle can come close to approaching reality. For example, arguments for steep subduction and slab melting during the Archean have conventionally relied on the requirement of a plagioclase-free eclogite-facies metabasic source rock (e.g. Section 3.4.2), with high Mg# and Cr contents in so-called high-pressure TTGs interpreted to represent component exchange during ascent through the ultramafic mantle wedge (Rapp et al., 2003). While subsequent studies have shown that the geochemical signatures in Archean high-pressure TTGs can be replicated without steep subduction, it seems necessary that some interaction with the ultramafic mantle is required (Martin, 1999; Moyen, 2011). Effective constraints on residence or transport times through this wedge derived from reactive transport calculations may provide new constraints supporting or refuting the possibility of subduction-driven continental crust formation on the early Earth entirely, although a new generation of integrated petrological–geodynamic models will be required to do so.

7.3. Concluding remarks

Many research groups are already strongly invested in particular interpretations of secular change through Earth history, and it is possible that the details provided in this review are unlikely to change some hearts or minds. Nonetheless, the authors hope that it represents a somewhat concise introduction to the state of play at the turn of the decade, and we are excited to see how these scientific opinions may change over the next 10, 25, or 50 years! As so eloquently stated by Hooykaas (1963), we may be unfortunately hindered in our ability to discern what the Hadean, Archean, or even Proterozoic Earth may have looked like, given our vast knowledge of how the Phanerozoic Earth has evolved: *"By explaining past changes by analogy with present phenomena, a limit is set to conjecture, for there is only one way in which two things are equal, but there is an infinity of ways in which they could be supposed different."* In this case, looking and working 'outside of the box' may be of critical importance to making advances in this field, which we are now being given the opportunity to do so with the recent resurgence of interest in exploration of our neighboring rocky planets and moons. It truly is a Golden Age to study petrology, tectonics, and comparative planetology.

Declaration of Competing Interest

The authors declare that they have no known competing financial interests or personal relationships that could have appeared to influence the work reported in this paper.

References

Abbott, D., Burgess, L., Longhi, J., Smith, W.H., 1994. An empirical thermal history of the Earth's upper mantle. J. Geophys. Res. Solid Earth 99, 13835–13850.
Abe, Y., 1997. Thermal and chemical evolution of the terrestrial magma ocean. Phys. Earth Planet. Inter. 100, 27–39.

Abe, Y., Abe-Ouchi, A., Sleep, N.H., Zahnle, K.J., 2011. Habitable zone limits for dry planets. Astrobiology 11, 443–460.

Acuña, M.H., Connerney, J.E.P., Ness, N.F., Lin, R.P., Mitchell, D., Carlson, C.W., McFadden, J., Anderson, K.A., Rème, H., Mazelle, C., Vignes, D., Wasilewski, P., Cloutier, P., 1999. Global distribution of crustal magnetization discovered by the Mars Global Surveyor MAG/ER experiment. Science 284, 790–793.

Adam, J., Rushmer, T., O'Neil, J., Francis, D., 2012. Hadean greenstones from the Nuvvuagittuq fold belt and the origin of the Earth's early continental crust. Geology 40, 363–366.

Agard, P., Yamato, P., Jolivet, L., Burov, E., 2009. Exhumation of oceanic blueschists and eclogites in subduction zones: Timing and mechanisms. Earth Sci. Rev. 92, 53–79.

Agard, P., Zuo, X., Funiciello, F., Bellahsen, N., Faccenna, C., Savva, D., 2014. Obduction: Why, how and where. Clues from analog models. Earth Planet. Sci. Lett. 393, 132–145.

Anbar, A.D., Duan, Y., Lyons, T.W., Arnold, G.L., Kendall, B., Creaser, R.A., Kaufman, A.J., Gordon, G.W., Scott, C., Garvin, J., Buick, R., 2007. A whiff of oxygen before the great oxidation event? Science 317, 1903–1906.

Anderson, D.L., 1995. Lithosphere, asthenosphere, and perisphere. Rev. Geophys. 33, 125–149.

Anderson, D.L., 2000. The thermal state of the upper mantle; no role for mantle plumes. Geophys. Res. Lett. 27, 3623–3626.

Anderson, D.L., Bass, J.D., 1986. Transition region of the Earth's upper mantle. Nature 320, 321–325.

Anderson, R.N., Honnorez, J., Becker, K., Adamson, A.C., Alt, J.C., Emmermann, R., Kempton, P.D., Kinoshita, H., Laverne, C., Mottl, M.J., Newmark, R.L., 1982. DSDP Hole 504B, the first reference section over 1 km through Layer 2 of the oceanic crust. Nature 300, 589–593.

Andrews-Hanna, J.C., 2011. The formation of Valles Marineris, Mars. Lunar and Planet. Sci. Conf. Abs. 42, 2182.

Anovitz, L.M., Essene, E.J., 1990. Thermobarometry and pressure–temperature paths in the Grenville Province of Ontario. J. Petrol. 31, 197–241.

Armstrong, R., 1981. Radiogenic isotopes: The case for crustal recycling on a near-steady-state no-continental-growth Earth. Phil. Trans. R. Soc. Lond. Ser. A. Math. Phys. Sci. 301, 443–472.

Arndt, N.T., 2003. Komatiites, kimberlites, and boninites. J. Geophys. Res. 108 (B6), 2293.

Arndt, N.T., Goldstein, S.L., 1987. Use and abuse of crust-formation ages. Geology 15, 893–895.

Arndt, N.T., Kerr, A.C., Tarney, J., 1997. Dynamic melting in plume heads: The formation of Gorgona komatiites and basalts. Earth Planet. Sci. Lett. 146, 289–301.

Artemieva, I.M., 2006. Global 1° × 1° thermal model TC1 for the continental lithosphere: Implications for lithosphere secular evolution. Tectonophysics 416, 245–277.

Aspler, L.B., Chiarenzelli, J.R., 1998. Two Neoarchean supercontinents? Evidence from the Paleoproterozoic. Sediment. Geol. 120, 75–104.

Audet, P., Bostock, M.G., Christensen, N.I., Peacock, S.M., 2009. Seismic evidence for overpressured subducted oceanic crust and megathrust fault sealing. Nature 457, 76–80.

Austrheim, H., 1990. The granulite-eclogite facies transition: A comparison of experimental work and a natural occurrence in the Bergen Arcs, western Norway. Lithos 25, 163–169.

Bada, J.L., Korenaga, J., 2018. Exposed areas above sea level on Earth > 3.5 Gyr ago: Implications for prebiotic and primitive biotic chemistry. Life 8, 55.

Bailey, E.H., 1961. Metamorphic facies of the Franciscan formation of California and their geologic significance. Geol. Soc. Am. Spec. Publ. 68, 4–5.

Bajracharya, M., Maimone, M.W., Helmick, D., 2008. Autonomy for mars rovers: Past, present, and future. Computer 41, 44–50.

Baker, V.R., Strom, R.G., Gulick, V.C., Kargel, J.S., Komatsu, G., Kale, V.S., 1991. Ancient oceans, ice sheets and the hydrological cycle on Mars. Nature 352, 589–593.

Balestro, G., Festa, A., Borghi, A., Castelli, D., Gattiglio, M., Tartarotti, P., 2018. Role of Late Jurassic intra-oceanic structural inheritance in the Alpine tectonic evolution of the Monviso meta-ophiolite complex (Western Alps). Geol. Mag. 155, 233–249.

Barley, M.E., Brown, S.J.A., Krapez, B., 2006. Felsic volcanism in the eastern Yilgarn craton, Western Australia: Evolution of a late Archean convergent margin. Geochim. Cosmochim. Acta 70, A35.

Barnes, S.J., van Kranendonk, M.J., 2014. Archean andesites in the east Yilgarn craton, Australia: Products of plume-crust interaction? Lithosphere 6, 80–92.

Barrell, J., 1914. The strength of the Earth's crust. J. Geol. 22, 289–314.

Becker, T.W., Faccenna, C., 2009. A review of the role of subduction dynamics for regional and global plate motions. In: Subduction Zone Geodynamics. Springer, Berlin, Heidelberg, pp. 3–34.

Bédard, J.H., 2006. A catalytic delamination-driven model for coupled genesis of Archaean crust and sub-continental lithospheric mantle. Geochim. Cosmochim. Acta 70, 1188–1214.

Bédard, J.H., 2013. How many arcs can dance on the head of a plume? A 'Comment' on: A critical assessment of Neoarchean 'plume only' geodynamics: Evidence from the Superior province, by Derek Wyman. Precambrian Res. 229, 189–197.

Bédard, J.H., 2018. Stagnant lids and mantle overturns: Implications for Archaean tectonics, magmagenesis, crustal growth, mantle evolution, and the start of plate tectonics. Geosci. Front. 9, 19–49.

Bédard, J.H., Brouillette, P., Madore, L., Berclaz, A., 2003. Archaean cratonization and deformation in the northern Superior Province, Canada: An evaluation of plate tectonic versus vertical tectonic models. Precambrian Res. 127, 61–87.

Bekker, A., Holland, H.D., Wang, P.L., Rumble Iii, D., Stein, H.J., Hannah, J.L., Coetzee, L.L., Beukes, N.J., 2004. Dating the rise of atmospheric oxygen. Nature 427, 117–121.

Bercovici, D., 2003. The generation of plate tectonics from mantle convection. Earth Planet. Sci. Lett. 205, 107–121.

Bickle, M.J., Nisbet, E.G., Martin, A., 1994. Archean greenstone belts are not oceanic crust. J. Geol. 102, 121–138.

Birch, F., LeComte, P., 1960. Temperature–pressure plane for albite composition. Am. J. Sci. 258, 209–217.

Bjørnerud, M.G., Austrheim, H., 2004. Inhibited eclogite formation: The key to the rapid growth of strong and buoyant Archean continental crust. Geology 32, 765–768.

Bland, M.T., McKinnon, W.B., 2016. Mountain building on Io driven by deep faulting. Nat. Geosci. 9, 429–433.

Bleeker, W., 2003. The late Archean record: A puzzle in ca. 35 pieces. Lithos 71, 99–134.

Blundy, J., Wood, B., 2003. Partitioning of trace elements between crystals and melts. Earth Planet. Sci. Lett. 210, 383–397.

Boak, J.L., Dymek, R.F., 1982. Metamorphism of the ca. 3800 Ma supracrustal rocks at Isua, West Greenland: Implications for early Archaean crustal evolution. Earth Planet. Sci. Lett. 59, 155–176.

Boehnke, P., Bell, E.A., Stephan, T., Trappitsch, R., Keller, C.B., Pardo, O.S., Davis, A.M., Harrison, T.M., Pellin, M.J., 2018. Potassic, high-silica Hadean crust. Proc. Natl. Acad. Sci. 115, 6353–6356.

Bohlen, S.R., 1987. Pressure–temperature–time paths and a tectonic model for the evolution of granulites. J. Geol. 95, 617–632.

Bohlen, S.R., 1991. On the formation of granulites. J. Metamorph. Geol. 9, 223–229.

Bohlen, S.R., Mezger, K., 1989. Origin of granulite terranes and the formation of the lowermost continental crust. Science 244, 326–329.

Boily, M., Dion, C., 2002. Geochemistry of boninite-type volcanic rocks in the Frotet-Evens greenstone belt, Opatica subprovince, Quebec: Implications for the evolution of Archean greenstone belts. Precambr. Res. 115, 349–371.

Borucki, W.J., Koch, D., Basri, G., Batalha, N., Brown, T., Caldwell, D., Caldwell, J., Christensen-Dalsgaard, J., Cochran, W.D., DeVore, E., Dunham, E.W., 2010. Kepler planet-detection mission: Introduction and first results. Science 327, 977–980.

Bottke, W.F., Norman, M.D., 2017. The late heavy bombardment. Annu. Rev. Earth Planet. Sci. 45.

Bown, J.W., White, R.S., 1994. Variation with spreading rate of oceanic crustal thickness and geochemistry. Earth Planet. Sci. Lett. 121, 435–449.

Bowring, S.A., Williams, I.S., 1999. Priscoan (4.00–4.03 Ga) orthogneisses from north-western Canada. Contrib. Mineral. Petrol. 134, 3–16.

Brandt, S., Klemd, R., Okrusch, M., 2003. Ultrahigh-temperature metamorphism and multistage evolution of garnet–orthopyroxene granulites from the Proterozoic Epupa Complex, NW Namibia. J. Petrol. 44, 1121–1144.

Brasier, M.D., Lindsay, J.F., 1998. A billion years of environmental stability and the emergence of eukaryotes: New data from northern Australia. Geology 26, 555–558.

Breuer, D., Spohn, T., 1993. Cooling of the Earth, Urey ratios, and the problem of potassium in the core. Geophys. Res. Lett. 20, 1655–1658.

Brown, M., Johnson, T.E., 2018. Secular change in metamorphism and the onset of global plate tectonics. Am. Mineral. 103, 181–196.

Brown, M., Johnson, T., Gardiner, N.J., 2020. Plate tectonics and the Archean Earth. Annu. Rev. Earth Planet. Sci. 48.

Buchan, K.L., 2013. Key paleomagnetic poles and their use in Proterozoic continent and supercontinent reconstructions: A review. Precambrian Res. 238, 93–110.

Buchan, K.L., Mitchell, R.N., Bleeker, W., Hamilton, M.A., LeCheminant, A.N., 2016. Paleomagnetism of ca. 2.13–2.11 Ga Indin and ca. 1.885 Ga Ghost dyke swarms of the Slave craton: Implications for the Slave craton APW path and relative drift of Slave, Superior and Siberian cratons in the Paleoproterozoic. Precambrian Res. 275, 151–175.

Bucher, K., Grapes, R., 2011. Metamorphism of Mafic Rocks. In: Petrogenesis of Metamorphic Rocks. Springer, Berlin, Heidelberg, pp. 339–393.

Bunge, H.P., Richards, M.A., Baumgardner, J.R., 1996. Effect of depth-dependent viscosity on the planform of mantle convection. Nature 379, 436–440.

Burke, K., Kidd, W.S.F., 1978. Were Archean continental geothermal gradients much steeper than those of today? Nature 272, 240–244.

Burov, E.B., 2011. Rheology and strength of the lithosphere. Mar. Pet. Geol. 28, 1402–1443.

Burov, E., Cloetingh, S., 2010. Plume-like upper mantle instabilities drive subduction initiation. Geophys. Res. Lett. 37 (3).

Campbell, I.H., Allen, C.M., 2008. Formation of supercontinents linked to increases in atmospheric oxygen. Nat. Geosci. 1, 554–558.

Campbell, I.H., Griffiths, R.W., Hill, R.I., 1989. Melting in an Archean mantle plume: Heads it's basalts, tails it's komatiites. Nature 339, 697–701.

Canup, R.M., 2012. Forming a Moon with an Earth-like composition via a giant impact. Science 338, 1052–1055.

Cao, W., Gilotti, J.A., Massonne, H.J., Ferrando, S., Foster Jr., C.T., 2019. Partial melting due to breakdown of an epidote-group mineral during exhumation of ultrahigh-pressure eclogite: An example from the North-East Greenland Caledonides. J. Metamorph. Geol. 37, 15–39.

Capitanio, F.A., Nebel, O., Cawood, P.A., Weinberg, R.F., Chowdhury, P., 2019. Reconciling thermal regimes and tectonics of the early Earth. Geology 47, 923–927.

Carbotte, S.M., Scheirer, D.S., 2004. The global mid-ocean ridge. Hydrogeol. Oceanic Lithos. 1, 59–74.

Carswell, D.A., O'Brien, P.J., 1993. Thermobarometry and geotectonic significance of high-pressure granulites: Examples from the Moldanubian Zone of the Bohemian Massif in Lower Austria. J. Petrol. 34, 427–459.

Catling, D.C., Zahnle, K.J., McKay, C.P., 2001. Biogenic methane, hydrogen escape, and the irreversible oxidation of early Earth. Science 293, 839–843.

Cawood, P.A., Kröner, A., Pisarevsky, S., 2006. Precambrian plate tectonics: Criteria and evidence. GSA Today 16, 4–11.

Cawood, P.A., Kröner, A., Collins, W.J., Kusky, T.M., Mooney, W.D., Windley, B.F., 2009. Accretionary orogens through Earth history. Geol. Soc. Lond., Spec. Publ. 318, 1–36.

Cawood, P.A., Hawkesworth, C.J., Pisarevsky, S.A., Dhuime, B., Capitanio, F.A., Nebel,

O., 2018. Geological archive of the onset of plate tectonics. Philos. Trans. R. Soc. A Math. Phys. Eng. Sci. 376, 20170405.

Charbonneau, D., Berta, Z.K., Irwin, J., Burke, C.J., Nutzman, P., Buchhave, L.A., Lovis, C., Bonfils, X., Latham, D.W., Udry, S., Murray-Clay, R.A., 2009. A super-Earth transiting a nearby low-mass star. Nature 462, 891–895.

Chardon, D., Choukroune, P., Jayananda, M., 1996. Strain patterns, décollement and incipient sagducted greenstone terrains in the Archaean Dharwar craton (south India). J. Struct. Geol. 18, 991–1004.

Chase, C.G., Patchett, P.J., 1988. Stored mafic/ultramafic crust and early Archean mantle depletion. Earth Planet. Sci. Lett. 91, 66–72.

Chen, Y.J., 1992. Oceanic crustal thickness versus spreading rate. Geophys. Res. Lett. 19, 753–756.

Cheng, Q., 2018. Extrapolations of secular trends in magmatic intensity and mantle cooling: Implications for future evolution of plate tectonics. Gondwana Res. 63, 268–273.

Chopin, C., 1984. Coesite and pure pyrope in high-grade blueschists of the Western Alps: A first record and some consequences. Contrib. Mineral. Petrol. 86, 107–118.

Christensen, N.I., Mooney, W.D., 1995. Seismic velocity structure and composition of the continental crust: A global view. J. Geophys. Res. Solid Earth 100 (B6), 9761–9788.

Ciborowski, T.J.R., Kerr, A.C., 2016. Did mantle plume magmatism help trigger the Great Oxidation Event? Lithos 246, 128–133.

Citron, R.I., Manga, M., Hemingway, D.J., 2018. Timing of oceans on Mars from shoreline deformation. Nature 555, 643–647.

Clark, C., Fitzsimons, I.C., Healy, D., Harley, S.L., 2011. How does the continental crust get really hot? Elements 7, 235–240.

Clarke, G.L., Powell, R., Fitzherbert, J.A., 2006. The lawsonite paradox: A comparison of field evidence and mineral equilibria modelling. J. Metamorph. Geol. 24, 715–725.

Clemens, J.D., 1990. The granulite—granite connexion. In: Granulites and crustal evolution. Springer, Dordrecht, pp. 25–36.

Clift, P.D., Vannucchi, P., Morgan, J.P., 2009. Crustal redistribution, crust–mantle recycling and Phanerozoic evolution of the continental crust. Earth Sci. Rev. 97, 80–104.

Collins, W.J., 2002. Hot orogens, tectonic switching, and creation of continental crust. Geology 30, 535–538.

Collins, G.C., McKinnon, W.B., Moore, J.M., Nimmo, F., Pappalardo, R.T., Prockter, L.M., Schenk, P.M., 2009. Tectonics of the outer planet satellites. Planet. Tecton. 11, 229.

Condie, K.C., 1981. Archean greenstone belts. Vol. 3 Elsevier.

Condie, K.C., 1985. Secular variation in the composition of basalts: An index to mantle evolution. J. Petrol. 26, 545–563.

Condie, K.C., 1994. Greenstones through time. In: Condie, K.C. (Ed.), Archean Crustal Evolution. Elsevier, Amsterdam, pp. 85–120.

Condie, K.C., 2001. Mantle Plumes and their Record in Earth History. Cambridge University Press, U.K., pp. 303.

Condie, K.C., 2003. Incompatible element ratios in oceanic basalts and komatiites: Tracking deep mantle sources and continental growth rates with time. Geochem. Geophys. Geosyst. 4, 1–28.

Condie, K.C., 2004. Supercontinents and superplume events: Distinguishing signals in the geologic record. Phys. Earth Planet. Inter. 146, 319–332.

Condie, K.C., 2005. Earth as an Evolving Planetary System. Academic Press.

Condie, K.C., 2015. Changing tectonic settings through time: Indiscriminate use of geochemical discriminant diagrams. Precambrian Res. 266, 587–591.

Condie, K.C., 2018. A planet in transition: The onset of plate tectonics on Earth between 3 and 2 Ga? Geosci. Front. 9, 51–60.

Condie, K.C., Aster, R.C., 2010. Episodic zircon age spectra of orogenic granitoids: The supercontinent connection and continental growth. Precambrian Res. 180, 227–236.

Condie, K.C., Benn, K., 2006. Archean geodynamics: Similar to or different from modern geodynamics? Am. Geophys. Union Monogr. 164, 47–59.

Condie, K.C., Kröner, A., 2008. When did plate tectonics begin? Evidence from the geologic record. Geol. Soc. Am. Spec. Pap. 440, 281–294.

Condie, K.C., Aster, R.C., van Hunen, J., 2016. A great thermal divergence in the mantle beginning 2.5 Ga: Geochemical constraints from greenstone basalts and komatiites. Geosci. Front. 7, 543–553.

Connerney, J.E.P., Acuña, M.H., Wasilewski, P.J., Ness, N.F., Rème, H., Mazelle, C., Vignes, D., Lin, R.P., Mitchell, D.L., Cloutier, P.A., 1999. Magnetic lineations in the ancient crust of Mars. Science 284, 794–798.

Connerney, J.E.P., Acuña, M.H., Wasilewski, P.J., Ness, N.F., Reme, H., Lin, R.P., Mitchell, D.L., 2001. The global magnetic field of Mars and implications for crustal evolution. Geophys. Res. Lett. 28, 4015–4018.

Connolly, J.A., 2005. Computation of phase equilibria by linear programming: A tool for geodynamic modeling and its application to subduction zone decarbonation. Earth Planet. Sci. Lett. 236, 524–541.

Conrad, C.P., Lithgow-Bertelloni, C., 2002. How mantle slabs drive plate tectonics. Science 298, 207–209.

Crosby, A.G., McKenzie, D., Sclater, J.G., 2006. The relationship between depth, age and gravity in the oceans. Geophys. J. Int. 166, 553–573.

Crowley, J.L., 2003. U–Pb geochronology of 3810–3630 Ma granitoid rocks south of the Isua greenstone belt, southern West Greenland. Precambrian Res. 126, 235–257.

Ćuk, M., Stewart, S.T., 2012. Making the Moon from a fast-spinning Earth: A giant impact followed by resonant de-spinning. Science 338, 1047–1052.

Cutts, J.A., Balint, T.S., Chassefiere, E., Kolawa, E.A., 2007. Technology perspectives in the future exploration of Venus. Geophys. Monogr. Am. Geophys. Union 176, 207–211.

Dann, J.C., 1997. Pseudostratigraphy and origin of the early Proterozoic Payson ophiolite, central Arizona: Geol. Soc. Am. Bull., 109, 347–365.

Davaille, A., Smrekar, S.E., Tomlinson, S., 2017. Experimental and observational evidence for plume-induced subduction on Venus. Nat. Geosci. 10, 349–353.

Davies, G.F., 1992. On the emergence of plate tectonics. Geology 20, 963–966.

Davies, G.F., 2009. Effect of plate bending on the Urey ratio and the thermal evolution of the mantle. Earth Planet. Sci. Lett. 287, 513–518.

Day, H.W., 2012. A revised diamond-graphite transition curve. Am. Mineral. 97, 52–62.

De Paoli, M.C., Clarke, G.L., Daczko, N.R., 2012. Mineral equilibria modeling of the granulite–eclogite transition: Effects of whole-rock composition on metamorphic facies type-assemblages. J. Petrol. 53, 949–970.

De Wit, M.J., de Ronde, C.E., Tredoux, M., Roering, C., Hart, R.J., Armstrong, R.A., Green, R.W., Peberdy, E., Hart, R.A., 1992. Formation of an Archaean continent. Nature 357, 553–557.

Debaille, V., O'Neill, C., Brandon, A.D., Haenecour, P., Yin, Q.Z., Mattielli, N., Treiman, A.H., 2013. Stagnant-lid tectonics in early Earth revealed by ^{142}Nd variations in late Archean rocks. Earth Planet. Sci. Lett. 373, 83–92.

Deines, P., 1980. The carbon isotopic composition of diamonds: Relationship to diamond shape, color, occurrence and vapor compositon. Geochim. Cosmochim. Acta 44, 943–961.

Deng, J.C., Kusky, T., Polat, A., Wang, L., Wang, J., Wang, S., 2013. Geochemistry of Neoarchean mafic volcanic rocks and late mafic dikes in the Zanhuang Complex, Central Orogenic Belt, North China Craton: Implications for geodynamic setting. Lithos 175–176, 193–212.

Dewey, J.F., 1976. Ophiolite obduction. Tectonophysics 31, 93–120.

Dewey, J.F., Horsfield, B., 1970. Plate tectonics, orogeny and continental growth. Nature 225, 521.

Dewey, J., Spall, H., 1975. Pre-Mesozoic plate tectonics: How far back in Earth history can the Wilson Cycle be extended? Geology 3, 422–424.

Dhuime, B., Hawkesworth, C.J., Cawood, P.A., Storey, C.D., 2012. A change in the geodynamics of continental growth 3 billion years ago. Science 335, 1334–1336.

Dhuime, B., Wuestefeld, A., Hawkesworth, C.J., 2015. Emergence of modern continental crust about 3 billion years ago. Nat. Geosci. 8, 552–556.

Di Achille, G., Hynek, B.M., 2010. Ancient ocean on Mars supported by global distribution of deltas and valleys. Nat. Geosci. 3, 459–463.

Diener, J.F.A., Powell, R., 2012. Revised activity–composition models for clinopyroxene and amphibole. J. Metamorph. Geol. 30, 131–142.

Diener, J.F., Stevens, G., Kisters, A.F., Poujol, M., 2005. Metamorphism and exhumation of the basal parts of the Barberton greenstone belt, South Africa: Constraining the rates of Mesoarchaean tectonism. Precambrian Res. 143, 87–112.

Diener, J.F.A., Powell, R., White, R.W., Holland, T.J.B., 2007. A new thermodynamic model for clino-and orthoamphiboles in the system Na$_2$O–CaO–FeO–MgO–Al$_2$O$_3$–SiO$_2$–H$_2$O–O. J. Metamorph. Geol. 25, 631–656.

Dilek, Y., Furnes, H., 2011. Ophiolite genesis and global tectonics: Geochemical and tectonic fingerprinting of ancient oceanic lithosphere. Geol. Soc. Am. Bull. 123, 387–411.

Dilek, Y., Furnes, H., 2014. Ophiolites and their origins. Elements 10, 93–100.

Dokukina, K.A., Kaulina, T.V., Konilov, A.N., Mints, M.V., Van, K.V., Natapov, L., Belousova, E., Simakin, S.G., Lepekhina, E.N., 2014. Archean to Palaeoproterozoic high-grade evolution of the Belomorian eclogite province in the Gridino area, Fennoscandian Shield: Geochronological evidence. Gondwana Res. 25, 585–613.

Dorn, C., Khan, A., Heng, K., Connolly, J.A., Alibert, Y., Benz, W., Tackley, P., 2015. Can we constrain the interior structure of rocky exoplanets from mass and radius measurements? Astron. Astrophys. 577, A83–92.

Drummond, M.S., Defant, M.J., 1990. A model for trondhjemite-tonalite-dacite genesis and crustal growth via slab melting: Archean to modern comparisons. J. Geophys. Res. Solid Earth 95 (B13), 21503–21521.

Duffield, W.A., 1972. A naturally occurring model of global plate tectonics. J. Geophys. Res. 77, 2543–2555.

Duretz, T., Agard, P., Yamato, P., Ducassou, C., Burov, E.B., Gerya, T.V., 2016. Thermomechanical modeling of the obduction process based on the Oman ophiolite case. Gondwana Res. 32, 1–10.

Dziggel, A., Stevens, G., Poujol, M., Anhaeusser, C.R., Armstrong, R.A., 2002. Metamorphism of the granite–greenstone terrane south of the Barberton greenstone belt, South Africa: An insight into the tectono-thermal evolution of the 'lower' portions of the Onverwacht Group. Precambrian Res. 114, 221–247.

Eaton, D.W., Darbyshire, F., Evans, R.L., Grütter, H., Jones, A.G., Yuan, X., 2009. The elusive lithosphere–asthenosphere boundary (LAB) beneath cratons. Lithos 109, 1–22.

Edwards, S.J., Schellart, W.P., Duarte, J.C., 2015. Geodynamic models of continental subduction and obduction of overriding plate forearc oceanic lithosphere on top of continental crust. Tectonics 34, 1494–1515.

Elkins-Tanton, L.T., 2008. Linked magma ocean solidification and atmospheric growth for Earth and Mars. Earth Planet. Sci. Lett. 271, 181–191.

Elkins-Tanton, L.T., 2012. Magma oceans in the inner solar system. Annu. Rev. Earth Planet. Sci. 40, 113–139.

Ellis, D.J., 1987. Origin and evolution of granulites in normal and thickened crusts. Geology 15, 167–170.

Ellis, D.J., Maboko, M.A.H., 1992. Precambrian tectonics and the physicochemical evolution of the continental crust. I. The gabbro-eclogite transition revisited. Precambrian Res. 55, 491–506.

England, P.C., Bickle, M., 1984. Continental thermal and tectonic regimes during the Archaean. J. Geol. 92, 353–367.

England, P.C., Richardson, S.W., 1977. The influence of erosion upon the mineral facies of rocks from different metamorphic environments. J. Geol. Soc. 134, 201–213.

England, P.C., Thompson, A.B., 1984. Pressure–temperature–time paths of regional metamorphism I. Heat transfer during the evolution of regions of thickened continental crust. J. Petrol. 25, 894–928.

Ernst, W.G., 1963. Petrogenesis of glaucophane schists. J. Petrol. 4, 1–30.

Ernst, W.G., 2003. High-pressure and ultrahigh-pressure metamorphic belts—Subduction,

recrystallization, exhumation, and significance for ophiolite studies. In: Dilek, Y., Newcombe, S. (Eds.), Ophiolite Concept and Evolution of Geological Thought. Geological Society of America Special Paper 373. pp. 365–384.

Ernst, W.G., 2009. Archean plate tectonics, rise of Proterozoic supercontinentality, and onset of regional, episodic stagnant-lid behavior. Gondwana Res. 15, 243–253.

Ernst, W.G., 2017a. Earth's thermal evolution, mantle convection, and Hadean onset of plate tectonics. J. Asian Earth Sci. 145B, 334–348.

Ernst, W.G., 2017b. Kimberlites and the start of plate tectonics: Comment. Geology 44, 405.

Ernst, R.E., Desnoyers, D.W., 2004. Lessons from Venus for understanding mantle plumes on Earth. Phys. Earth Planet. Inter. 146, 195–229.

Ernst, R.E., Wingate, M.T.D., Buchan, K.L., Li, Z.X., 2008. Global record of 1600–700 Ma Large Igneous Provinces (LIPs): Implications for the reconstruction of the proposed Nuna (Columbia) and Rodinia supercontinents. Precambrian Res. 160, 159–178.

Eskola, P.E., 1920. The Mineral Facies of Rocks. Brøgger.

Evans, B.W., 1990. Phase relations of epidote-blueschists. Lithos 25, 3–23.

Evans, B.W., Brown, E.H. eds., 1986. Blueschists and Eclogites (Vol. 164). Geological Society of America.

Evans, D.A.D., Halls, H.C., 2010. Restoring Proterozoic deformation within the Superior craton. Precambrian Res. 183, 474–489.

Evans, D.A., Pisarevsky, S.A., 2008. Plate tectonics on early Earth? Weighing the paleo-magnetic evidence. GSA Special Paper 440, 249–263.

Faccenda, M., Burlini, L., Gerya, T.V., Mainprice, D., 2008. Fault-induced seismic aniso-tropy by hydration in subducting oceanic plates. Nature 455, 1097–1101.

Fairén, A.G., Ruiz, J., Anguita, F., 2002. An origin for the linear magnetic anomalies on Mars through accretion of terranes: Implications for dynamo timing. Icarus 160, 220–223.

Feisel, Y., White, R.W., Palin, R.M., Johnson, T.E., 2018. New constraints on granulite facies metamorphism and melt production in the Lewisian Complex, northwest Scotland. J. Metamorph. Geol. 36, 799–819.

Festa, A., Pini, G.A., Dilek, Y., Codegone, G., 2010. Mélanges and mélange-forming processes: A historical overview and new concepts. Int. Geol. Rev. 52, 1040–1105.

Festa, A., Pini, G.A., Ogata, K., Dilek, Y., 2019. Diagnostic features and field-criteria in recognition of tectonic, sedimentary and diapiric mélanges in orogenic belts and exhumed subduction-accretion complexes. Gondwana Res. 74, 7–30.

Fink, J.H., Bridges, N.T., Grimm, R.E., 1993. Shapes of Venusian "pancake" domes imply episodic emplacement and silicic composition. Geophys. Res. Lett. 20, 261–264.

Fischer, R., Gerya, T., 2016a. Early Earth plume-lid tectonics: A high-resolution 3D nu-merical modelling approach. J. Geodyn. 100, 198–214.

Fischer, R., Gerya, T., 2016b. Regimes of subduction and lithospheric dynamics in the Precambrian: 3D thermomechanical modelling. Gondwana Res. 37, 53–70.

Fischer, K.M., Ford, H.A., Abt, D.L., Rychert, C.A., 2010. The lithosphere-asthenosphere boundary. Annu. Rev. Earth Planet. Sci. 38, 551–575.

Fischer, D.A., Howard, A.W., Laughlin, G.P., Macintosh, B., Mahadevan, S., Sahlmann, J., Yee, J.C., 2014. Exoplanet detection techniques. In: Beuther, H. (Ed.), Protostars and Planets VI. Univ. of Arizona, Tucson, pp. 715–737. https://doi.org/10.2458/azu_uapress_9780816531240-ch031.

Flament, N., Coltice, N., Rey, P.F., 2008. A case for late-Archaean continental emergence from thermal evolution models and hypsometry. Earth Planet. Sci. Lett. 275, 326–336.

Floyd, P.A., Winchester, J.A., 1978. Identification and discrimination of altered. and metamorphosed volcanic rocks using immobile elements. Chem. Geol. 21, 291–306.

Foley, S.F., Tiepolo, M., Vannucci, R., 2002. Growth of early continental crust controlled by melting of amphibolite in subduction zones. Nature 417, 837–841.

Foley, S.F., Buhre, S., Jacob, D.E., 2003. Evolution of the Archaean crust by delamination and shallow subduction. Nature 421, 249–253.

Foley, B.J., Bercovici, D., Landuyt, W., 2012. The conditions for plate tectonics on super-Earths: Inferences from convection models with damage. Earth Planet. Sci. Lett. 331, 281–290.

Ford, P.G., Pettengill, G.H., 1992. Venus topography and kilometer-scale slopes. J. Geophys. Res. Planets 97, 13,103–13,114.

Forsyth, D., Uyeda, S., 1975. On the relative importance of the driving forces of plate motion. Geophys. J. R. Astron. Soc. 43, 163–200.

Foster, G., Parrish, R.R., 2003. Metamorphic monazite and the generation of *P–T–t* paths. Geol. Soc. Lond., Spec. Publ. 220, 25–47.

François, C., Debaille, V., Paquette, J.L., Baudet, D., Javaux, E.J., 2018. The earliest evidence for modern-style plate tectonics recorded by HP–LT metamorphism in the Paleoproterozoic of the Democratic Republic of the Congo. Sci. Rep. 8, 15452.

Frey, H., Schultz, R.A., 1988. Large impact basins and the mega-impact origin for the crustal dichotomy on Mars. Geophys. Res. Lett. 15, 229–232.

Friend, C.R., Nutman, A.P., 2010. Eoarchean ophiolites? New evidence for the debate on the Isua supracrustal belt, southern West Greenland. Am. J. Sci. 310, 826–861.

Fripp, R.E.P., Van Nierop, D.A., Callow, M.J., Lilly, P.A., Du Plessis, L.U., 1980. Deformation in part of the Archean Kaapvaal craton, South Africa. Precambrian Res. 13, 241–251.

Frost, B.R., Frost, C.D., 1987. CO_2, melts and granulite metamorphism. Nature 327, 503–507.

Fukao, Y., Hori, S., Ukawa, M., 1983. A seismological constraint on the depth of ba-salt–eclogite transition in a subducting oceanic crust. Nature 303, 413–417.

Furnes, H., Safonova, I., 2019. Ophiolites of the Central Asian Orogenic Belt: Geochemical and petrological characterization and tectonic settings. Geosci. Front. 10, 1255–1284.

Furnes, H., Rosing, M., Dilek, Y., de Wit, M., 2009. Isua supracrustal belt (Greenland) — a vestige of a 3.8 Ga suprasubduction zone ophiolite, and implications for Archean geology. Lithos 113, 115–132.

Furnes, H., Dilek, Y., De Wit, M., 2014a. Precambrian greenstone sequences represent different ophiolite types. Gondwana Res. 27, 649–685.

Furnes, H., De Wit, M., Dilek, Y., 2014b. Four billion years of ophiolites reveal secular trends in oceanic crust formation. Geosci. Front. 5, 571–603.

Fyfe, W.S., 1958. Metamorphic reactions and metamorphic facies. Geol. Soc. Am. 73.

Ganne, J., Feng, X., 2017. Primary magmas and mantle temperatures through time. Geochem. Geophys. Geosyst. 18, 872–888.

Ganne, J., De Andrade, V., Weinberg, R.F., Vidal, O., Dubacq, B., Kagambega, N., Naba, S., Baratoux, L., Jessell, M., Allibon, J., 2011. Modern-style plate subduction pre-served in the Palaeoproterozoic West African craton. Nat. Geosci. 5, 60–65.

Gao, P., Santosh, M., 2019. Building the Wutai arc: Insights into the Archean – Paleoproterozoic crustal evolution of the North China Craton. Precambrian Res. 333, 105429.

Gao, S., Rudnick, R.L., Yuan, H.L., Liu, X.M., Liu, Y.S., Xu, W.L., Ling, W.L., Ayers, J., Wang, X.C., Wang, Q.H., 2004. Recycling lower continental crust in the North China craton. Nature 432, 892–896.

Gao, S., Yang, J., Zhou, L., Li, M., Hu, Z., Guo, J., Yuan, H., Gong, H., Xiao, G., Wei, J., 2011. Age and growth of the Archean Kongling terrain, South China, with emphasis on 3.3 Ga granitoid gneisses. Am. J. Sci. 311, 153–182.

Gardiner, N.J., Kirkland, C.L., Hollis, J., Szilas, K., Steenfelt, A., Yakymchuk, C., Heide-Jørgensen, H., 2019. Building Mesoarchaean crust upon Eoarchaean roots: The Akia Terrane, West Greenland. Contrib. Mineral. Petrol. 174, 20–34.

Ge, R., Zhu, W., Wilde, S.A., Wu, H., 2018. Remnants of Eoarchean continental crust derived from a subducted proto-arc. Sci. Adv. 4, 3159–3162.

Gerya, T.V., 2014. Precambrian geodynamics: Concepts and models. Gondwana Res. 25, 442–463.

Gerya, T.V., 2015. Tectonic overpressure and underpressure in lithospheric tectonics and metamorphism. J. Metamorph. Geol. 33, 785–800.

Gerya, T.V., 2019. Geodynamics of the early Earth: Quest for the missing paradigm. Geology 47, 1006–1007.

Gerya, T.V., Connolly, J.A., Yuen, D.A., 2008. Why is terrestrial subduction one-sided? Geology 36, 43–46.

Gerya, T.V., Stern, R.J., Baes, M., Sobolev, S.V., Whattam, S.A., 2015. Plate tectonics on the Earth triggered by plume-induced subduction initiation. Nature 527, 221–225.

Giardini, D., Lognonné, P., Banerdt, W.B., et al., 2020. The seismicity of Mars. Nat. Geosci. 13, 205–212.

Gibbons, W., Mann, A., 1983. Pre-Mesozoic lawsonite in Anglesey, northern Wales: Preservation of ancient blueschists. Geology 11, 3–6.

Gill, R.C.O., 1979. Comparative petrogenesis of Archean and modern low-K tholeiites. A critical review of some geochemical aspects. Phys. Chem. Earth 11, 431–447.

Gioia, G., Chakraborty, P., Marshak, S., Kieffer, S.W., 2007. Unified model of tectonics and heat transport in a frigid Enceladus. Proc. Natl. Acad. Sci. 104, 13578–13581.

Girardeau, J., Mercier, J.C.C., Yougong, Z., 1985. Structure of the Xigaze ophiolite, Yarlung Zangbo suture zone, southern Tibet, China: Genetic implications. Tectonics 4, 267–288.

Glassley, W.E., Korstgård, J.A., Sørensen, K., Platou, S.W., 2014. A new UHP meta-morphic complex in the ~1.8 Ga Nagssugtoqidian Orogen of West Greenland. Am. Mineral. 99, 1315–1334.

Goodwin, A.M., 1996. Principles of Precambrian Geology. Elsevier.

Gorczyk, W., Smithies, H., Korhonen, F., Howard, H., De Gromard, R.Q., 2015. Ultra-hot Mesoproterozoic evolution of intracontinental central Australia. Geosci. Front. 6, 23–37.

Green, E.C.R., 2018. Metamorphic reactions and processes. In: White, W.M. (Ed.), Encyclopedia of Geochemistry. Encyclopedia of Earth Sciences Series Springer, Cham.

Green, D.H., Ringwood, A.E., 1967. An experimental investigation of the gabbro to eclogite transformation and its petrological applications. Geochim. Cosmochim. Acta 31, 767–833.

Green, E.C.R., Holland, T.J.B., Powell, R., 2007. An order-disorder model for omphacitic pyroxenes in the system jadeite-diopside-hedenbergite-acmite, with applications to eclogitic rocks. Am. Mineral. 92, 1181–1189.

Green, D.H., Hibberson, W.O., Kovács, I., Rosenthal, A., 2010. Water and its influence on the lithosphere–asthenosphere boundary. Nature 467, 448–452.

Green, E.C.R., White, R.W., Diener, J.F.A., Powell, R., Holland, T.J.B., Palin, R.M., 2016. Activity–composition relations for the calculation of partial melting equilibria in metabasic rocks. J. Metamorph. Geol. 34, 845–869.

Greenough, J.D., Ya'acoby, A., 2013. A comparative geochemical study of Mars and Earth basalt petrogenesis. Can. J. Earth Sci. 50, 78–93.

Griffin, W.L., Belousova, E.A., O'Neill, C.O.S.Y., O'Reilly, S.Y., Malkovets, V., Pearson, N.J., Spetsius, S., Wilde, S.A., 2014. The world turns over: Hadean–Archean crust--mantle evolution. Lithos 189, 2–15.

Grigné, C., Labrosse, S., Tackley, P.J., 2005. Convective heat transfer as a function of wavelength: Implications for the cooling of the Earth. J. Geophys. Res. Solid Earth 110 (B3).

Grove, T.L., Kinzler, R.J., Bryan, W.B., 1992. Fractionation of mid-ocean ridge basalt (MORB). In: Mantle Flow and Melt Generation at Mid-Ocean Ridges. 71. pp. 281–310.

Gumsley, A.P., Chamberlain, K.R., Bleeker, W., Söderlund, U., de Kock, M.O., Larsson, E.R., Bekker, A., 2017. Timing and tempo of the great oxidation event. Proc. Natl Acad. Sci. 114, 1811–1816.

Guo, J.H., O'Brien, P.J., Zhai, M., 2002. High-pressure granulites in the Sanggan area, North China craton: Metamorphic evolution, *P–T* paths and geotectonic significance. J. Metamorph. Geol. 20, 741–756.

Guo, Q., Strauss, H., Kaufman, A.J., Schröder, S., Gutzmer, J., Wing, B., Baker, M.A., Bekker, A., Jin, Q., Kim, S.T., Farquhar, J., 2009. Reconstructing Earth's surface oxidation across the Archean-Proterozoic transition. Geology 37, 399–402.

Guo, R., Liu, S., Santosh, M., Li, Q., Bai, X., Wang, W., 2013. Geochemistry, zircon U–Pb geochronology and Lu–Hf isotopes of metavolcanics from eastern Hebei reveal

Neoarchean subduction tectonics in the North China Craton. Gondwana Res. 24, 664–686.

Gurnis, M., Hall, C., Lavier, L., 2004. Evolving force balance during incipient subduction. Geochem. Geophys. Geosyst. 5 (7).

Hacker, B.R., 2006. Pressures and temperatures of ultrahigh-pressure metamorphism: Implications for UHP tectonics and H_2O in subducting slabs. Int. Geol. Rev. 48, 1053–1066.

Hacker, B.R., Wang, Q., 1995. Ar/Ar geochronology of ultrahigh-pressure metamorphism in central China. Tectonics 14, 994–1006.

Hacker, B.R., Abers, G.A., Peacock, S.M., 2003. Subduction factory 1. Theoretical mineralogy, densities, seismic wave speeds, and H_2O contents. J. Geophys. Res. Solid Earth 108 (B1).

Hacker, B., Luffi, P., Lutkov, V., Minaev, V., Ratschbacher, L., Plank, T., Ducea, M., Patiño-Douce, A., McWilliams, M., Metcalf, J., 2005. Near-ultrahigh pressure processing of continental crust: Miocene crustal xenoliths from the Pamir. J. Petrol. 46, 1661–1687.

Hacker, B.R., Kelemen, P.B., Behn, M.D., 2011. Differentiation of the continental crust by relamination. Earth Planet. Sci. Lett. 307, 501–516.

Hacker, B.R., Kelemen, P.B., Behn, M.D., 2015. Continental lower crust. Annu. Rev. Earth Planet. Sci. 43, 167–205.

Haggerty, S.E., 1986. Diamond genesis in a multiply constrained model. Nature 320, 34–37.

Hajná, J., Žák, J., Ackerman, L., Svojtka, M., Pašava, J., 2019. A giant late Precambrian chert-bearing olistostrome discovered in the Bohemian Massif: A record of Ocean Plate Stratigraphy (OPS) disrupted by mass-wasting along an outer trench slope. Gondwana Res. 74, 173–188.

Hall, C.E., Gurnis, M., Sdrolias, M., Lavier, L.L., Muller, R.D., 2003. Catastrophic initiation of subduction following forced convergence across fractures zones. Earth Planet. Sci. Lett. 212, 15–30.

Hamano, K., Abe, Y., Genda, H., 2013. Emergence of two types of terrestrial planet on solidification of magma ocean. Nature 497, 607–611.

Hamilton, W.B., 1998. Archean magmatism and deformation were not products of plate tectonics. Precambrian Res. 91, 143–179.

Hamilton, W.B., 2007. Comment on "A vestige of Earth's oldest ophiolite". Science 318, 746.

Hamilton, W.B., 2011. Plate tectonics began in Neoproterozoic time, and plumes from deep mantle have never operated. Lithos 123, 1–20.

Hansen, V.L., 2000. Geologic mapping of tectonic planets. Earth Planet. Sci. Lett. 176, 527–542.

Hansen, V.L., Olive, A., 2010. Artemis, Venus: The largest tectonomagmatic feature in the solar system? Geology 38, 467–470.

Harley, S.L., 1989. The origins of granulites: A metamorphic perspective. Geol. Mag. 126, 215–247.

Harley, S.L., 1998. On the occurrence and characterization of ultrahigh-temperature crustal metamorphism. Geol. Soc. Lond., Spec. Publ. 138, 81–107.

Harlow, G.E., Sorensen, S.S., Sisson, V.B., Shi, G., 2014. The geology of jade deposits. Mineral. Assoc. Can. Short-Course Ser. 44, 305–374.

Harlow, G.E., Tsujimori, T., Sorensen, S.S., 2015. Jadeitites and plate tectonics. Annu. Rev. Earth Planet. Sci. 43, 105–138.

Harris, P.T., 2020. Oceans created: Oceans destroyed. In Mysterious Ocean (pp. 13-22). Springer, Cham.

Harris, N.B.W., Caddick, M., Kosler, J., Goswami, S., Vance, D., Tindle, A.G., 2004. The pressure–temperature–time path of migmatites from the Sikkim Himalaya. J. Metamorph. Geol. 22, 249–264.

Harrison, T.M., 2009. The Hadean crust: evidence from > 4 Ga zircons. Annu. Rev. Earth Planet. Sci. 37, 479–505.

Harte, B., 2010. Diamond formation in the deep mantle: The record of mineral inclusions and their distribution in relation to mantle dehydration zones. Mineral. Mag. 74, 189–215.

Hartmann, W.K., Malin, M., McEwen, A., Carr, M., Soderblom, L., Thomas, P., Danielson, E., James, P., Veverka, J., 1999. Evidence for recent volcanism on Mars from crater counts. Nature 397, 586–590.

Hassani, R., Jongmans, D., Chery, J., 1997. Study of plate deformation and stress in subduction processes using two-dimensional numerical models. J. Geophys. Res. 102, 17951–17965.

Hastie, A.R., Fitton, J.G., Bromiley, G.D., Butler, I.B., Odling, N.W., 2016. The origin of Earth's first continents and the onset of plate tectonics. Geology 44, 855–858.

Hauber, E., Brož, P., Jagert, F., Jodłowski, P., Platz, T., 2011. Very recent and wide-spread basaltic volcanism on Mars. Geophys. Res. Lett. 38 (10).

Hauck II, S.A., Dombard, A.J., Phillips, R.J., Solomon, S.C., 2004. Internal and tectonic evolution of Mercury. Earth Planet. Sci. Lett. 222, 713–728.

Hawkesworth, C.J., Dhuime, B., Pietranik, A.B., Cawood, P.A., Kemp, A.I.S., Storey, C.D., 2010. The generation and evolution of the continental crust. J. Geol. Soc. 167, 229–248.

Hawkesworth, C.J., Cawood, P.A., Dhuime, B., 2016. Tectonics and crustal evolution. GSA Today, v. 26 26, 4–11.

Hawkesworth, C.J., Cawood, P.A., Dhuime, B., Kemp, T.I., 2017. Earth's continental lithosphere through time. Annu. Rev. Earth Planet. Sci. 45, 169–198.

Head, J.W., Crumpler, L.S., 1987. Evidence for divergent plate-boundary characteristics and crustal spreading on Venus. Science 238, 1380–1385.

Head, J.W., Solomon, S.C., 1981. Tectonic evolution of the terrestrial planets. Science 213, 62–76.

Head, J.W., Hiesinger, H., Ivanov, M.A., Kreslavsky, M.A., Pratt, S., Thomson, B.J., 1999. Possible ancient oceans on Mars: evidence from Mars Orbiter Laser Altimeter data. Science 286, 2134–2137.

Helmstaedt, H., Padgham, W.A., Brophy, J.A., 1986. Multiple dikes in Lower Kam Group,

Yellowknife greenstone belt: Evidence for Archean seafloor spreading? Geology 14, 562–566.

Hernández-Uribe, D., Palin, R.M., 2019a. A revised petrological model for subducted oceanic crust: Insights from phase equilibrium modelling. J. Metamorph. Geol. 37, 745–768.

Hernández-Uribe, D., Palin, R.M., 2019b. Catastrophic shear-removal of subcontinental lithospheric mantle beneath the Colorado Plateau by the subducted Farallon slab. Sci. Rep. 9, 8153–8159.

Hernández-Uribe, D., Gutiérrez-Aguilar, F., Mattinson, C.G., Palin, R.M., Neill, O.K., 2019. A new record of deeper and colder subduction in the Acatlán complex, Mexico: Evidence from phase equilibrium modelling and Zr-in-rutile thermometry. Lithos 324, 551–568.

Hernández-Uribe, D., Hernández-Montenegro, J.D., Cone, K.A., Palin, R.M., 2020. Oceanic slab-top melting during subduction: Implications for trace-element recycling and adakite petrogenesis. Geology 48, 216–220.

Herzberg, C., 1999. Phase equilibrium constraints on the formation of cratonic mantle. Geochem. Soc. Spec. Publ. 6, 241–257.

Herzberg, C., Asimow, P.D., Arndt, N., Niu, Y., Lesher, C.M., Fitton, J.G., Cheadle, M.J., Saunders, A.D., 2007. Temperatures in ambient mantle and plumes: Constraints from basalts, picrites, and komatiites. Geochem. Geophys. Geosyst. 8 (2).

Herzberg, C., Condie, K., Korenaga, J., 2010. Thermal history of the Earth and its petrological expression. Earth Planet. Sci. Lett. 292, 79–88.

Hoffman, P.F., 1997. Tectonic genealogy of North America. In: van der Pluijm, B.A., Marshak, S. (Eds.), Earth Structure: An Introduction to Structural Geology and Tectonics. McGraw-Hill, New York, pp. 459–464.

Hoffman, C., Keller, J., 1979. Xenoliths of lawsonite-ferroglaucophane rocks from a Quaternary volcano of Milos (Aegean Sea, Greece). Lithos 12, 209–219.

Hofmann, A.W., 1997. Mantle geochemistry: The message from oceanic volcanism. Nature 385, 219–225.

Hofmann, A.W., White, W.M., 1982. Mantle plumes from ancient oceanic crust. Earth Planet. Sci. Lett. 57, 421–436.

Hofmeister, A.M., 1983. Effect of a Hadean terrestrial magma ocean on crust and mantle evolution. J. Geophys. Res. Solid Earth 88 (B6), 4963–4983.

Holder, R.M., Hacker, B.R., Horton, F., Rakotondrazafy, A.M., 2018. Ultrahigh-temperature osumilite gneisses in southern Madagascar record combined heat advection and high rates of radiogenic heat production in a long-lived high-T orogen. J. Metamorph. Geol. 36, 855–880.

Holland, H.D., 2002. Volcanic gases, black smokers, and the Great Oxidation Event. Geochim. Cosmochim. Acta 66, 3811–3826.

Holland, T.J.B., Powell, R., 2011. An improved and extended internally consistent thermodynamic dataset for phases of petrological interest, involving a new equation of state for solids. J. Metamorph. Geol. 29, 333–383.

Holland, T.J., Green, E.C.R., Powell, R., 2018. Melting of peridotites through to granites: A simple thermodynamic model in the system KNCFMASHTOCr. J. Petrol. 59, 881–900.

Hooykaas, R., 1963. The Principle of Uniformity in Geology, Biology, and Theology. E.J. Brill, London.

Hopkins, M., Harrison, T.M., Manning, C.E., 2008. Low heat flow inferred from > 4 Gyr zircons suggests Hadean plate boundary interactions. Nature 456, 493–496.

Hoskin, P.W., 2005. Trace-element composition of hydrothermal zircon and the alteration of Hadean zircon from the Jack Hills, Australia. Geochim. Cosmochim. Acta 69, 637–648.

Hosono, N., Karato, S.I., Makino, J., Saitoh, T.R., 2019. Terrestrial magma ocean origin of the Moon. Nat. Geosci. 12, 418–423.

Houseman, G.A., McKenzie, D.P., Molnar, P., 1981. Convective instability of a thickened boundary layer and its relevance for the thermal evolution of continental convergent belts. J. Geophys. Res. Solid Earth 86 (B7), 6115–6132.

Howell, S.M., Pappalardo, R.T., 2019. Can Earth-like plate tectonics occur in ocean world ice shells? Icarus 322, 69–79.

Huang, G., Guo, J., Jiao, S., Palin, R.M., 2019. What drives the continental crust to be extremely hot so quickly? J. Geophys. Res. Solid Earth 124, 11218–11231.

Humphris, S.E., Herzig, P.M., Miller, D.J., Alt, J.C., Becker, K., Brown, D., Brügmann, G., Chiba, H., Fouquet, Y., Gemmell, J.B., Guerin, G., 1995. The internal structure of an active sea-floor massive sulphide deposit. Nature 377, 713–715.

Hutton, J., 1795. Theory of the Earth with Proofs and Illustrations. pp. 297.

Iizuka, T., Komiya, T., Ueno, Y., Katayama, I., Uehara, Y., Maruyama, S., Hirata, T., Johnson, S.P., Dunkley, D.J., 2007. Geology and zircon geochronology of the Acasta Gneiss Complex, northwestern Canada: New constraints on its tectonothermal history. Precambrian Res. 153, 179–208.

Ingersoll, A.P., 1970. Mars: Occurrence of liquid water. Science 168, 972–973.

Irving, E., Lapointe, P.L., 1975. Paleomagnetism of Precambrian Rocks of Laurentia. Geosci. Can. 2.

Isozaki, Y., Aoki, K., Nakama, T., Yanai, S., 2010. New insight into a subduction-related orogen: A reappraisal of the geotectonic framework and evolution of the Japanese islands. Gondwana Res. 18, 82–105.

Ito, K., Kennedy, G.C., 1971. An experimental study of the basalt-garnet granulite-eclogite transition. In: The Structure and Physical Properties of the Earth's Crust. 14. pp. 303–314.

Iwamori, H., 1998. Transportation of H_2O and melting in subduction zones. Earth Planet. Sci. Lett. 160, 65–80.

Jackson, S.L., Fyon, J.A., Corfu, F., 1994. Review of Archean supracrustal assemblages of the southern Abitibi greenstone belt in Ontario, Canada: Products of microplate interaction within a large-scale plate-tectonic setting. Precambrian Res. 65, 183–205.

Jacob, D.E., Piazolo, S., Schreiber, A., Trimby, P., 2016. Redox-freezing and nucleation of diamond via magnetite formation in the Earth's mantle. Nat. Commun. 7, 11891.

Jahn, B.M., 2010. Accretionary orogen and evolution of the Japanese Islands:

Implications from a Sr–Nd isotopic study of the Phanerozoic granitoids from SW Japan. Am. J. Sci. 310, 1210–1249.

Jahn, B.M., Zhang, Z.Q., 1984. Archean granulite gneisses from eastern Hebei Province, China: Rare earth geochemistry and tectonic implications. Contrib. Mineral. Petrol. 85, 224–243.

Jahn, B.M., Glikson, A.Y., Peucat, J.J., Hickman, A.H., 1981. REE geochemistry and isotopic data of Archean silicic volcanics and granitoids from the Pilbara Block, Western Australia: Implications for the early crustal evolution. Geochim. Cosmochim. Acta 45, 1633–1652.

Jahn, B.M., Caby, R., Monie, P., 2001. The oldest UHP eclogites of the world: Age of UHP metamorphism, nature of protoliths and tectonic implications. Chem. Geol. 178, 143–158.

Jaupart, C., Labrosse, S., Mareschal, J.-C., 2007. Temperatures, heat, and energy in the mantle of the Earth. In: Schubert, G. (Ed.), Treatise on Geophysics. 7. pp. 253–303 eds.

Jayananda, M., Santosh, M., Aadhiseshan, K.R., 2018. Formation of Archean (3600–2500 Ma) continental crust in the Dharwar craton, southern India. Earth Sci. Rev. 181, 12–42.

Jayananda, M., Aadhiseshan, K.R., Kusiak, M.A., Wilde, S.A., Sekhamo, K., Santosh, M., Gireessh, R.V., 2020. Multi-stage crustal growth and Neoarchean geodynamics in the Eastern Dharwar Craton, southern India. Gondwana Res. 78, 228–260.

Jenner, F.E., Bennett, V.C., Nutman, A.P., Friend, C.R.L., Norman, M.D., Yaxley, G., 2009. Evidence for subduction at 3.8 Ga: Geochemistry of arc-like metabasalts from the southern edge of the Isua Supracrustal Belt. Chem. Geol. 261, 83–98.

Jennings, E.S., Holland, T.J., 2015. A simple thermodynamic model for melting of peridotite in the system NCFMASOCr. J. Petrol. 56, 869–892.

Johnson, M.C., Plank, T., 2000. Dehydration and melting experiments constrain the fate of subducted sediments. Geochem. Geophys. Geosyst. 1. https://doi.org/10.1029/1999GC000014.

Johnson, T.E., Brown, M., Gardiner, N.J., Kirkland, C.L., Smithies, R.H., 2017. Corrigendum: Earth's first stable continents did not form by subduction. Nature 545, 510. https://doi.org/10.1038/nature22385.

Johnson, T.E., Gardiner, N.J., Miljković, K., Spencer, C.J., Kirkland, C.L., Bland, P.A., Smithies, H., 2018. An impact melt origin for Earth's oldest known evolved rocks. Nat. Geosci. 11, 795–799.

Kaczmarek, M.A., Reddy, S.M., Nutman, A.P., Friend, C.R., Bennett, V.C., 2016. Earth's oldest mantle fabrics indicate Eoarchaean subduction. Nat. Commun. 7, 10665.

Kamber, B.S., 2010. Archean mafic–ultramafic volcanic landmasses and their effect on ocean–atmosphere chemistry. Chem. Geol. 274, 19–28.

Kamber, B.S., 2015. The evolving nature of terrestrial crust from the Hadean, through the Archaean, into the Proterozoic. Precambrian Res. 258, 48–82.

Kamber, B.S., Whitehouse, M.J., Bolhar, R., Moorbath, S., 2005. Volcanic resurfacing and the early terrestrial crust: zircon U–Pb and REE constraints from the Isua Greenstone Belt, southern West Greenland. Earth Planet. Sci. Lett. 240, 276–290.

Kankanamge, D.G., Moore, W.B., 2016. Heat transport in the Hadean mantle: From heat pipes to plates. Geophys. Res. Lett. 43, 3208–3214.

Kankanamge, D.G., Moore, W.B., 2019. A parameterization for volcanic heat flux in heat-pipe planets. J. Geophys. Res. Planets 124, 114–127.

Kargel, J.S., Pozio, S., 1996. The volcanic and tectonic history of Enceladus. Icarus 119, 385–404.

Kawai, T., Windley, B.F., Terabayashi, M., Yamamoto, H., Maruyama, S., Omori, S., Shibuya, T., Sawaki, Y., Isozaki, Y., 2007. Geotectonic framework of the Blueschist Unit on Anglesey–Lleyn, UK, and its role in the development of a Neoproterozoic accretionary orogen. Precambrian Res. 153, 11–28.

Kawai, K., Yamamoto, S., Tsuchiya, T., Maruyama, S., 2013. The second continent: Existence of granitic continental materials around the bottom of the mantle transition zone. Geosci. Front. 4, 1–6.

Kay, S.M., Kay, R.W., 1985. Role of crystal cumulates and the oceanic crust in the formation of the lower crust of the Aleutian arc. Geology 13, 461–464.

Keller, C.B., Schoene, B., 2012. Statistical geochemistry reveals disruption in secular lithospheric evolution about 2.5 Gyr ago. Nature 485, 490–493.

Keller, C.B., Schoene, B., 2018. Plate tectonics and continental basaltic geochemistry throughout Earth history. Earth Planet. Sci. Lett. 481, 290–304.

Kelsey, D.E., 2008. On ultrahigh-temperature crustal metamorphism. Gondwana Res. 13, 1–29.

Kelsey, D.E., Hand, M., 2015. On ultrahigh temperature crustal metamorphism: Phase equilibria, trace element thermometry, bulk composition, heat sources, timescales and tectonic settings. Geosci. Front. 6, 311–356.

Kemp, A.I.S., Hawkesworth, C.J., 2014. Growth and differentiation of the continental crust from isotope studies of accessory minerals. In: Treatise on Geochemistry, Second edition. Elsevier Inc, pp. 379–421.

Kerrick, D.M., Connolly, J.A.D., 2001. Metamorphic devolatilization of subducted marine sediments and the transport of volatiles into the Earth's mantle. Nature 411, 293–297.

Khaliullin, R.Z., Eshet, H., Kühne, T.D., Behler, J., Parrinello, M., 2011. Nucleation mechanism for the direct graphite-to-diamond phase transition. Nat. Mater. 10, 693–697.

Kiefer, W.S., Hager, B.H., 1991. A mantle plume model for the equatorial highlands of Venus. J. Geophys. Res. 96, 20947–20966.

Kimura, J.I., Yoshida, T., 2006. Contributions of slab fluid, mantle wedge and crust to the origin of Quaternary lavas in the NE Japan arc. J. Petrol. 47, 2185–2232.

King, S.D., 2001. Subduction zones: Observations and geodynamic models. Phys. Earth Planet. Inter. 127, 9–24.

Kinzler, R.J., Grove, T.L., 1992. Primary magmas of mid-ocean ridge basalts 1. Experiments and methods. J. Geophys. Res. Solid Earth 97 (B5), 6885–6906.

Kirby, S.H., Durham, W.B., Stern, L.A., 1991. Mantle phase changes and deep-earthquake faulting in subducting lithosphere. Science 252, 216–225.

Kitajima, K., Maruyama, S., Utsunomiya, S., Liou, J.G., 2001. Seafloor hydrothermal alteration at an Archean mid-ocean ridge. J. Metamorph. Geol. 19, 583–600.

Klápová, H., Konopásek, J., Schulmann, K., 1998. Eclogites from the Czech part of the Erzgebirge: Multi-stage metamorphic and structural evolution. J. Geol. Soc. 155, 567–583.

Klein, B.Z., Jagoutz, O., Behn, M.D., 2017. Archean crustal compositions promote full mantle convection. Earth Planet. Sci. Lett. 474, 516–526.

Komiya, T., Maruyama, S., Masuda, T., Nohda, S., Hayashi, M., Okamoto, K., 1999. Plate tectonics at 3.8–3.7 Ga: Field evidence from the Isua accretionary complex, southern West Greenland. J. Geol. 107, 515–554.

Komiya, T., Maruyama, S., Hirata, T., Yurimoto, H., Nohda, T., 2004. Geochemistry of the oldest MORB and OIB in the Isua supracrustal belt (3.8 Ga), southern West Greenland: Implications for the composition and temperature of early Archean upper mantle. Island Arc 13, 47–72.

Korenaga, J., 2006. Archean geodynamics and the thermal evolution of Earth. In: Benn, K., Mareschal, J.-C., Condie, K. (Eds.), Archean Geodynamics and Environments. Vol. 164. AGU, Washington, D.C., pp. 7–32 Eds.

Korenaga, J., 2008a. Plate tectonics, flood basalts, and the evolution of Earth's oceans. Terra Nova 20, 419–439.

Korenaga, J., 2008b. Urey ratio and the structure and evolution of Earth's mantle. Rev. Geophys. 46 (2), RG2007.

Korenaga, J., 2010. Scaling of plate-tectonic convection with pseudoplastic rheology. J. Geophys. Res. 115, B11405.

Korenaga, J., 2011. Thermal evolution with a hydrating mantle and the initiation of plate tectonics in the early Earth. J. Geophys. Res. Solid Earth 116 (B12).

Korenaga, J., 2013. Initiation and evolution of plate tectonics on Earth: Theories and observations. Annu. Rev. Earth Planet. Sci. 41, 117–151.

Korenaga, J., 2016. Plate tectonics: Metamorphic myth. Nat. Geosci. 9, 9.

Korenaga, J., Jordan, T.H., 2003. Physics of multiscale convection in Earth's mantle: Onset of sub-lithospheric convection. J. Geophys. Res. Solid Earth 108 (B7).

Kröner, A., 1985. Evolution of the Archean continental crust. Annu. Rev. Earth Planet. Sci. 13, 49–74.

Kröner, A., Kovach, V., Belousova, E., Hegner, E., Rytsk, E., 2014. Reassessment of continental growth during the accretionary history of the Central Asian Orogenic Belt. Gondwana Res. 25, 103–125.

Kröner, A., Nagel, T.J., Hoffmann, J.E., Liu, X., Wong, J., Hegner, E., Xie, H., Kasper, U., Hofmann, A., Liu, D., 2018. High-temperature metamorphism and crustal melting at ca. 3.2 Ga in the eastern Kaapvaal craton, southern Africa. Precambrian Res. 317, 101–116.

Kump, L.R., Kasting, J.F., Barley, M.E., 2001. Rise of atmospheric oxygen and the "upside-down" Archean mantle. Geochem. Geophys. Geosyst. 2. https://doi.org/10.1029/2000GC000114.

Kunz, B.E., White, R.W., 2019. Phase equilibrium modelling of the amphibolite to granulite facies transition in metabasic rocks (Ivrea Zone, NW Italy). J. Metamorph. Geol. 37, 935–950.

Kusky, T.M., 1998. Tectonic setting and terrane accretion of the Archean Zimbabwe craton. Geology 26, 163–166.

Kusky, T.M., Li, J.H., Tucker, R.D., 2001. The Archean Dongwanzi ophiolite complex, North China Craton: 2.505-billion-year-old oceanic crust and mantle. Science 292, 1142–1145.

Kusky, T.M., Windley, B.F., Safonova, I., Wakita, K., Wakabayashi, J., Polat, A., Santosh, M., 2013. Recognition of ocean plate stratigraphy in accretionary orogens through Earth history: A record of 3.8 billion years of sea floor spreading, subduction, and accretion. Gondwana Res. 24, 501–547.

Labrosse, S., Jaupart, C., 2007. Thermal evolution of the Earth: Secular changes and fluctuations of plate characteristics mantle. Earth Planet. Sci. Lett. 260, 465–481.

Lamont, T.N., Searle, M.P., Waters, D.J., Roberts, N.M., Palin, R.M., Smye, A., Dyck, B., Gopon, P., Weller, O.M., St-Onge, M.R., 2019. Compressional origin of the Naxos metamorphic Core Complex, Greece: Structure, petrography, and thermobarometry. Geol. Soc. Am. Bull. https://doi.org/10.1130/B31978.1. in press.

Lancaster, M.G., Guest, J.E., Magee, K.P., 1995. Great lava flow fields on Venus. Icarus 118, 69–86.

Laurent, O., Martin, H., Moyen, J.F., Doucelance, R., 2014. The diversity and evolution of late-Archean granitoids: Evidence for the onset of "modern-style" plate tectonics between 3.0 and 2.5 Ga. Lithos 205, 208–235.

Laurie, A., Stevens, G., 2012. Water-present eclogite melting to produce Earth's early felsic crust. Chem. Geol. 314, 83–95.

Laurie, A., Stevens, G., van Hunen, J., 2013. The end of continental growth by TTG magmatism. Terra Nova 25, 130–136.

Le Bas, M.L., Maitre, R.L., Streckeisen, A., Zanettin, B., IUGS Subcommission on the Systematics of Igneous Rocks, 1986. A chemical classification of volcanic rocks based on the total alkali-silica diagram. J. Petrol. 27, 745–750.

Lécuyer, C., 2013. Water and plate tectonics. In: Water on Earth: Physicochemical and Biological Properties, pp. 113–154.

Leitch, A.M., Yuen, D.A., 1989. Internal heating and thermal constraints on the mantle. Geophys. Res. Lett. 16, 1407–1410.

Lenardic, A., 2018. The diversity of tectonic modes and thoughts about transitions between them. Philos. Trans. R. Soc. A Math. Phys. Eng. Sci. 376, 20170416.

Lenoir, X., Garrido, C.J., Bodinier, J.L., Dautria, J.M., 2000. Contrasting lithospheric mantle domains beneath the Massif Central (France) revealed by geochemistry of peridotite xenoliths. Earth Planet. Sci. Lett. 181, 359–375.

Lenton, T.M., Schellnhuber, H.J., Szathmáry, E., 2004. Climbing the co-evolution ladder. Nature 431, 913.

Levine, J.S., Garvin, J.B., Head III, J.W., 2010. Martian geology investigations. Planning for the scientific exploration of Mars by humans. Part 2. J. Cosmol. 12, 3636–3646.

Li, Z.X., Bogdanova, S.V., Collins, A.S., Davidson, A., De Waele, B., Ernst, R.E., Fitzsimons,

I.C.W., Fuck, R.A., Gladkochub, D.P., Jacobs, J., Karlstrom, K.E., Lu, S., Natapov, L.M., Pease, V., Pisarevsky, S.A., Thrane, K., Vernikovsky, V., 2008. Assembly, configuration, and break-up history of Rodinia: A synthesis. Precambrian Res. 160, 179–210.

Li, Z.H., Gerya, T.V., Burg, J.-P., 2010. Influence of tectonic overpressure on *P–T* paths of HP-UHP rocks in continental collision zones: Thermomechanical modelling. J. Metamorph. Geol. 28, 227–247.

Li, C., Arndt, N.T., Tang, Q., Ripley, E.M., 2015. Trace element indiscrimination diagrams. Lithos 232, 76–83.

Li, S.S., Santosh, M., Teng, X.M., He, X.F., 2016. Paleoproterozoic arc-continent collision in the North China Craton: Evidence from the Zanhuang complex. Precambrian Res. 286, 281–305.

Li, S.S., Santosh, M., Ganguly, S., Thanooja, P.V., Sajeev, K., Pahari, A., 2018a. Neoarchean microblock amalgamation in southern India: Evidence from the Nallamalai Suture Zone. Precambrian Res. 314, 1–27.

Li, S.S., Santosh, M., Palin, R.M., 2018b. Metamorphism during the Archaean–Paleoproterozoic transition associated with microblock amalgamation in the Dharwar Craton, India. J. Petrol. 59, 2435–2462.

Li, X., Niu, M., Yakymchuk, C., Wu, Q., Fu, C., 2019. A paired metamorphic belt in a subduction-to-collision orogen: An example from the South Qilian–North Qaidam orogenic belt, NW China. J. Metamorph. Geol. 37, 479–508.

Li, S.S., Palin, R.M., Santosh, M., Shaji, E., Tsunogae, T., 2020. Extreme thermal metamorphism associated with Gondwana assembly: Evidence from sapphirine-bearing granulites of Rajapalayam, southern India. Bulletin 132 (5-6), 1013–1030.

Liou, J.G., Hacker, B.R., Zhang, R.Y., 2000. Into the forbidden zone. Science 287, 1215–1216.

Liou, J.G., Tsujimori, T., Zhang, R.Y., Katayama, I., Maruyama, S., 2004. Global UHP metamorphism and continental subduction/collision: The Himalayan model. Int. Geol. Rev. 46, 1–27.

Liu, H., Zhang, H.F., 2019. Paleoproterozoic ophiolite remnants in the northern margin of the North China Craton: Evidence from the Chicheng peridotite massif. Lithos 344, 311–323.

Liu, Y., Zhong, D., 1997. Petrology of high-pressure granulites from the eastern Himalayan syntaxis. J. Metamorph. Geol. 15, 451–466.

Liu, J., Bohlen, S.R., Ernst, W.G., 1996. Stability of hydrous phases in subducting oceanic crust. Earth Planet. Sci. Lett. 143, 161–171.

Lourenço, D.L., Rozel, A.B., Gerya, T., Tackley, P.J., 2018. Efficient cooling of rocky planets by intrusive magmatism. Nat. Geosci. 11, 322–326.

Lowman Jr., P.D., 1989. Comparative planetology and the origin of continental crust. Precambrian Res. 44, 171–195.

Lubnina, N.V., Pisarevsky, S.A., Stepanova, A.V., Bogdanova, S.V., Sokolov, S.J., 2017. Fennoscandia before Nuna/Columbia: Paleomagnetism of 1.98–1.96 Ga mafic rocks of the Karelian craton and paleogeographic implications. Precambrian Res. 292, 1–12.

Lucchitta, B.K., 1987. Recent mafic volcanism on Mars. Science 235, 565–567.

Lunine, J.I., 2001. The occurrence of Jovian planets and the habitability of planetary systems. Proc. Natl. Acad. Sci. 98, 809–814.

Lunine, J.I., 2017. Ocean worlds exploration. Acta Astron. 131, 123–130.

Maas, R., Kinny, P.D., Williams, I.S., Froude, D.O., Compston, W., 1992. The Earth's oldest known crust: A geochronological and geochemical study of 3900–4200 Ma old detrital zircons from Mt. Narryer and Jack Hills, Western Australia. Geochim. Cosmochim. Acta 56, 1281–1300.

MacDonald, G.J., 1959. Calculations on the thermal history of the earth. J. Geophys. Res. 64, 1967–2000.

Macdonald, F.A., Swanson-Hysell, N.L., Park, Y., Lisiecki, L., Jagoutz, O., 2019. Arc-continent collisions in the tropics set Earth's climate state. Science 364, 181–184.

MacGregor, I.D., Manton, W.I., 1986. Roberts Victor eclogites: Ancient oceanic crust. J. Geophys. Res. Solid Earth 91 (B14), 14063–14079.

Mahapatro, S.N., Pant, N.C., Bhowmik, S.K., Tripathy, A.K., Nanda, J.K., 2012. Archaean granulite-facies metamorphism at the Singhbhum Craton–Eastern Ghats Mobile Belt interface: Implication for the Ur supercontinent assembly. Geol. J. 47, 312–333.

Maniar, P.D., Piccoli, P.M., 1989. Tectonic discrimination of granitoids. Geol. Soc. Am. Bull. 101, 635–643.

Manikyamba, C., Kerrich, R., Khanna, T.C., Krishna, A.K., Satyanarayanan, M., 2008. Geochemical systematics of komatiite-tholeiite and adakite-arc basalt associations: The role of a mantle plume and convergent margin in formation of the Sandur Superterrane, Dharwar craton. Lithos 106, 155–172.

Manikyamba, C., Kerrich, R., Khanna, T.C., Satyanarayanan, M., Krishna, A.K., 2009. Enriched and depleted arc basalts, with Mg-andesites and adakites: A potential paired arc–back-arc of the 2.6 Ga Hutti greenstone terrane, India. Geochim. Cosmochim. Acta 73, 1711–1736.

Marchi, S., Bottke, W.F., Elkins-Tanton, L.T., Bierhaus, M., Wuennemann, K., Morbidelli, A., Kring, D.A., 2014. Widespread mixing and burial of Earth's Hadean crust by asteroid impacts. Nature 511, 578.

Marsh, J.H., Kelly, E.D., 2017. Petrogenetic relations among titanium-rich minerals in an anatectic high-P mafic granulite. J. Metamorph. Geol. 35, 717–738.

Marshak, S., 1999. Deformation style way back when: thoughts on the contrasts between Archean/Paleoproterozoic and contemporary orogens. J. Struct. Geol. 21, 1175–1182.

Martin, H., 1993. The mechanisms of petrogenesis of the Archaean continental crust—comparison with modern processes. Lithos 30, 373–388.

Martin, H., 1994. The Archean grey gneisses and the genesis of continental crust. In Developments in Precambrian Geology, 11, 205–259, Elsevier.

Martin, H., 1999. Adakitic magmas: Modern analogues of Archaean granitoids. Lithos 46, 411–429.

Martin, H., Moyen, J.F., 2002. Secular changes in tonalite–trondhjemite–granodiorite

composition as markers of the progressive cooling of Earth. Geology 30, 319–322.

Martin, H., Moyen, J.F., Guitreau, M., Blichert-Toft, J., Le Pennec, J.L., 2014. Why Archaean TTG cannot be generated by MORB melting in subduction zones. Lithos 198, 1–13.

Maruyama, S., Liou, J.G., Terabayashi, M., 1996. Blueschists and eclogites of the world and their exhumation. Int. Geol. Rev. 38, 485–594.

Maruyama, S., Santosh, M., Zhao, D., 2007. Superplume, supercontinent, and post-perovskite: Mantle dynamics and anti-plate tectonics on the core–mantle boundary. Gondwana Res. 11, 7–37.

Maruyama, S., Santosh, M., Azuma, S., 2018. Initiation of plate tectonics in the Hadean: Eclogitization triggered by the ABEL Bombardment. Geosci. Front. 9, 1033–1048.

Matsuda, T., Isozaki, Y., 1991. Well-documented travel history of Mesozoic pelagic chert in Japan: From remote ocean to subduction zone. Tectonics 10, 475–499.

Maurice, C., Francis, D., Madore, L., 2003. Constraints on early Archean crustal extraction and tholeiitic-komatiitic volcanism in greenstone belts of the Northern Superior Province. Can. J. Earth Sci. 40, 431–445.

McCauley, J.F., Carr, M.H., Cutts, J.A., Hartmann, W.K., Masursky, H., Milton, D.J., Sharp, R.P., Wilhelms, D.E., 1972. Preliminary Mariner 9 report on the geology of Mars. Icarus 17, 289–327.

McCoy-West, A.J., Chowdhury, P., Burton, K.W., Sossi, P., Nowell, G.M., Fitton, J.G., Kerr, A.C., Cawood, P.A., Williams, H.M., 2019. Extensive crustal extraction in Earth's early history inferred from molybdenum isotopes. Nat. Geosci. 12, 946–951.

McGregor, V.R., 1979. Archean gray gneisses and the origin of the continental crust: Evidence the Godthåb region, West Greenland. In: Developments in Petrology. 6. Elsevier, pp. 169–204.

McKenzie, D., Bickle, M.J., 1988. The volume and composition of melt generated by extension of the lithosphere. J. Petrol. 29, 625–679.

McKenzie, D., Weiss, N., 1975. Speculations on the thermal and tectonic history of the Earth. Geophys. J. Int. 42, 131–174.

McKenzie, D., Ford, P.G., Johnson, C., Parsons, B., Sandwell, D., Saunders, S., Solomon, S.C., 1992. Features on Venus generated by plate boundary processes. J. Geophys. Res. Planets 97 (E8), 13,533–13,544.

McKinnon, W.B., Nimmo, F., Wong, T., Schenk, P.M., White, O.L., Roberts, J.H., Moore, J.M., Spencer, J.R., Howard, A.D., Umurhan, O.M., Stern, S.A., 2016. Convection in a volatile nitrogen-ice-rich layer drives Pluto's geological vigour. Nature 534, 82–86.

McSween Jr, H.Y., 2015. Petrology on Mars. Am. Mineral., 100, 2380–2395.

Meert, J.G., 2012. What's in a name? The Columbia (Paleopangaea/Nuna) supercontinent. Gondwana Res. 21, 987–993.

Meert, J.G., Santosh, M., 2017. The Columbia supercontinent revisited. Gondwana Res. 50, 67–83.

Mège, D., 2001. Uniformitarian plume tectonics: The post-Archean Earth and Mars. In: Special papers – Geological Society of America, pp. 141–164.

Menneken, M., Nemchin, A.A., Geisler, T., Pidgeon, R.T., Wilde, S.A., 2007. Hadean diamonds in zircon from Jack Hills, Western Australia. Nature 448, 917–921.

Merdith, A.S., Collins, A.S., Williams, S.E., Pisarevsky, S., Foden, J.D., Archibald, D.B., Blades, M.L., Alessio, B.L., Armistead, S., Plavsa, D., Clark, C., Müller, R.D., 2017. A full-plate global reconstruction of the Neoproterozoic. Gondwana Res. 50, 84–134.

Michael, P.J., Langmuir, C.H., Dick, H.J.B., Snow, J.E., Goldstein, S.L., Graham, D.W., Lehnert, K., Kurras, G., Jokat, W., Mühe, R., Edmonds, H.N., 2003. Magmatic and amagmatic seafloor generation at the ultraslow-spreading Gakkel ridge, Arctic Ocean. Nature 423, 956–961.

Miller, S., Coustenis, A., Read, P., Tennyson, J., 2014. Characterizing exoplanets. Philos. Trans. R. Soc. London, Ser. A 372, 20130375.

Mints, M.V., Belousova, E.A., Konilov, A.N., Natapov, L.M., Shchipansky, A.A., Griffin, W.L., O'Reilly, S.Y., Dokukina, K.A., Kaulina, T.V., 2010. Mesoarchean subduction processes: 2.87 Ga eclogites from the Kola Peninsula, Russia. Geology 38, 739–742.

Mitchell, R.N., Bleeker, W., van Breemen, O., Lecheminant, T.N., Peng, P., Nilsson, M.K.M., Evans, D.A.D., 2014. Plate tectonics before 2.0 Ga: Evidence from paleomagnetism of cratons within supercontinent Nuna. Am. J. Sci. 314, 878–894.

Miyashiro, A., 1961. Evolution of metamorphic belts. J. Petrol. 2, 277–311.

Miyashiro, A., 1975. Classification, characteristics, and origin of ophiolites. J. Geol. 83, 249–281.

Möller, A., Appel, P., Mezger, K., Schenk, V., 1995. Evidence of a 2 Ga subduction zone: Eclogites in the Usagaran belt of Tanzania. Geology 23, 1067–1070.

Monecke, T., Kempe, U., Götze, J., 2002. Genetic significance of the trace element content in metamorphic and hydrothermal quartz: A reconnaissance study. Earth Planet. Sci. Lett. 202, 709–724.

Monteux, J., Andrault, D., Samuel, H., 2016. On the cooling of a deep terrestrial magma ocean. Earth Planet. Sci. Lett. 448, 140–149.

Moorbath, S., Allaart, J.H., Bridgwater, D., McGregor, V.R., 1977. Rb–Sr ages of early Archaean supracrustal rocks and Amîtsoq gneisses at Isua. Nature 270, 43–47.

Moore, W.B., Webb, A.A.G., 2013. Heat-pipe Earth. Nature 501, 501–505.

Moore, W.B., Simon, J.I., Webb, A.A.G., 2017. Heat-pipe planets. Earth Planet. Sci. Lett. 474, 13–19.

Moores, E.M., 1982. Origin and emplacement of ophiolites. Rev. Geophys. 20, 735–760.

Moresi, L., Solomatov, V., 1998. Mantle convection with a brittle lithosphere: Thoughts on the global tectonic styles of the Earth and Venus. Geophys. J. Int. 133, 669–682.

Morgan, J.P., Chen, Y.J., 1993. The genesis of oceanic crust: Magma injection, hydrothermal circulation, and crustal flow. J. Geophys. Res. Solid Earth 98 (B4), 6283–6297.

Moyen, J.F., 2011. The composite Archaean grey gneisses: Petrological significance, and evidence for a non-unique tectonic setting for Archaean crustal growth. Lithos 123, 21–36.

Moyen, J.F., Laurent, O., 2017. Archaean tectonic systems: A view from igneous rocks. Lithos 302–303, 99–125.

Moyen, J.F., Martin, H., 2012. Forty years of TTG research. Lithos 148, 312–336.

Moyen, J.F., Stevens, G., 2006. Experimental constraints on TTG petrogenesis: implications for Archean geodynamics. Geophys. Monogr. Am. Geophys. Union 164, 149–171.

Moyen, J.F., Van Hunen, J., 2012. Short-term episodicity of Archaean plate tectonics. Geology 40, 451–454.

Moyen, J.F., Stevens, G., Kisters, A., 2006. Record of mid-Archaean subduction from metamorphism in the Barberton terrain, South Africa. Nature 442, 559–562.

Mueller, W.U., Corcoran, P.L., 2001. Volcano-sedimentary processes operating on a marginal continental arc: The Archean Raquette Lake Formation, Slave Province, Canada. Sediment. Geol. 141–142, 169–204.

Mueller, W.U., Daigneault, R., Mortensen, J.K., Chown, E.H., 1996. Archean terrane docking: Upper crust collision tectonics, Abitibi greenstone belt, Quebec, Canada. Tectonophysics 265, 127–150.

Müller, S., Dziggel, A., Kolb, J., Sindern, S., 2018a. Mineral textural evolution and PT-path of relict eclogite-facies rocks in the Paleoproterozoic Nagssugtoqidian Orogen, South-East Greenland. Lithos 296, 212–232.

Müller, S., Dziggel, A., Sindern, S., Kokfelt, T.F., Gerdes, A., Kolb, J., 2018b. Age and temperature-time evolution of retrogressed eclogite-facies rocks in the Paleoproterozoic Nagssugtoqidian Orogen, South-East Greenland: Constrained from U–Pb dating of zircon, monazite, titanite and rutile. Precambrian Res. 314, 468–486.

Munévar, G., 2019. Science and ethics in the exploration of Mars. In: The Human Factor in a Mission to Mars. Springer, Cham, pp. 185–200.

Myers, J.S., 2001. Protoliths of the 3.8–3.7 Ga Isua greenstone belt, west Greenland. Precambrian Res. 105, 129–141.

Nagel, T.J., Hoffmann, J.E., Münker, C., 2012. Generation of Eoarchean tonalite-trondhjemite-granodiorite series from thickened mafic arc crust. Geology 40, 375–378.

Nair, R., Chacko, T., 2008. Role of oceanic plateaus in the initiation of subduction and origin of continental crust. Geology 36, 583–586.

Nakajima, M., Stevenson, D.J., 2015. Melting and mixing states of the Earth's mantle after the Moon-forming impact. Earth Planet. Sci. Lett. 427, 286–295.

Nance, R.D., Murphy, J.D., Santosh, M., 2014. The supercontinent cycle: A retrospective essay. Gondwana Res. 25, 4–29.

Naqvi, S.M., Khan, R.M.K., Manikyamba, C., Ram Mohan, M., Khanna, T.C., 2006. Geochemistry of the Neoarchaean high-Mg basalts, boninites and adakites form the Kushtagi–Hungund greenstone belt of the eastern Dhawar craton (EDC): Implications for the tectonic setting. J. Asian Earth Sci. 27, 25–44.

Natland, J.H., Dick, H.J., 2001. Formation of the lower ocean crust and the crystallization of gabbroic cumulates at a very slowly spreading ridge. J. Volcanol. Geotherm. Res. 110, 191–233.

Nebel, O., Capitanio, F.A., Moyen, J.F., Weinberg, R.F., Clos, F., Nebel-Jacobsen, Y.J., Cawood, P.A., 2018. When crust comes of age: on the chemical evolution of Archaean, felsic continental crust by crustal drip tectonics. Philos. Trans. R. Soc. A Math. Phys. Eng. Sci. 376, 20180103.

Newton, R.C., 1992. Charnockitic alteration: evidence for CO_2 infiltration in granulite facies metamorphism. J. Metamorph. Geol. 10, 383–400.

Newton, M.S., Kennedy, G.C., 1968. Jadeite, analcime, nepheline and albite at high temperatures and pressures. Am. J. Sci. 266, 728–735.

Nicolas, A., Boudier, F., Ildefonse, B., 1994. Evidence from the Oman ophiolite for active mantle upwelling beneath a fast-spreading ridge. Nature 370, 51–55.

Nicoli, G., Dyck, B., 2018. Exploring the metamorphic consequences of secular change in the siliciclastic compositions of continental margins. Geosci. Front. 9, 967–975.

Nimmo, F., 2000. Dike intrusion as a possible cause of linear Martian magnetic anomalies. Geology 28, 391–394.

Nisbet, E.G., Fowler, C.M.R., 1983. Model for Archean plate tectonics. Geology 11, 376–379.

Nisbet, E.G., Bickle, M.J., Martin, A., 1977. The mafic and ultramafic lavas of the Belingwe greenstone belt, Rhodesia. J. Petrol. 18, 521–566.

Nishimura, Y., Shibata, K., 1989. Modes of occurrence and K–Ar ages of metagabbroic rocks in the "Sangun metamorphic belt", Southwest Japan. Mem. Geol. Soc. Jpn. 33, 343–357.

Noack, L., Breuer, D., 2014. Plate tectonics on rocky exoplanets: Influence of initial conditions and mantle rheology. Planet. Space Sci. 98, 41–49.

Noack, N.M., Kleinschrodt, R., Kirchenbaur, M., Raúl, O., Fonseca, C., Münker, C., 2013. Lu–Hf isotope evidence for Paleoproterozoic metamorphism and deformation of Archean oceanic crust along the Dharwar Craton margin, southern India. Precambrian Res. 233, 206–222.

Nutman, A.P., Friend, C.R.L., Bennett, V.C., 2002. Evidence for 3650–3600 Ma assembly of the northern end of the Itsaq Gneiss Complex, Greenland: Implication for early Archean tectonics. Tectonics 21, 1005.

O'Brien, P.J., 2018. Eclogites and other high-pressure rocks in the Himalaya: A review. Geol. Soc. Lond. Spec. Publ. 483, SP483–13.

O'Brien, P.J., Rötzler, J., 2003. High-pressure granulites: Formation, recovery of peak conditions and implications for tectonics. J. Metamorph. Geol. 21, 3–20.

Ogawa, M., 2008. Mantle convection: A review. Fluid Dynam. Res. 40, 379–391.

O'Hara, M.J., 1977. Geochemical evolution during fractional crystallisation of a periodically refilled magma chamber. Nature 266, 503–507.

Ohta, H., Maruyama, S., Takahashi, E., Watanabe, Y., Kato, Y., 1996. Field occurrence, geochemistry and petrogenesis of the Archean mid-oceanic ridge basalts (AMORBs) of the Cleaverville area, Pilbara craton, Western Australia. Lithos 37, 199–221.

Ohtani, E., 1985. The primordial terrestrial magma ocean and its implication for stratification of the mantle. Phys. Earth Planet. Inter. 38, 70–80.

O'Neil, J., Carlson, R.W., 2017. Building Archean cratons from Hadean mafic crust. Science 355, 1199–1202.

O'Neil, J., Carlson, R.W., Francis, D., Stevenson, R.K., 2008. Neodymium-142 evidence for Hadean mafic crust. Science 321, 1828–1831.

O'Neil, J., Francis, D., Carlson, R.W., 2011. Implications of the Nuvvuagittuq greenstone belt for the formation of Earth's early crust. J. Petrol. 52, 985–1009.

O'Neill, C., Roberts, N.M., 2018. Lid tectonics. Preface. Geosci. Front. 9, 1–2.

O'Neill, C., Jellinek, A.M., Lenardic, A., 2007. Conditions for the onset of plate tectonics on terrestrial planets and moons. Earth Planet. Sci. Lett. 261, 20–32.

O'Neill, C., Lenardic, A., Weller, M., Moresi, L., Quenette, S., Zhang, S., 2016. A window for plate tectonics in terrestrial planet evolution? Phys. Earth Planet. Inter. 255, 80–92.

O'Neill, C., Turner, S., Rushmer, T., 2018. The inception of plate tectonics: A record of failure. Philos. Trans. R. Soc. A Math. Phys. Eng. Sci. 376, 20170414.

O'Neill, C., Marchi, S., Bottke, W., Fu, R., 2020. The role of impacts on Archean tectonics. Geology 48, 174–178.

O'Reilly, S.Y., Griffin, W.L., 2010. The continental lithosphere–asthenosphere boundary: Can we sample it? Lithos 120, 1–13.

Othman, D.B., White, W.M., Patchett, J., 1989. The geochemistry of marine sediments, island arc magma genesis, and crust-mantle recycling. Earth Planet. Sci. Lett. 94, 1–21.

Palin, R.M., Dyck, B., 2018. Metamorphic consequences of secular changes in oceanic crust composition and implications for uniformitarianism in the geological record. Geosci. Front. 9, 1009–1019.

Palin, R.M., Spencer, C.J., 2018. Secular change in earth processes: Preface. Geosci. Front. 9, 965–966.

Palin, R.M., White, R.W., 2016. Emergence of blueschists on Earth linked to secular changes in oceanic crust composition. Nat. Geosci. 9, 60–64.

Palin, R.M., Searle, M.P., Waters, D.J., Horstwood, M.S.A., Parrish, R.R., 2012. Combined thermobarometry and geochronology of peraluminous metapelites from the Karakoram metamorphic complex, North Pakistan; New insight into the tecto-nothermal evolution of the Baltoro and Hunza Valley regions. J. Metamorph. Geol. 30, 793–820.

Palin, R.M., Searle, M.P., St-Onge, M.R., Waters, D.J., Roberts, N.M.W., Horstwood, M.S.A., Parrish, R.R., Weller, O.M., Chen, S., Yang, J., 2014a. Monazite geochronology and petrology of kyanite-and sillimanite-grade migmatites from the north-western flank of the eastern Himalayan syntaxis. Gondwana Res. 26, 323–347.

Palin, R.M., St-Onge, M.R., Waters, D.J., Searle, M.P., Dyck, B., 2014b. Phase equilibria modelling of retrograde amphibole and clinozoisite in mafic eclogite from the Tso Morari massif, northwest India: Constraining the $P–T–M(H_2O)$ conditions of exhumation. J. Metamorph. Geol. 32, 675–693.

Palin, R.M., White, R.W., Green, E.C.R., Diener, J.F.A., Powell, R., Holland, T.J.B., 2016a. High-grade metamorphism and partial melting of basic and intermediate rocks. J. Metamorph. Geol. 34, 871–892.

Palin, R.M., White, R.W., Green, E.C.R., 2016b. Partial melting of metabasic rocks and the generation of tonalitic–trondhjemitic–granodioritic (TTG) crust in the Archean: constraints from phase equilibrium modelling. Precambrian Res. 287, 73–90.

Palin, R.M., Reuber, G.S., White, R.W., Kaus, B.J.P., Weller, O.M., 2017. Subduction metamorphism in the Himalayan ultrahigh-pressure Tso Morari massif: An integrated geodynamic and petrological modelling approach. Earth Planet. Sci. Lett. 467, 108–119.

Pallister, J.S., 1981. Structure of the sheeted dike complex of the Samail ophiolite near Ibra, Oman. J. Geophys. Res. Solid Earth 86, 2661–2672.

Parman, S.W., Grove, T.L., Dann, J.C., 2001. The production of Barberton komatiites in an Archean subduction zone. Geophys. Res. Lett. 28, 2513–2516.

Parmentier, E.M., Hess, P.C., 1992. Chemical differentiation of a convecting planetary interior: Consequences for a one plate planet such as Venus. Geophys. Res. Lett. 19, 2015–2018.

Parsons, B., McKenzie, D., 1978. Mantle convection and the thermal structure of the plates. J. Geophys. Res. 83, 4485–4496.

Parsons, A.J., Hosseini, K., Palin, R.M., Sigloch, K., 2020. Geological, geophysical and plate kinematic constraints for models of the India-Asia collision and the post-Triassic central Tethys oceans. Earth Sci. Rev. 103084. https://doi.org/10.1016/j.earscirev.2020.103084.

Patterson, C., 1956. Age of meteorites and the Earth. Geochim. Cosmochim. Acta 10, 230–237.

Pattison, D.R.M., 2003. Petrogenetic significance of orthopyroxene-free garnet + clinopyroxene + plagioclase ± quartz-bearing metabasites with respect to the amphibolite and granulite facies. J. Metamorph. Geol. 21, 21–34.

Păun, D.A., 2015. A systems approach to the exploration and resource utilization of Venus and Mercury. In: Inner Solar System. Springer, Cham, pp. 365–381.

Pawley, A.R., 1994. The pressure and temperature stability limits of lawsonite: implications for H2O recycling in subduction zones. Contributions to Mineralogy and Petrology 118 (1), 99–108.

Payne, J.J., Ferris, G., Barovich, K.M., Hand, M., 2010. Pitfalls of classifying ancient magmatic suites with tectonic discrimination diagrams: An example from the Paleoproterozoic Tunkillia Suite, southern Australia. Precambrian Res. 177, 227–240.

Peacock, S., 1990. Fluid processes in subduction zones. Science 248, 329–337.

Peacock, S., 1996. Thermal and petrologic structure of subduction zones. In: Bebout, G.E., Scholl, D.W., Kirby, S.H., Platt, J.P. (Eds.), Subduction: Top to Bottom. 96. pp. 119–133 eds.

Peacock, S.M., Wang, K., 1999. Seismic consequences of warm versus cool subduction metamorphism: Examples from southwest and northeast Japan. Science 286, 937–939.

Pearce, J.A., 1996. A user's guide to basalt discrimination diagrams. Trace element geochemistry of volcanic rocks: Applications for massive sulphide exploration. Geol. Assoc. Can., Short Course Notes 12, 79–113.

Pearce, J.A., 2008. Geochemical fingerprinting of oceanic basalts with applications to ophiolite classification and the search for Archean oceanic crust. Lithos 100, 14–48.

Pearce, J.A., Cann, J.R., 1973. Tectonic setting of basic volcanic rock determined using

trace elements analyses. Earth Planet. Sci. Lett. 19, 290–300.

Peltonen, P., Kontinen, A., Huhma, H., 1996. Petrology and geochemistry of metabasalts from the 1.95 Ga Jormua ophiolite, northeastern Finland. J. Petrol. 37, 1359–1383.

Peng, T., Wilde, S.A., Fan, W., Peng, B., 2013. Neoarchean siliceous high-Mg basalt (SHMB) from the Taishan granite-greenstone terrane, Eastern North China Craton: Petrogenesis and tectonic implications. Precambrian Res. 228, 233–249.

Peng, H., Kusky, T., Deng, H., Wang, L., Wang, J., Huang, Y., Huang, B., Ning, W., 2020. Identification of the Neoarchean Jianping pyroxenite-mélange in the Central Orogenic Belt, North China Craton: A fore-arc accretional assemblage. Precambrian Res. 336, 105495.

Penniston-Dorland, S.C., Kohn, M.J., Manning, C.E., 2015. The global range of subduction zone thermal structures from exhumed blueschists and eclogites: Rocks are hotter than models. Earth Planet. Sci. Lett. 428, 243–254.

Pepe, F., Ehrenreich, D., Meyer, M.R., 2014. Instrumentation for the detection and characterization of exoplanets. Nature 513, 358–362.

Petersen, R.I., Stegman, D.R., Tackley, P.J., 2015. A regime diagram of mobile lid convection with plate-like behavior. Phys. Earth Planet. Inter. 241, 65–76.

Petrini, K., Podladchikov, Y., 2000. Lithospheric pressure-depth relationship in compressive regions of thickened crust. J. Metamorph. Geol. 18, 67–77.

Phillips, G.N., 1981. Water activity changes across an amphibolite-granulite facies transition, Broken Hill, Australia. Contrib. Mineral. Petrol. 75, 377–386.

Phillips, C.B., Pappalardo, R.T., 2014. Europa Clipper mission concept: Exploring Jupiter's ocean moon. Eos, Trans. Am. Geophys. Union 95, 165–167.

Phillips, R.J., Kaula, W.M., McGill, G.E., Malin, M.C., 1981. Tectonics and evolution of Venus. Science 212, 879–887.

Piccolo, A., Palin, R.M., Kaus, B.J., White, R.W., 2019. Generation of Earth's early continents from a relatively cool Archean mantle. Geochem. Geophys. Geosyst. 20, 1679–1697.

Pisarevsky, S.A., Elming, S.-Å., Pesonen, L.J., Li, Z.-X., 2014. Mesoproterozoic paleogeography: Supercontinent and beyond. Precambrian Res. 244, 207–225.

Polat, A., 2012. Growth of Archean continental crust in oceanic island arcs. Geology 40, 383–384.

Polat, A., Hofmann, A.W., 2003. Alteration and geochemical patterns in the 3.7–3.8 Ga Isua greenstone belt, West Greenland. Precambrian Res. 126, 197–218.

Polat, A., Kerrich, R., 1999. Formation of an Archean tectonic mélange in the Schreiber-Hemlo greenstone belt, Superior Province, Canada: Implications for Archean subduction-accretion process. Tectonics 18, 733–755.

Polat, A., Hofmann, A.W., Rosing, M.T., 2002. Boninite-like volcanic rocks in the 3.7–3.8 Ga Isua greenstone belt, West Greenland: geochemical evidence for intra-oceanic subduction zone processes in the early Earth. Chem. Geol. 184, 231–254.

Poli, S., Schmidt, M.W., 2002. Petrology of subducted slabs. Annu. Rev. Earth Planet. Sci. 30, 207–235.

Pollack, H.N., Chapman, D.S., 1977. On the regional variation of heat flow, geotherms, and lithospheric thickness. Tectonophysics 38, 279–296.

Powell, R., Holland, T.J.B., 2008. On thermobarometry. J. Metamorph. Geol. 26, 155–179.

Powell, W.G., Carmichael, D.M., Hodgson, C.J., 1995. Conditions and timing of metamorphism in the southern Abitibi greenstone belt, Quebec. Can. J. Earth Sci. 32, 787–805.

Presnall, D.C., Gudfinnsson, G.H., Walter, M.J., 2002. Generation of mid-ocean ridge basalts at pressures from 1 to 7 GPa. Geochim. Cosmochim. Acta 66, 2073–2090.

Prockter, L.M., Nimmo, F., Pappalardo, R.T., 2005. A shear heating origin for ridges on Triton. Geophys. Res. Lett. 32.

Prouteau, G., Scaillet, B., Pichavant, M., Maury, R., 2001. Evidence for mantle metasomatism by hydrous silicic melts derived from subducted oceanic crust. Nature 410, 197–201.

Quick, J.E., Denlinger, R.P., 1993. Ductile deformation and the origin of layered gabbro in ophiolites. J. Geophys. Res. Solid Earth 98, 14015–14027.

Rajesh, H.M., Belyanin, G.A., Van Reenen, D.D., 2018. Three tier transition of Neoarchean TTG-sanukitoid magmatism in the Beit Bridge Complex, Southern Africa. Lithos 296, 431–451.

Rapp, R.P., Watson, E.B., 1995. Dehydration melting of metabasalt at 8–32 kbar: Implications for continental growth and crust–mantle recycling. J. Petrol. 36, 891–931.

Rapp, R.P., Watson, E.B., Miller, C.F., 1991. Partial melting of amphibolite/eclogite and the origin of Archaean trondhjemites and tonalites (Eds.) In: Haapala, I., Condie, K.C. (Eds.), Precambrian Granitoids–Petrogenesis, Geochemistry and Metallogeny. 51. pp. 1–25.

Rapp, R.P., Shimizu, N., Norman, M.D., 2003. Growth of early continental crust by partial melting of eclogite. Nature 425, 605–609.

Rapp, R.P., Irifune, T., Shimizu, N., Nishiyama, N., Norman, M.D., Inoue, T., 2008. Subduction recycling of continental sediments and the origin of geochemically enriched reservoirs in the deep mantle. Earth Planet. Sci. Lett. 271, 14–23.

Reese, C.C., Solomatov, V.S., Moresi, L.N., 1999. Non-newtonian stagnant lid convection and magmatic resurfacing on Venus. Icarus 139, 67–80.

Reese, C.C., Solomatov, V.S., Orth, C.P., 2007. Mechanisms for cessation of magmatic resurfacing on Venus. J. Geophys. Res. Planets 112 (E4).

Regenauer-Lieb, K., Yuen, D.A., Branlund, J., 2001. The initiation of subduction: Criticality by addition of water? Science 294, 578–580.

Reimink, J.R., Chacko, T., Stern, R.A., Heaman, L.M., 2014. Earth's earliest evolved crust generated in an Iceland-like setting. Nat. Geosci. 7, 529–533.

Reimink, J.R., Davies, J.H.F.L., Chacko, T., Stern, R.A., Heaman, L.M., Sarkar, C., Schaltegger, U., Creaser, R.A., Pearson, D.G., 2016. No evidence for Hadean continental crust within Earth's oldest evolved rock unit. Nat. Geosci. 9, 777–781.

Reimink, J.R., Chacko, T., Carlson, R.W., Shirey, S.B., Liu, J., Stern, R.A., Bauer, A.M., Pearson, D.G., Heaman, L.M., 2018. Petrogenesis and tectonics of the Acasta Gneiss

Complex derived from integrated petrology and ^{142}Nd and ^{182}W extinct nuclide-geochemistry. Earth Planet. Sci. Lett. 494, 12–22.

Reuber, G., Kaus, B.J.P., Schmalholz, S.M., White, R.W., 2016. Non-lithostatic pressure during subduction and collision and the formation of (ultra)high-pressure rocks. Geology 44, 343–346.

Revenaugh, J., Reasoner, C., 1997. Cumulative offset of the San Andreas fault in central California: A seismic approach. Geology 25, 123–126.

Rino, S., Kon, Y., Sato, W., Maruyama, S., Santosh, M., Zhao, D., 2008. The Grenvillian and Pan-African orogens: World's largest orogenies through geologic time, and their implications on the origin of superplume. Gondwana Res. 14, 51–72.

Roberts, N.M.W., 2012. Increased loss of continental crust during supercontinent amalgamation. Gondwana Res. 21, 994–1000.

Roberts, J.H., Nimmo, F., 2008. Tidal heating and the long-term stability of a subsurface ocean on Enceladus. Icarus 194, 675–689.

Roberts, N.M.W., Spencer, C.J., 2015. The zircon archive of continent formation through time. Geol. Soc. Lond., Spec. Publ. 389, 197–225.

Roberts, J.H., Zhong, S., 2004. Plume-induced topography and geoid anomalies and their implications for the Tharsis rise on Mars. J. Geophys. Res. Planets 109 (E3).

Robertson, E.C., Birch, F., MacDonald, G.J.F., 1957. Experimental determination of jadeite stability relations to 25,000 bars. Am. J. Sci. 255, 115–137.

Robinson, A.C., 2009. Geologic offsets across the northern Karakorum fault: Implications for its role and terrane correlations in the western Himalayan-Tibetan orogen. Earth Planet. Sci. Lett. 279, 123–130.

Rogers, J.J.W., Santosh, M., 2002. Configuration of Columbia, a Mesoproterozoic supercontinent. Gondwana Res. 5, 5–22.

Rogers, J.J.W., Santosh, M., 2004. Continents and Supercontinents. Oxford University Press, New York, pp. 289.

Rolf, T., Coltice, N., Tackley, P.J., 2012. Linking continental drift, plate tectonics and the thermal state of the Earth's mantle. Earth Planet. Sci. Lett. 351–352, 134–146.

Rollinson, H., 2017. There were no large volumes of felsic continental crust in the early Earth. Geosphere 13, 235–246.

Rozel, A.B., Golabek, G.J., Jain, C., Tackley, P.J., Gerya, T., 2017. Continental crust formation on early Earth controlled by intrusive magmatism. Nature 545, 332–335.

Rubie, D.C., Melosh, H.J., Reid, J.E., Liebske, C., Righter, K., 2003. Mechanisms of metal–silicate equilibration in the terrestrial magma ocean. Earth Planet. Sci. Lett. 205, 239–255.

Rudnick, R.L., 1995. Making continental crust. Nature 378, 571.

Rudnick, R.L., Fountain, D.M., 1995. Nature and composition of the continental crust: A lower crustal perspective. Rev. Geophys. 33, 267–309.

Rudnick, R.L., Gao, S., 2003. Composition of the continental crust. In: Treatise on Geochemistry. 3. Elsevier Inc, pp. 659.

Rudnick, R.L., Gao, S., 2014. Composition of the continental crust. In: Treatise on Geochemistry, Second edition. Elsevier Inc, pp. 1–51.

Rudnick, R.L., Presper, T., 1990. Geochemistry of intermediate/−to high-pressure granulites. In Granulites and crustal evolution (pp. 523–550). Springer, Dordrecht.

Rushmer, T., 1991. Partial melting of two amphibolites: Contrasting experimental results under fluid-absent conditions. Contrib. Mineral. Petrol. 107, 41–59.

Saccani, E., 2015. A new method of discriminating different types of post-Archean ophiolitic basalts and their tectonic significance using Th–Nb and Ce–Dy–Yb systematics. Geosci. Front. 6, 481–501.

Safonova, I. Yu, Santosh, M., 2014. Accretionary complexes in the Asia-Pacific region: Tracing archives of ocean plate stratigraphy and tracking mantle plumes. Gondwana Res. 25, 126–158.

Sagan, C., 2011. The Demon-Haunted World: Science as a Candle in the Dark. Ballantine Books.

Sajeev, K., Osanai, Y., Santosh, M., 2004. Ultrahigh-temperature metamorphism followed by two-stage decompression of garnet–orthopyroxene–sillimanite granulites from Ganguvarpatti, Madurai block, southern India. Contrib. Mineral. Petrol. 139, 29–46.

Samuel, V.O., Santosh, M., Liu, S., Wang, W., Sajeev, K., 2014. Neoarchean continental growth through arc magmatism in the Nilgiri Block, southern India. Precambrian Res. 245, 146–173.

Sandwell, D.T., Schubert, G., 1992. Evidence for retrograde lithospheric subduction on Venus. Science 257, 766–770.

Santosh, M., 2010. A synopsis of recent conceptual models on supercontinent tectonics in relation to mantle dynamics, life evolution and surface environment. J. Geodyn. 50, 116–133.

Santosh, M., Kusky, T., 2010. Origin of paired high pressure–ultrahigh-temperature orogens: A ridge subduction and slab window model. Terra Nova 22, 35–42.

Santosh, M., Yokoyama, K., Biju-Sekhar, S., Rogers, J.J.W., 2003. Multiple tectonothermal events in the granulite blocks of southern India revealed from EPMA dating: Implications on the history of supercontinents. Gondwana Res. 6, 29–63.

Santosh, M., Sajeev, K., Li, J.H., 2006. Extreme crustal metamorphism during Columbia supercontinent assembly: Evidence from North China Craton. Gondwana Res. 10, 256–266.

Santosh, M., Maruyama, S., Sato, K., 2009. Anatomy of a Cambrian suture in Gondwana: Pacific type orogeny in southern India? Gondwana Res. 16, 321–341.

Santosh, M., Liu, S.J., Tsunogae, T., Li, J.H., 2012. Paleoproterozoic ultrahigh-temperature granulites in the North China Craton: Implications for tectonic models on extreme crustal metamorphism. Precambrian Res. 222, 77–106.

Santosh, M., Teng, X.M., He, X.F., Tang, L., Yang, Q.Y., 2015a. Discovery of Neoarchean suprasubduction zone ophiolite suite from Yishui complex in the North China Craton. Gondwana Res. 38, 1–27.

Santosh, M., Arai, T., Maruyama, S., 2017. Hadean Earth and primordial continents: The cradle of prebiotic life. Geosci. Front. 8, 309–327.

Sartini-Rideout, C., Gilotti, J.A., McClelland, W.C., 2009. Reaction progress and timing of retrogression of eclogite-facies rocks, Danmarkshavn, North-East Greenland

Caledonides. Eur. J. Mineral. 21, 1149–1172.

Sasaki, S., Nakazawa, K., 1986. Metal-silicate fractionation in the growing Earth: Energy source for the terrestrial magma ocean. J. Geophys. Res. Solid Earth 91, 9231–9238.

Saunders, A.D., Norry, M.J., Tarney, J., 1988. Origin of MORB and chemically depleted mantle reservoirs: Trace element constraints. J. Petrol. 1, 415–445.

Schellart, W.P., 2004. Quantifying the net slab pull force as a driving mechanism for plate tectonics. Geophys. Res. Lett. 31.

Schirrmeister, B.E., de Vos, J.M., Antonelli, A., Bagheri, H.C., 2013. Evolution of multi-cellularity coincided with increased diversification of cyanobacteria and the Great Oxidation Event. Proc. Natl. Acad. Sci. 110, 1791–1796.

Schmalholz, S.M., Podladchikov, Y.Y., 2013. Tectonic overpressure in weak crustal-scale shear zones and implications for the exhumation of high-pressure rocks. Geophys. Res. Lett. 40, 1984–1988.

Schmalholz, S.M., Podladchikov, Y., 2014. Metamorphism under stress: the problem of relating minerals to depth. Geology 42, 733–734.

Schmidt, M.W., Poli, S., 1998. Experimentally based water budgets for dehydrating slabs and consequences for arc magma generation. Earth and Planetary Science Letters 163 (1-4), 361–379.

Schneider, J., Dedieu, C., Le Sidaner, P., Savalle, R., Zolotukhin, I., 2011. Defining and cataloging exoplanets: The exoplanet.eu database. Astron. Astrophys. 532, 79–85.

Scholl, D.W., von Huene, R., 2007. Crustal recycling at modern subduction zones applied to the past—Issues of growth and preservation of continental basement crust, mantle geochemistry, and supercontinent reconstruction. Geol. Soc. Am. Mem. 200, 9–32.

Scholl, D.W., von Huene, R., 2010. Subduction zone recycling processes and the rock record of crustal suture zones. Can. J. Earth Sci. 47, 633–654.

Schubert, G., Sandwell, D.T., 1995. A global survey of possible subduction sites on Venus. Icarus 117, 173–196.

Schubert, G., Spohn, T., 1990. Thermal history of Mars and the sulfur content of its core. J. Geophys. Res. Solid Earth 95 (B9), 14,095–14,104.

Schulze, D.E., Harte, B., Valley, J.W., Brenan, J.M., Channer, D.M.R., 2003. Extreme crustal oxygen isotope signatures preserved in coesite in diamond. Nature 423, 68–70.

Sclater, J.G., Anderson, R.N., Bell, M.L., 1971. Elevation of ridges and evolution of the central eastern Pacific. J. Geophys. Res. 76, 7888–7915.

Scott, D.J., Helmstaedt, H., Bickle, M.J., 1992. Purtuniq ophiolite, Cape Smith belt, northern Quebec, Canada: A reconstructed section of early Proterozoic oceanic crust. Geology 20, 173–176.

Sen, C., Dunn, T., 1994. Dehydration melting of a basaltic composition amphibolite at 1.5 and 2.0 GPa: Implications for the origin of adakites. Contrib. Mineral. Petrol. 117, 394–409.

Sepidbar, F., Ao, S., Palin, R.M., Li, Q.L., Zhang, Z., 2019. Origin, age and petrogenesis of barren (low-grade) granitoids from the Bezenjan-Bardsir magmatic complex, south-east of the Urumieh-Dokhtar magmatic belt, Iran. Ore Geol. Rev. 104, 132–147.

Sessions, A.L., Doughty, D.M., Welander, P.V., Summons, R.E., Newman, D.K., 2009. The continuing puzzle of the great oxidation event. Curr. Biol. 19, R567–R574.

Shea, J.H., 1982. Twelve fallacies of uniformitarianism. Geology 10, 455–460.

Sheraton, J.W., 1984. Chemical changes associated with high-grade metamorphism of mafic rocks in the East Antarctic Shield. Chem. Geol. 47, 135–157.

Shervais, J.W., 2001. Birth, death, and resurrection: The life cycle of suprasubduction zone ophiolites. Geochem. Geophys. Geosyst. 2 (1).

Shervais, J.W., 2006. The significance of subduction-related accretionary complexes in early Earth processes. eds In: Reimold, W.U., Gibson, R.L. (Eds.), Processes on Early Earth: Geological Society of America Special Paper. 405. pp. 173–192.

Shirey, S.B., Richardson, S.H., 2011. Start of the Wilson cycle at 3 Ga shown by diamonds from subcontinental mantle. Science 333, 434–436.

Shirey, S.B., Kamber, B.S., Whitehouse, M.J., Mueller, P.A., Basu, A.R., 2008. A review of the isotopic and trace element evidence for mantle and crustal processes in the Hadean and Archean: Implications for the onset of plate tectonic subduction. GSA Special Papers 440, 1–29.

Sieh, K.E., Jahns, R.H., 1984. Holocene activity of the San Andreas fault at Wallace creek, California. Geol. Soc. Am. Bull. 95, 883–896.

Simons, M., Solomon, S.C., Hager, B.H., 1997. Localization of gravity and topography: Constraints on the tectonics and mantle dynamics of Venus. Geophys. J. Int. 131, 24–44.

Sizova, E., Gerya, T., Stüwe, K., Brown, M., 2015. Generation of felsic crust in the Archean: A geodynamic modeling perspective. Precambrian Res. 271, 198–224.

Sleep, N.H., 1975. Formation of oceanic crust: Some thermal constraints. J. Geophys. Res. 80, 4037–4042.

Sleep, N.H., 1994. Martian plate tectonics. J. Geophys. Res. Planets 99, 5639–5655.

Smart, K.A., Tappe, S., Stern, R.A., Webb, S.J., Ashwal, L.D., 2016. Early Archaean tectonics and mantle redox recorded in Witwatersrand diamonds. Nat. Geosci. 9, 255–259.

Smit, K.V., Shirey, S.B., Hauri, E.H., Stern, R.A., 2019. Sulfur isotopes in diamonds reveal differences in continent construction. Science 364, 383–385.

Smith, D.C., 1984. Coesite in clinopyroxene in the Caledonides and its implications for geodynamics. Nature 310, 641.

Smith, D.E., Zuber, M.T., Frey, H.V., Garvin, J.B., Head, J.W., Muhleman, D.O., Pettengill, G.H., Phillips, R.J., Solomon, S.C., Zwally, H.J., Banerdt, W.B., 1998. Topography of the northern hemisphere of Mars from the Mars Orbiter Laser Altimeter. Science 279, 1686–1692.

Smithies, R.H., Champion, D.C., Cassidy, K.F., 2003. Formation of Earth's early Archaean continental crust. Precambrian Res. 127, 89–101.

Smithies, R.H., Champion, D.C., Sun, S.-S., 2004. The case for Archean bon- inites. Contrib. Mineral. Petrol. 147, 705–721.

Smrekar, S.E., Davaille, A., Sotin, C., 2018. Venus interior structure and dynamics. Space Sci. Rev. 214, 88.

Snow, C.A., 2006. A reevaluation of tectonic discrimination diagrams and a new probabilistic approach using large geochemical databases: Moving beyond binary and ternary plots. J. Geophys. Res. Solid Earth 111 (B6).

Snyder, C.W., Moroz, V.I., 1992. Spacecraft exploration of Mars. Mars 71–119.

So, B.D., Yuen, D.A., 2015. Generation of tectonic over-pressure inside subducting oceanic lithosphere involving phase-loop of olivine–wadsleyite transition. Earth Planet. Sci. Lett. 413, 59–69.

Sobolev, S.V., Babeyko, A.Y., 2005. What drives orogeny in the Andes? Geology 33, 617–620.

Solomatov, V.S., Moresi, L.N., 1996. Stagnant lid convection on Venus. J. Geophys. Res. Planets 101 (E2), 4737–4753.

Song, S., Zhang, L., Niu, Y., Song, B., Zhang, G., Wang, Q., 2004. Zircon U-Pb SHRIMP ages of eclogites from the North Qilian Mountains in NW China and their tectonic implication. Chin. Sci. Bull. 49, 848–852.

Spandler, C., Hermann, J., Arculus, R., Mavrogenes, J., 2003. Redistribution of trace elements during prograde metamorphism from lawsonite blueschist to eclogite facies; implications for deep subduction-zone processes. Contributions to Mineralogy and Petrology 146 (2), 205–222.

Spencer, C.J., Roberts, N.M.W., Santosh, M., 2017. Growth, destruction, and preservation of Earth's continental crust. Earth Sci. Rev. 172, 87–106.

Spohn, T., 1991. Mantle differentiation and thermal evolution of Mars, Mercury, and Venus. Icarus 90, 222–236.

Spudich, P., Orcutt, J., 1980. A new look at the seismic velocity structure of the oceanic crust. Rev. Geophys. 18, 627–645.

Stern, R.J., 2005. Evidence from ophiolites, blueschists, and ultrahigh-pressure metamorphic terranes that the modern episode of subduction tectonics began in Neoproterozoic time. Geology 33, 557–560.

Stern, R.J., 2016. Is plate tectonics needed to evolve technological species on exoplanets? Geosci. Front. 7, 573–580.

Stern, R.J., Reagan, M., Ishizuka, O., Ohara, Y., Whattam, S., 2012. To understand subduction initiation, study forearc crust: To understand forearc crust, study ophiolites. Lithosphere 4, 469–483.

Stern, S.A., Bagenal, F., Ennico, K., Gladstone, G.R., Grundy, W.M., McKinnon, W.B., Moore, J.M., Olkin, C.B., Spencer, J.R., Weaver, H.A., Young, L.A., 2015. The Pluto system: Initial results from its exploration by New Horizons. Science 350, 1815–1819.

Stern, R.J., Leybourne, M.I., Tsujimori, T., 2016. Kimberlites and the start of plate tectonics. Geology 44, 799–802.

Stern, R.J., Gerya, T., Tackley, P.J., 2018. Stagnant lid tectonics: Perspectives from silicate planets, dwarf planets, large moons, and large asteroids. Geosci. Front. 9, 103–119.

Stevenson, D.J., 2003. Styles of mantle convection and their influence on planetary evolution. C. R. Geosci. 335, 99–111.

Štípská, P., Powell, R., 2005. Constraining the *P–T* path of a MORB-type eclogite using pseudosections, garnet zoning and garnet-clinopyroxene thermometry: An example from the Bohemian Massif. J. Metamorph. Geol. 23, 725–743.

Stofan, E.R., Anderson, S.W., Crown, D.A., Plaut, J.J., 2000. Emplacement and composition of steep-sided domes on Venus. J. Geophys. Res. Planets 105, 26,757–26,771.

St-Onge, M.R., Searle, M.P., Wodicka, N., 2006. Trans-Hudson Orogen of North America and Himalaya-Karakoram-Tibetan Orogen of Asia: Structural and thermal characteristics of the lower and upper plates. Tectonics 25.

St-Onge, M.R., Rayner, N., Palin, R.M., Searle, M.P., Waters, D.J., 2013. Integrated pressure–temperature–time constraints for the Tso Morari dome (Northwest India): Implications for the burial and exhumation path of UHP units in the western Himalaya. J. Metamorph. Geol. 31, 469–504.

Stracke, A., 2012. Earth's heterogeneous mantle: A product of convection-driven interaction between crust and mantle. Chem. Geol. 330, 274–299.

Streckeisen, A., 1974. Classification and nomenclature of plutonic rocks recommendations of the IUGS subcommission on the systematics of igneous rocks. Geol. Rundsch. 63, 773–786.

Strom, R.G., Schaber, G.G., Dawson, D.D., 1994. The global resurfacing of Venus. J. Geophys. Res. Planets 99, 10899–10926.

Stuck, T.J., Diener, J.F.A., 2018. Mineral equilibria constraints on open-system melting in metamafic compositions. J. Metamorph. Geol. 36, 255–281.

Syracuse, E.M., van Keken, P.E., Abers, G.A., 2010. The global range of subduction zone thermal models. Phys. Earth Planet. Inter. 183, 73–90.

Tackley, P.J., 2000. Self-consistent generation of tectonic plates in time-dependent, three-dimensional mantle convection simulations. Geochem. Geophys. Geosyst. 1. https://doi.org/10.1029/2000GC000036.

Tagawa, M., Nakakuki, T., Kameyama, M., Tajima, F., 2007. The role of history-dependent rheology in plate boundary lubrication for generating one-sided subduction. Pure Appl. Geophys. 164, 879–907.

Takahashi, E., Brearley, M., 1990. Speculations on the Archean mantle: Missing link between komatiite and depleted garnet peridotite. J. Geophys. Res. 95, 15,941–15,954.

Tang, L., Santosh, M., 2018. Neoarchean granite-greenstone belts and related ore mineralization in the North China Craton: An overview. Geosci. Front. 9, 751–768.

Tang, M., Chen, K., Rudnick, R.L., 2016. Archean upper crust transition from mafic to felsic marks the onset of plate tectonics. Science 351, 372–375.

Tao, W.C., O'Connell, R.J., 1992. Ablative subduction: A two-sided alternative to the conventional subduction model. J. Geophys. Res. Solid Earth 97, 8877–8904.

Tappert, R., Stachel, T., Harris, J.W., Muehlenbachs, K., Ludwig, T., Brey, G.P., 2005. Subducting oceanic crust: The source of deep diamonds. Geology 33, 565–568.

Taylor, R.J., Kirkland, C.L., Clark, C., 2016. Accessories after the facts: Constraining the timing, duration and conditions of high-temperature metamorphic processes. Lithos 264, 239–257.

Thurston, P.C., Chivers, K.M., 1990. Secular variation in greenstone sequence

development emphasizing Superior Province, Canada. Precambrian Res. 46, 21–58.

Timmerman, S., Honda, M., Burnham, A.D., Amelin, Y., Woodland, S., Pearson, D.G., Jaques, A.L., Le Losq, C., Bennett, V.C., Bulanova, G.P., Smith, C.B., 2019. Primordial and recycled helium isotope signatures in the mantle transition zone. Science 365, 692–694.

Tosi, N., Godolt, M., Stracke, B., Ruedas, T., Grenfell, J.L., Höning, D., Nikolaou, A., Plesa, A.C., Breuer, D., Spohn, T., 2017. The habitability of a stagnant-lid Earth. Astron. Astrophys. 605, A71.

Toth, J., Gurnis, M., 1998. Dynamics of subduction initiation at preexisting fault zones. J. Geophys. Res. Solid Earth 103 (B8), 18,053–18,067.

Trebi-Ollennu, A., Kim, W., Ali, K., Khan, O., Sorice, C., Bailey, P., Umland, J., Bonitz, R., Ciarleglio, C., Knight, J., Haddad, N., 2018. InSight Mars lander robotics instrument deployment system. Space Sci. Rev. 214, 93–103.

Treloar, P.J., Palin, R.M., Searle, M.P., 2019. Towards resolving the metamorphic enigma of the Indian Plate in the NW Himalaya of Pakistan. Geol. Soc. Lond. Spec. Publ. 483, 255–279.

Tsujimori, T., Ernst, W.G., 2014. Lawsonite blueschists and lawsonite eclogites as proxies for palaeo-subduction zone processes: A review. J. Metamorph. Geol. 32, 437–454.

Tsujimori, T., Harlow, G.E., 2012. Petrogenetic relationships between jadeitite and associated high-pressure and low-temperature metamorphic rocks in worldwide jadeitite localities: A review. Eur. J. Mineral. 24, 371–390.

Tsujimori, T., Sisson, V.B., Liou, J.G., Harlow, G.E., Sorensen, S.S., 2006. Very-low-temperature record of the subduction process: A review of worldwide lawsonite eclogites. Lithos 92, 609–624.

Turcotte, D.L., 1980. On the thermal evolution of the Earth. Earth Planet. Sci. Lett. 48, 53–58.

Turcotte, D.L., 1993. An episodic hypothesis for Venusian tectonics. J. Geophys. Res. Planets 98, 17,061–17,068.

Turner, S.P., George, R.M.M., Evans, P.J., Hawkesworth, C.J., Zellmer, G.F., 2000. Timescales of magma formation, ascent and storage beneath subduction-zone volcanoes. Phil. Trans. R. Soc. Lond. Ser. A Math. Phys. Eng. Sci., 358, 1443–1464.

Turner, S., Rushmer, T., Reagan, M., Moyen, J-F., 2014. Heading down early on? Start of subduction on Earth. Geology 42, 139–142.

Ueda, K., Gerya, T., Sobolev, S.V., 2008. Subduction initiation by thermal–chemical plumes: Numerical studies. Phys. Earth Planet. Inter. 171, 296–312.

Unterborn, C.T., Kabbes, J.E., Pigott, J.S., Reaman, D.M., Panero, W.R., 2014. The role of carbon in extrasolar planetary geodynamics and habitability. Astrophys. J. 793, 124–132.

Usui, T., Nakamura, E., Kobayashi, K., Maruyama, S., Helmstaedt, H., 2003. Fate of the subducted Farallon plate inferred from eclogite xenoliths in the Colorado Plateau. Geology 31, 589–592.

Usui, T., Kobayashi, K., Nakamura, E., Helmstaedt, H., 2007. Trace element fractionation in deep subduction zones inferred from a lawsonite-eclogite xenolith from the Colorado Plateau. Chemical Geology 239 (3-4), 336–351.

Valencia, D., O'Connell, R.J., Sasselov, D.D., 2007. Inevitability of plate tectonics on super-Earths. Astrophys. J. Lett. 670, 45–49.

Van der Voo, R., 1982. Pre-Mesozoic paleomagnetism and plate tectonics. Annu. Rev. Earth Planet. Sci., 10, 191–220.

Van der Voo, R., 1990. The reliability of paleomagnetic data. Tectonophysics 184, 1–9.

Van Heck, H.J., Tackley, P.J., 2011. Plate tectonics on super-Earths: Equally or more likely than on Earth. Earth Planet. Sci. Lett. 310, 252–261.

Van Hunen, J., Moyen, J-F., 2012. Archean subduction: Fact or fiction? Annu. Rev. Earth Planet. Sci. 40, 195–219.

Van Hunen, J., van den Berg, A.P., 2008. Plate tectonics on the early Earth: Limitations imposed by strength and buoyancy of subducted lithosphere. Lithos 103, 217–235.

Van Hunen, J., van Keken, P.E., Hynes, A., Davies, G.F., Condie, K.C., Pease, V., 2008. Tectonics of early Earth: Some geodynamic considerations (eds.) In: Condie, K.C., Pease, V. (Eds.), When Did Plate Tectonics Begin on Planet Earth. Geological Society of America Special Paper 440pp. 157–171.

Van Keken, P.E., Hacker, B.R., Syracuse, E.M., Abers, G.A., 2011. Subduction factory: 4. Depth-dependent flux of H$_2$O from subducting slabs worldwide. J. Geophys. Res. Solid Earth 116 (B1).

Van Kranendonk, M.J., Collins, W.J., Hickman, A., Pawley, M.J., 2004. Critical tests of vertical vs. horizontal tectonic models for the Archaean East Pilbara granite–greenstone terrane, Pilbara craton, western Australia. Precambrian Res. 13, 173–211.

Van Kranendonk, M.J., Smithies, R.H., Hickman, A.H., Champion, D., 2007. Review: secular tectonic evolution of Archean continental crust: Interplay between horizontal and vertical processes in the formation of the Pilbara Craton, Australia. Terra Nova 19, 1–38.

Van Thienen, P., van den Berg, A.P., Vlaar, N., 2004. Production and recycling of oceanic crust in the early Earth. Tectonophysics 386, 41–65.

Vance, D., Mahar, E., 1998. Pressure-temperature paths from *P–T* pseudosections and zoned garnets: Potential, limitations and examples from the Zanskar Himalaya, NW India. Contrib. Mineral. Petrol. 132, 225–245.

Verma, S.K., Verma, S.P., 2013. Identification of Archaean plate tectonic processes from multidimensional discrimination diagrams and probability calculations. Int. Geol. Rev. 55, 225–248.

Vermeesch, P., 2006. Tectonic discrimination diagrams revisited. Geochem. Geophys. Geosyst. 7. https://doi.org/10.1029/2005GC001092.

Vidale, J.E., Benz, H.M., 1992. Upper-mantle seismic discontinuities and the thermal structure of subduction zones. Nature 356, 678–682.

Viete, D.R., Holder, R.M., 2019. Modern-style metamorphism in the Paleoproterozoic: A product of stochasticity in 'time to subduction initiation' within ocean basins? In: Abstract for GSA Annual Meeting in Phoenix, Arizona.

Vine, F.J., Matthews, D.H., 1963. Magnetic anomalies over oceanic ridges. Nature 199, 947–949.

Vlaar, N.J., Van Keken, P.E., Van den Berg, A.P., 1994. Cooling of the Earth in the Archaean: Consequences of pressure-release melting in a hotter mantle. Earth Planet. Sci. Lett. 121, 1–18.

Wade, J., Dyck, B., Palin, R.M., Moore, J.D., Smye, A.J., 2017. The divergent fates of primitive hydrospheric water on Earth and Mars. Nature 552, 391–395.

Wahrhaftig, C., 1984. Structure of the Marin Headlands block, California: A progress report (Ed.) In: Blake, M.C.J. (Ed.), Franciscan Geology of Northern California. 43. Pacific Section S.E.P.M, pp. 31–50.

Wakabayashi, J., 2019. Sedimentary compared to tectonically deformed serpentinites and tectonic serpentinite mélanges at outcrop to petrographic scales: Unambiguous and disputed examples from California. Gondwana Res. 74, 51–67.

Wakita, K., 2019. Tectonic setting required for the preservation of sedimentary mélanges in Palaeozoic and Mesozoic accretionary complexes of southwest Japan. Gondwana Res. 74, 90–100.

Wang, Z., Wilde, S.A., Wang, K., Yu, L., 2004. A MORB-arc basalt-adakite association in the 2.5 Ga Wutai greenstone belt: Late Archean magmatism and crustal growth in the North China Craton. Precambrian Res. 131, 323–343.

Wang, S., Wang, C., Phillips, R.J., Murphy, M.A., Fang, X., Yue, Y., 2012. Displacement along the Karakoram fault, NW Himalaya, estimated from LA-ICP-MS U–Pb dating of offset geologic markers. Earth Planet. Sci. Lett. 337, 156–163.

Warren, R.G., 1983. Metamorphic and tectonic evolution of granulites, Arunta Block, central Australia. Nature 305, 300–304.

Waters, D.J., 2019. Metamorphic constraints on the tectonic evolution of the High Himalaya in Nepal: The art of the possible. Geol. Soc. Lond., Spec. Publ. 483, SP483–2018.

Watters, T.R., Nimmo, F., 2010. The tectonics of Mercury. Planet. Tecton. 11, 15–21.

Watters, T.R., McGovern, P.J., Irwin Iii, R.P., 2007. Hemispheres apart: The crustal dichotomy on Mars. Annu. Rev. Earth Planet. Sci. 35, 621–652.

Wei, C.J., Clarke, G.L., 2011. Calculated phase equilibria for MORB compositions: A re-appraisal of the metamorphic evolution of lawsonite eclogite. J. Metamorph. Geol. 29, 939–952.

Wei, Y., Zhou, W., Hu, Z., Li, H., Huang, X., Zhao, X., Xu, D., 2019. Geochronology and geochemistry of Archean TTG and tremolite schist xenoliths in Yemadong Complex: Evidence for ≥3.0 Ga Archean continental crust in Kongling high-grade metamorphic terrane, Yangtze Craton, China. Minerals 9, 689–698.

Weller, M.B., Lenardic, A., 2018. On the evolution of terrestrial planets: Bi-stability, stochastic effects, and the non-uniqueness of tectonic states. Geosci. Front. 9, 91–102.

Weller, O.M., St-Onge, M.R., 2017. Record of modern-style plate tectonics in the Palaeoproterozoic Trans-Hudson orogen. Nat. Geosci. 10, 305–311.

Weller, M.B., Lenardic, A., O'Neill, C., 2015a. The effects of internal heating and large-scale climate variations on tectonic bi-stability in terrestrial planets. Earth Planet. Sci. Lett. 420, 85–94.

Weller, O.M., St-Onge, M.R., Searle, M.P., Waters, D.J., Rayner, N., Chen, S., Chung, S.L., Palin, R.M., 2015b. Quantifying the *P–T–t* conditions of north–south Lhasa terrane accretion: New insight into the pre-Himalayan architecture of the Tibetan plateau. J. Metamorph. Geol. 33, 91–113.

Weller, O.M., St-Onge, M.R., Rayner, N., Waters, D.J., Searle, M.P., Palin, R.M., 2016. U–Pb zircon geochronology and phase equilibria modelling of a mafic eclogite from the Sumdo complex of south-east Tibet: Insights into prograde zircon growth and the assembly of the Tibetan plateau. Lithos 262, 729–741.

Weller, O.M., Copley, A., Miller, W.G.R., Palin, R.M., Dyck, B., 2019. The relationship between mantle potential temperature and oceanic lithosphere buoyancy. Earth Planet. Sci. Lett. 518, 86–99.

White, W.M., Klein, E.M., 2014. 4.13—Composition of the Oceanic Crust. In: Treatise on Geochemistry, Second edition. 4. pp. 457–496.

White, R.W., Palin, R.M., Green, E.C., 2017. High-grade metamorphism and partial melting in Archean composite grey gneiss complexes. J. Metamorph. Geol. 35, 181–195.

Whitney, D.L., Davis, P.B., 2006. Why is lawsonite eclogite so rare? Metamorphism and preservation of lawsonite eclogite, Sivrihisar, Turkey. Geology 34, 473–476.

Wiemer, D., Schrank, C.E., Murphy, D.T., Wenham, L., Allen, C.M., 2018. Earth's oldest stable crust in the Pilbara Craton formed by cyclic gravitational overturns. Nat. Geosci. 11, 357–361.

Wilhelms, D.E., Squyres, S.W., 1984. The Martian hemispheric dichotomy may be due to a giant impact. Nature 309, 138–142.

Wilke, F.D., O'Brien, P.J., Gerdes, A., Timmerman, M.J., Sudo, M., Khan, M.A., 2010. The multistage exhumation history of the Kaghan Valley UHP series, NW Himalaya, Pakistan from U–Pb and ^{40}Ar/^{39}Ar ages. Eur. J. Mineral. 22, 703–719.

Wilson, B.M., 2007. Igneous Petrogenesis a Global Tectonic Approach. Springer Science & Business Media.

Wilson, J.F., Orpen, J.L., Bickle, M.J., Hawkesworth, C.J., Martin, A., Nisbet, E.G., 1978. Granite-greenstone terrains of the Rhodesian Archean craton. Nature 271, 23–27.

Winchester, J.A., Floyd, P.A., 1976. Geochemical magma type discrimination: Application to altered. and metamorphosed basic igneous rocks. Earth Planet. Sci. Lett. 28, 459–469.

Wolf, M.B., Wyllie, P.J., 1994. Dehydration melting of amphibolite at 10 kbar: The effects of temperature and time. Contrib. Mineral. Petrol. 115, 369–383.

Wood, D.A., 1980. The application of a Th–Hf–Ta diagram to problems of tectonomagmatic classification and to establishing the nature of crustal contamination of basaltic lavas of the British Tertiary volcanic province. Earth Planet. Sci. Lett. 50, 11–30.

Wood, D.A., Joron, J.L., Treuil, M., 1979. A re-appraisal of the use of trace elements to classify and discriminate between magma series erupted in different tectonic settings. Earth Planet. Sci. Lett. 45, 326–336.

Wu, W., Liu, W., Qiao, D., Jie, D., 2012. Investigation on the development of deep space exploration. Sci. China Technol. Sci. 55, 1086–1091.

Xiao, W.J., Sun, M., Santosh, M., 2015. Continental reconstruction and metallogeny of the

Circum-Junggar areas and termination of the southern Central Asian Orogenic Belt. Geosci. Front. 6, 137–140.

Xie, Q., Kerrich, R., Fan, J., 1993. HFSE/REE fractionations recorded in three komatiite-basalt sequences, Archean Abitibi greenstone belt: Implications for multiple plume sources and depths. Geochim. Cosmochim. Acta 57, 4111–4118.

Yamamoto, S., Senshu, H., Rino, S., Omori, S., Maruyama, S., 2009. Granite subduction: Arc subduction, tectonic erosion and sediment subduction. Gondwana Res. 15, 443–453.

Yang, X.M., Drayson, D., Polat, A., 2019. S-type granites in the western Superior Province: A marker of Archean collision zones. Can. J. Earth Sci. 56, 1409–1436.

Yardley, B.W., Bodnar, R.J., 2014. Fluids in the continental crust. Geochem. Perspect. 3, 1–125.

Yin, A., 2012. Structural analysis of the Valles Marineris fault zone: Possible evidence for large-scale strike-slip faulting on Mars. Lithosphere 4, 286–330.

Zack, T., Rivers, T., Brumm, R., Kronz, A., 2004. Cold subduction of oceanic crust: Implications from a lawsonite eclogite from the Dominican Republic. Eur. J. Mineral. 16, 909–916.

Zegers, T.E., van Keken, P.E., 2001. Middle Archean continent formation by crustal de-lamination. Geology 29, 1083–1086.

Zhai, M.G., Santosh, M., 2011. The early Precambrian odyssey of the North China Craton: A synoptic overview. Gondwana Res. 20, 6–25.

Zhai, M.G., Zhao, G., Zhang, Q., 2002. Is the Dongwanzi complex an Archean ophiolite? Science 295, 923.

Zhang, C., Holtz, F., Koepke, J., Wolff, P.E., Ma, C., Bédard, J.H., 2013. Constraints from experimental melting of amphibolite on the depth of formation of garnet-rich restites, and implications for models of Early Archean crustal growth. Precambrian Res. 231, 206–217.

Zhang, S., Wei, C., Duan, Z., 2017. Petrogenetic simulation of the Archean trondhjemite from Eastern Hebei, China. Sci. China Earth Sci. 60, 958–971.

Zhang, Z., Ding, H., Palin, R.M., Dong, X., Tian, Z., Chen, Y., 2020. The lower crust of the Gangdese magmatic arc, southern Tibet, implication for the growth of continental crust. Gondwana Res. 77, 136–146.

Zhao, G., Cawood, P.A., Wilde, S.A., Lu, L., 2001. High-pressure granulites (retrograded eclogites) from the Hengshan Complex, North China Craton: Petrology and tectonic implications. J. Petrol. 42, 1141–1170.

Zhao, G., Wilde, S.A., Li, S., Sun, M., Grant, M.L., Li, X., 2007. U–Pb zircon age constraints on the Dongwanzi ultramafic–mafic body, North China, confirm it is not an Archean ophiolite. Earth Planet. Sci. Lett. 255, 85–93.

Zhong, S., Zuber, M.T., 2001. Degree-1 mantle convection and the crustal dichotomy on Mars. Earth Planet. Sci. Lett. 189, 75–84.

Ziaja, K., Foley, S.F., White, R.W., Buhre, S., 2014. Metamorphism and melting of picritic crust in the early Earth. Lithos 189, 173–184.